ABSTRACT

KONONCHIK JR, JOSEPH PETER. Assembly and Entry of Alphaviruses. (Under the direction of Dennis Brown.)

Sindbis virus, the prototype virus for alphaviruses, is a membrane containing virus with T=4 icosahedral symmetry. It contains two icosahedral shells sandwiching a host-derived lipid bilayer. The outer shell consists of the glycoproteins E1 and E2 and the inner shell is made of capsid and along with the RNA make up the nucleocapsid. The symmetry of the particle has been shown to be directed by the nucleocapsid. Here, data is presented that supports this hypothesis. Using previously generated SV mutants containing furin protease sites at the base of the viral glycoproteins, E1 and E2, the last step of encapsulation can be inhibited. This is hypothesized to be a loss of capsid-glycoprotein interaction at the last critical step of encapsulation. As a result, the virus particles that normally release into the extracellular medium continue to recruit glycoproteins. This creates long tubular protrusions from the plasma membrane that release with agitation. Analysis of the tubular viruses shows assembly consistent with Casper and Klug's hypothesis that simple subunits (E1/E2 trimers in this case) can create icosahedral, tubular and planar symmetry.

Recent crystal structures of soluble constructs of E1 and an E1-E2 fusion protein have been fitted into a cryo-electron microscopy reconstruction giving a pseudo-atomic model of the virus structure. Analysis of this and of these soluble proteins at low pH (6.0) has resulted in a hypothetical conformation of SV at low pH. These data are critically reviewed and highlight unanswered questions and concerns that bring question to their model. An alternative mechanism of entry is also reviewed and compared to the widely accepted mechanism of entry by endocytosis. This mechanism involves infection at the

plasma membrane via the use of a proteinaceous pore. Supporting this hypothesis, novel data is presented that show SV cross-linked to a protein complex on the surface of mosquito cells via freeze-fracture replicas. These intramembrane particles (IMPs) are labeled with SV protein antibodies as well as Vacuolar-type H^+-ATPase (V-ATPase) antibody suggesting a correlation between the virus receptor and the V-ATPase. In addition to freeze-fracture replicas, thin-sections of SV bound to BHK-21 cells co-label with anti SV and anti-V-ATPase, further supporting the hypothesis that SV and the V-ATPase are associated during infection at the plasma membrane.

Assembly and Entry of Alphaviruses

by
Joseph Peter Kononchik Jr.

A dissertation submitted to the Graduate Faculty of
North Carolina State University
in partial fulfillment of the
requirements for the Degree of
Doctor of Philosophy

Biochemistry

Raleigh, North Carolina

March, 21st 2011

APPROVED BY:

Dr. Dennis Brown Chair of Advisory Committee	Dr. John Cavanagh
Dr. Paul Wollenzein	Dr. John Mackenzie

DEDICATION

This work is dedicated to my wife Genevieve Anne Holzapfel. Together we have made it through some of the worst times and some of the best of times. I will never stop learning from her.

BIOGRAPHY

My name is Joseph Peter Kononchik Jr. I was born in Connecticut to Ellen and Joseph Kononchik. My mother is a registered nurse, and my father has had a variety of professions. My first experience in school was in Texas, when my father decided to go to seminary to become a pastor. The two years I spent in Texas were very exciting, and I have many pleasant memories from there. After two years in TX, we returned to CT where I began 2nd grade. New London is one of the harsher places to live in CT with a high crime rate and a high poverty rate. Consequently the New London County school system is not one of the best in the country. As a result, I never had to open a book or study for an exam for the 6 years I spent in that school system. During these years, we moved into a nice colonial house (my favorite house still) and my parents divorced.

Once I finished middle school, my mother remarried and we moved to the next town over; Waterford. Waterford is a more affluent town which had an excellent school system. As a result, I was taken aback when I entered high school and realized that I actually had to study and I could not just watch movies and disregard the speaker at the front of the class. I also gained an appreciation of a good, challenging education. Here is where I met most of my friends that I have today, which is a testament to our friendship and loyalty throughout the last decade. We were personally motivated to do our best and we all ended up getting significant degrees in college. My high school chemistry and physics classes were where I became interested in chemistry and physical sciences.

College was the University of Connecticut from 2002 to 2006. Here I obtained a B.S. in Molecular and Cell Biology. In the wide breadth of this degree I was exposed to everything from plant biology, anatomy and physiology, alternative medicines, genetics, microbiology, immunology, virology and biochemistry. I completely and wholeheartedly enjoyed all of the classes and laboratories that I took, and all of the new friends that came with them. Here I really became interested in biochemistry, partly because the hardest class was biochemistry, and I managed to be successful. In the end, it won my heart and I decided that it was something that I would like continue to pursue.

Once I was accepted into the PhD program at NC State I concentrated on what specific part of biochemistry I would like focus on, as each field has its specializations. During the first rotation, my entire class really decided to stay where they were. I felt like I immediately fell into my place in Dennis Brown’s lab. I really enjoy all the work I have done in this lab, and I feel as though I have left a positive impression on all of the people in the lab. We’ve had some good times, and some tough times, but in the end we’re all (lab) family.

Here, at NC State, I met Genevieve Holzapfel. I fell in love with her smile and her drive to get what she wanted; along with her curly hair. We married on October 30th, 2009. We decided to expand our family sometime afterwards and felt that the end of grad school would be good time to start. Our little girl arrived on July 29th, 2010. She has given my life a new perspective and new motivation to be my best for her. Looking back at my childhood education, I want to give her a challenging and exciting experience that will develop her skills and hopefully give her enough experience to do the same for her children.

ACKNOWLEDGEMENTS

I would like to acknowledge Dennis Brown and Raquel Hernandez for their tireless mentoring of a young, naïve graduate student. I hope I make them proud. I would also like to acknowledge John Mackenzie and Valerie Knowlton for teaching me everything I know about electron microscopy and image processing. This knowledge will be invaluable in my future career and beyond. John Cavanagh and Paul Wollenzien have been put through torture during my annual reviews, preliminary defense and thesis defense; I appreciate their patience in my ongoing learning process.

I would lastly like to acknowledge all of the past grad students that I have had the pleasure of working with; Gongbo Wang, Steevenson Nelson and Helen Rho especially for helping me when I’ve been in trouble, or just to keep me sane.

TABLE OF CONTENTS

LIST OF TABLES

LIST OF FIGURES

CHAPTER 1

An Alternative Pathway for Alphavirus Entry

Joseph P. Kononchik Jr., Raquel Hernandez and Dennis T. Brown

Submitted to:

Adv. In Virol. 2011 Jan 1

Summary

The study of alphavirus entry has been complicated by an inability to clearly identify a receptor and experiments which only tangentially and indirectly examine the process producing results that are difficult to interpret. The mechanism of entry has been widely accepted to be by endocytosis followed by acidification of the endosome resulting in virus membrane-endosome membrane fusion. This mechanism has come under scrutiny as better purification protocols and improved methods of analysis have been brought to the study. Results have been obtained that suggest alphaviruses infect cells directly at the plasma membrane without the involvement of endocytosis or exposure to acid pH. In this review we compare the data which support the two models and make the case for an alternative pathway of entry by alphaviruses.

Alphaviruses

Alphaviruses are transmitted to vertebrates by hematophagic insects such as mosquitoes and ticks. These insects are the vectors in the enzootic cycle. Reptiles, small mammals and birds are primary reservoirs. Humans and larger mammals are largely a dead end in the virus life cycle due to the low levels of viremia produced. Symptoms of alphavirus infection vary from asymptomatic to encephalitis or arthritis. Of those that cause disease, Eastern, Western and Venezuelan encephalitis viruses contribute significantly to disease in large mammals and the well-being of humans. Chikungunya is reemerging as a threat to humans and has been gaining ground in Africa, Asia, the Philippines and Italy with imported cases in France and in international travelers returning to the United States and South America (2007; Angelini et al., 2007; Ledrans et al., 2007; Prevention, 2010).

Sindbis Virus (SINV), the prototype virus of genus *alphavirus* in the family *Togaviridae* is a group IV membrane containing virus with a positive sense RNA genome (Strauss and Strauss, 1994). It is widely used in laboratory studies due to its non-pathogenic phenotype in humans and biosafety level 2 containment status. SINV can be grown to high titer in both mammalian and insect cells (Brown and Condreay, 1986; Hernandez, Sinodis, and Brown, 2010), and has been shown to infect all cell types with the exclusion of those derived from plants. Certain strains of SINV, specifically the heat resistant SINV (SVHR) are ideal for Alphavirus entry studies. Purified SVHR, in contrast to other membrane containing viruses, can have a particle to plaque-forming-unit (pfu) ratio that approaches unity (Hernandez, Sinodis, and Brown, 2010). Knowing that every particle is infectious ensures that all observations of cell-virus interactions are of productive virus infections. These features of SINV are optimal for the study of entry of this class of membrane containing viruses including studies involving direct observation by electron microscopy. The term virus entry refers specifically to the mechanism by which the virus binds to the host cell receptor, penetrates the cell membrane barrier and releases the infectious RNA into the cell initiating the infection.

Alphavirus Structure

Alphaviruses are small 70nm viruses that have 240 copies each of three structural proteins, E1, E2 and capsid (C) assembled in a 1:1:1 stoichiometry. These three proteins create two nested T=4 icosahedral shells that sandwich a host derived lipid bilayer (Paredes

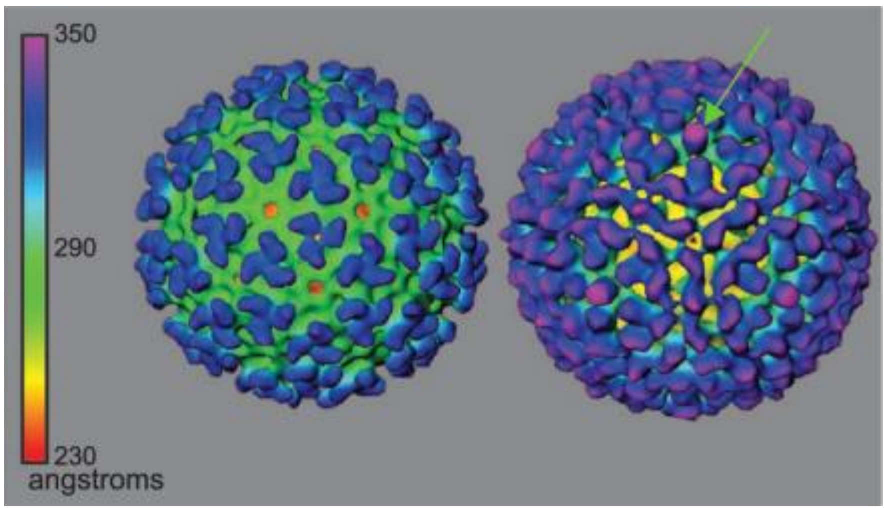

Figure 1.1: Cryo-EM reconstruction of Sindbis Virus

Cryo-EM reconstruction of Sindbis Virus at neutral pH (Left; pH 7.0) and at low pH (Right; pH 5.3) illustrating the conformational change that occurs at this threshold pH. The green arrow highlights the protrusion that appears at the 5-fold vertex at low pH.

Reprinted by permission from Elsevier from: *Paredes, A. M., Ferreira, D., Horton, M., Saad, A., Tsuruta, H., Johnston, R., Klimstra, W., Ryman, K., Hernandez, R., Chiu, W., and Brown, D. T. (2004). Conformational changes in Sindbis virions resulting from exposure to low pH and interactions with cells suggest that cell penetration may occur at the cell surface in the absence of membrane fusion. Virology* ***324****(2)****,*** *373-86.*

et al., 2004) (Figure 1.1). The outer protein shell is composed of E1 and E2 heterodimers that assemble into aggregates of three producing the three pronged spike which protrudes from the virus surface. The inner protein shell is made of only C, encapsulating the 49S RNA. This inner protein shell is the shape determining component of the virus (Ferreira et al., 2003a; Kononchik et al., 2009). The organization of the E1/E2 complexes on the cell membrane likely exist as a two-dimensional 6-fold symmetry sheet prior to capsid envelopment (VonBonsdorff and Harrison, 1978). When the membrane glycoproteins begin the process of encapsulation, the nucleocapsid recruits the E1-E2 trimers into the developing outer shell by specifically binding the E2 endodomains. Through its repeated 240 interactions between a hydrophobic cleft on C and the E2 endodomain this process organizes the glycoproteins into the 6-fold and requisite 5-fold rotational arrays necessary to form a three-dimensional icosahedral structure (Brown, Waite, and Pfefferkorn, 1972a). The resulting virus particle has 80 spikes that are primarily made of E2 (colored blue in Figure 1.1 pH 7.0) with a protein skirt that is mostly E1 (colored green in Figure 1.1 pH 7.0), which covers the incorporated membrane (Mukhopadhyay et al., 2006; Zhang et al., 2002). The two protein shells, with their significant level of lateral and transmembrane interactions (Hernandez et al., 2000; Whitehurst et al., 2006), result in a very rigid and precisely organized particle that is unlike that of other membrane containing viruses. It has been shown recently, that the particles of mammalian and insect grown SVHR are not identical (He et al.). The cellular response to infection by insect and mammalian derived virus has also been shown to be different (Shabman et al., 2007). Particles coming from insect cells are more compact, lacking some RNA intercalation into the capsid protein shell seen in mammalian grown virus. The thickness of the membrane of virus produced from mosquito and mammalian cells does not account for the difference in the structure of the virus particles; however the outer protein shell seems to be extended in the mammalian grown virus suggesting that the protein organization between the two particles may be in slightly different functional conformations.

The highly organized structure of the alphaviruses with the many protein-protein interactions stabilizing the structure and the membrane bilayer occluded by the outer protein shell have important implication for the process of entry of the viral genome into host cells. Whereas many membrane containing viruses such as influenza can be described as a membranous structure with embedded proteins the alphaviruses are protein shells with an associated membrane. This protein shell must be compromised if the virus is to transfer its RNA to the cell cytoplasm. The virus protein shell may provide the mechanism for genome delivery. The E1 protein in the mature alphavirus exists in a metastable configuration poised to use the energy stored during virus assembly for the entry process upon encountering an appropriate trigger (Carleton et al., 1997; Mulvey and Brown, 1994). The energy stored for this conformational change is considered to be partially the result of folding the E1 protein though a series of disulfide bonded intermediates as the protein is compacted into the metastable structure during the assembly of the spike heterotrimer (Mulvey and Brown, 1994). The metastable nature of the spike complex is revealed when the E1 protein is released from the mature virus using detergent and reorganizes into several disulfide bridged configurations which can be separated on non-denaturing gels(Mulvey and Brown, 1994).

The current molecular model for how the virus disassembles to expose the infectious RNA is supported by a crystal structure of E1* (PDB code: 1I9W) that was subsequently fit into a cryo-reconstruction of SINV (PDB code: 1Z8Y) (Gibbons et al., 2004b). This structure was obtained by expression of the E1 ectodomain from *E. coli* and by cleavage from purified Semliki Forest Virus (SFV) (Gibbons et al., 2004a; Lescar et al., 2001; Li et al., 2010). In this structure the protein has three primary domains I, II and III. Domain I is the NH proximal domain that contains the putative fusion loop. Domain II is the middle domain and domain III is the most distal domain. In the crystal structure, there are a number of disulfide bonds identified supporting the hypothesis that disulfide bonds are an energy source for virus entry (Abell and Brown, 1993); however some cystines identified as participating in disulfide bridges in the crystal structure were identified as free cystines using protein modification and mass spectrometry (Whitehurst et al., 2007). These conflicts are not unexpected because the protein crystal structure is dependent on how the protein is purified, the crystals are grown, and the structure is refined. By nature of the crystal analysis process the structure is of a protein in its lowest energy conformation. This means that the crystal structure could be any one of the various intermediate conformations assumed when E1 is extracted by detergent (described above). There is currently crystal structures of an E1-E2 fusion protein (PDB codes 3MUU), chikungunya glycoproteins (PDB codes: 3N40;3N41;3N42;3N43;3N44;2XFB;2XFC) and their fit into the SINV and/or Semliki Forest Virus cryo-reconstruction (PDB codes: 3MUW;2XFB;2XFC). These structures suffers from many of the same problems E1* struggles with including low energy conformations and lack of transmembrane domains, which have been shown to be essential in virus production and infectivity (Sjoberg and Garoff, 2003).

How is structure related to virus entry? The overall alphavirus icosahedral structure is unique in that it is a membrane containing virus that does not have the membrane exposed.

The membrane itself is not the form determining factor as with influenza, and because it is beneath the outer protein shell is not readily available to fuse with host membranes. The alphavirus could be considered a non-enveloped virus with an associated membrane. The essential role of the membrane may be to provide the scaffold upon which the virus is assembled.

Adsorption and receptor recognition

The process attachment/absorption is probably a multistep event that begins with a general "sticking" to the cell via one or more proteins (or the cell membrane itself) followed by "rolling" on the cell surface as it locates the proper receptor to initiate the penetration step of virus entry. This type of interaction has been recorded using single particle fluorescence resonance energy transfer (FRET). SINV with a membrane intercalated fluorescent self-quenching dye can be visualized when the dye is excited with a specific wavelength light (Wessels et al., 2007). Fusion of virus is detected when lipid mixing (fusion) releases the proteins and dequenching of the dye occurs causing it to fluoresce. Using this technique it has been shown that SINV moves on the cell surface in a neutral pH environment. If the pH of the medium bathing the cells is lowered the virus does not fuse with the cell surface as is the case with influenza, rather the virus "freezes" in place. These observations are interpreted to indicate that viruses probe the cell surface for the proper receptor molecule.

As arboviruses, alphaviruses infect insect and vertebrate hosts. Since alphaviruses need to effectively infect cells which provide widely divergent biochemical and genetic environments, it is likely that they either uses a ubiquitous receptor, or are able to use multiple proteins as a receptor. Many proteins have been implicated as being part of the receptor complex. The list includes, heparin sulfate (Byrnes and Griffin, 1998; Smit et al., 2002b; Zhang et al., 2005), the major histocompatability complex (MHC) (Helenius et al., 1978; Maassen and Terhorst, 1981), the major laminin receptor (Wang et al., 1992), DC sign, L sign (Klimstra et al., 2003), heat shock 70 protein (Ryan, Stevens, and Schlesinger, 1992), an unidentified 110kDa nerve protein (Ubol and Griffin, 1991), and a 63kDa protein in chicken cells (Wang et al., 1991). The length of the list of possible receptors strongly suggests that there are multiple proteins that alphaviruses can use, and that the specific receptor is both cell and virus specific. If, however, there is one widely used receptor it would have to be a fundamental piece of the cells' biochemical machinery that has been conserved throughout evolution. An alternative explanation is that the alphaviruses have evolved to use both highly conserved proteins that span the large breath of species and/or multiple proteins as a receptor for other cells.

The concept that the receptor is, at least in part, protein comes from a study that showed protease treatment of cells prior to adsorption decreased the number of infected cells whereas phospholipases and neuraminidases did not have an effect (Smith and Tignor, 1980). Using cross-linking, the first candidate as a receptor was identified by Maassen and Terhorst (Maassen and Terhorst, 1981) as a 90kDa protein. Following this study were a number of additional studies that employed various techniques to determine the receptor. One such study used soluble glycoproteins from Semliki Forest Virus (SFV) and showed that the MHC bound the glycoproteins and that detergent soluble MHC protein was able to inhibit SFV infection of HeLa cells (Helenius et al., 1978). Since then, a number of questions about the validity of this argument have arisen since cells that lack the MHC complex are not resistant to SFV infection (Oldstone et al., 1980). Additionally, mosquito cells, which fundamentally lack a human immune system and thus do not express MHC, are also readily infected by alphaviruses.

The use of anti-idiotypic antibodies as receptor locators has been used as well to determine the receptor for alphaviruses. This approach is responsible for the discovery of the 63kDa chicken protein (Wang et al., 1991) and eventually led to the implication of the high-affinity laminin receptor (Wang et al., 1992). While this is considered a major receptor for alphaviruses, reexamination of the original experiment that identified the 63kDa chicken protein revealed that this protein was not the chicken laminin receptor (Wang et al., 1991). Additionally antibody against the chicken laminin receptor did not inhibit infection significantly (<10%). This suggests that although the laminin receptor is conserved across many species, it is not the only virus receptor. It is entirely likely though that there are multi-protein complexes that are not required for, but enhance infection. Other investigations of the laminin receptor used antiidiotpye antibodies to examine the laminin receptor as a possible virus receptor in mosquito cells. In these studies a 32kDa protein was discovered in mosquito cells to which Venezuelan Equine Encephalitis Virus (VEE) bound as did laminin and SINV (Strauss and Strauss, 1994). Antibodies were also used to investigate virus binding with a strain of SINV which was selected to be a rapid penetrating virus (Olmsted, Meyer, and Johnston, 1986). Upon binding to the cell at neutral pH and assumingly to its receptor, SFV was shown to go through a conformational change as new antibody epitopes are exposed on the surface of the virus (Ahn et al., 1999). This is presumably related to the conformational change that is seen in reconstructed virus particles which were exposed to low pH (Paredes et al., 2004).

A measure of successful virus entry

There are numerous techniques that can be used to examine the interactions between the virus and the cell. These techniques can generally fall into two categories: direct and indirect observation. Direct observation uses familiar techniques such as thin-section microscopy, cryo-electron microscopy, tomography, and other less familiar techniques like freeze-fracture immunolabeling to examine virus-cell interactions. Electron microscopy (EM), both transmission and to a lesser extent scanning, is the crux of these observation methods. When properly prepared and processed, the interactions between the virus and cell seen in the microscope are the actual interactions that occurred at the time of fixation. By examining different times during the infection process, the possible mechanism and pathway of virus entry can be elucidated. Unfortunately, thin-sections and other direct observation techniques cannot distinguish between a successful infection process, and that of an unproductive interaction. This makes microscopy very subjective and is the primary problem when observing virus-cell interactions, as even with a relatively low particle/pfu ratio of 1:10, most observations are of virus-cell interactions that do not lead to a successful infection. For

SINV, the SVHR strain can be purified to a particle/pfu ratio of 1:1, and this virus was used in EM studies of virus infection that led to the direct cell penetration hypothesis of virus entry (Paredes et al., 2004). Many of the observations that have been made using EM are of viruses preparation made with strains or samples with high or undetermined particle/pfu ratio and therefore are difficult to interpret.

When direct observation is not possible, or cannot answer the question being asked, techniques that take advantage of indirect or secondary reporters have been used. Some indirect reporters that have been used as a measure of successful virus entry include virus RNA production (Glomb-Reinmund and Kielian, 1998), virus protein synthesis (DeTulleo and Kirchhausen, 1998), virus production (Perez and Carrasco, 1994). While these tools are useful and have shed light on many virus-cell interactions, these tools have a significant disadvantage insomuch that they cannot accurately determine if a virus has not entered the cell. Many of these biochemical reporters are significantly downstream of the initial virus adsorption and entry. As a result, each step between entry and the reporter has the potential to be inhibited giving a false negative. To give a time-scale to RNA translation and protein synthesis, super infection inhibition is detectable 15 minutes post infection (Johnston, Wan, and Bose, 1974; Karpf et al., 1997). This implies that entry is a very fast process, and that the genome is quickly unpacked and rapidly available for processing. The speed of infection, the problems of indirect reporters, and the limits of direct observation need to be carefully considered when building an assay to measure successful virus entry.

Alphavirus mode of entry

Once the virus has bound to its receptor, the virus outer shell must overcome the plasma membrane barrier. The classical mechanism of membrane containing viruses is to breach this barrier by triggering fusion of the virus membrane with the host cell membrane, releasing its contents into the cytoplasm (Harrison, 2008). This is accomplished by a conformational change that can occur by receptor recognition as with HIV (Kielian and Jungerwirth, 1990; Melikyan, 2008), or by environmental changes such as pH or artificially with heat or reducing agents as seen with SINV (Anthony, Paredes, and Brown, 1992; Meyer et al., 1992). The conformational change of SINV was visualized using cyro-electron microscopy reconstruction of particles exposed to low pH (Paredes et al., 2004). The change resulted in a protruding spike from the 5-fold axis of the virus, compared to the lack of this density in the untreated particles (Figure 1, green arrow). The location of the spike suggests that it is both 5-fold in symmetry, and that it is likely composed of E1, the glycoprotein that has the putative fusion loop. The following mode of entry would follow the traditional mechanism of vesicular fusion where the cell and viral membranes would be drawn together and fusion would occur. Discussed here are two suggested modes of entry for the alphavirus and the data supporting them.

Viral Endocytosis followed by membrane fusion

The most commonly accepted mechanism of entry for alphaviruses is proposed to be via endocytosis and the subsequent acidification of the vesicle; similar to influenza. The studies in support of this mechanism are extensive, and rely on the observations that alphaviruses have membrane fusion capabilities, and that inhibition of the acidification of endosomes inhibits the entry of the virus. The original fusion assays were done with cultured cells, and it was shown that treating cells with adsorbed virus to a brief low pH environment, resulted in cell-cell fusion (fusion from without) (White, Kartenbeck, and Helenius, 1980). This suggested the acid environment of an endosome could provide the requirements for fusion and penetration. However, unlike the situation encountered in an endosome, this fusion from without event required return to neutral pH (Edwards and Brown, 1986). The analysis of fusion was then moved from a live cell culture to an in vitro assay including liposomes and artificial membranes (White and Helenius, 1980). In these assays, the fusion process did not require a return to neutral pH, but required a significant amount of cholesterol (Kielian and Helenius, 1984). These data were supported by an experiment that showed cells grown in serum treated with Cab-O-sil, a silicate that removes cholesterol from the serum could not be infected as measured by immunofluorescent antibody labeling of newly folded virus protein (Lu, Cassese, and Kielian, 1999). There are two concerns regarding the cholesterol requirement for infection that have been neglected. First, the liposome is protein free and therefore receptor free and second the amount of cholesterol required to induce fusion of SINV to liposomes is high, up to 50 mol%. However, the requirement for such a high concentration of cholesterol is in direct conflict with the fact that alphaviruses infect and assemble mosquitoes, which are cholesterol auxotrophs (Hafer et al., 2009; Mitsuhashi, Nakasone, and Horie, 1983). Second, Cab-O-sil, while removing cholesterol also removes a significant number of other lipids, which may be required for proper function of the cells and virus stability (Hafer et al., 2009). In fact, growing the same cell type used in the Cab-O-sil experiment in serum-free media resulted in no significant change in their sensitivity to infection (Hafer et al., 2009). Together, these data imply that a large amount of cholesterol is not required for alphavirus infection. Thus, if cholesterol is not required for infection and fusion of living cells does not occur at acid pH the liposome model for studying virus penetration is not valid for this purpose.

Treatment of cells with chemicals that inhibit the acidification of endosomes has been used to assay the role of acid environment in the infection of mammalian cells by alphaviruses (Helenius, Marsh, and White, 1982; Marsh et al., 1982). The assays for successful penetration were virus RNA or protein production or the production of progeny virions. It was concluded from these studies that the mechanism of entry was via endocytosis and endosome acidification. Drug studies suffer from the fact that no drug is specific for a single target and secondary and tertiary effects can affect the observation made. Because of this inherent problem it is critical that all possible controls be done and that the results are interpreted with caution. Drugs such as Bafilomycin A1, chloroquine, monensin and ammonium chloride (NH_4Cl) were used to inhibit the endosome acidification (Helenius, Marsh, and White, 1982; Marsh et al., 1982; Talbot and Vance, 1980; Talbot and Vance, 1982). The initial intent of these experiments was to demonstrate what the effect of the lack of acidification using these chemicals would have on the infection process. It was found that virus, virus RNA, or virus protein were not produced in the presence of these agents and this was interpreted to indicate that lack of acidification inhibited the release of the nucleocapsid from the endosome into the cell cytoplasm. These early experiments led to the current model of alphavirus infection by low pH mediated membrane fusion. However upon more rigorous analysis it was discovered that these drugs have various inhibitory effects on virus production not directly related to virus penetration. Chloroquine was shown to reduce the amount of virus produced in mammalian cells, however in insect cells the virus titer was enhanced (Coombs et al., 1981; Hernandez, Luo, and Brown, 2001). Chloroquine did increase the pH of mosquito cell endosomes as the cells were protected from diphtheria toxin which is known to require an acid environment to enter cells. Also in mosquito cells ammonium chloride was shown to inhibit steps in the non-structural protein processing after initial translation of the incoming RNA; many steps from the initial virus entry which had to have occurred (Hernandez, Luo, and Brown, 2001). BafA1 has been shown to have additional effects on the cell in addition to the observed pH increase of endosomes (Hunt, Hernandez, and Brown, 2011b).

Using a SINV construct that contained a GFP reporter, a thorough study was done to assess the effect of Bafilomycin A1 on the entry of alphaviruses into mammalian and mosquito cells (Hunt, Hernandez, and Brown, 2011b). The results of this study showed that BafA1 did not stop virus entry into mammalian or mosquito cells or inhibit RNA synthesis.

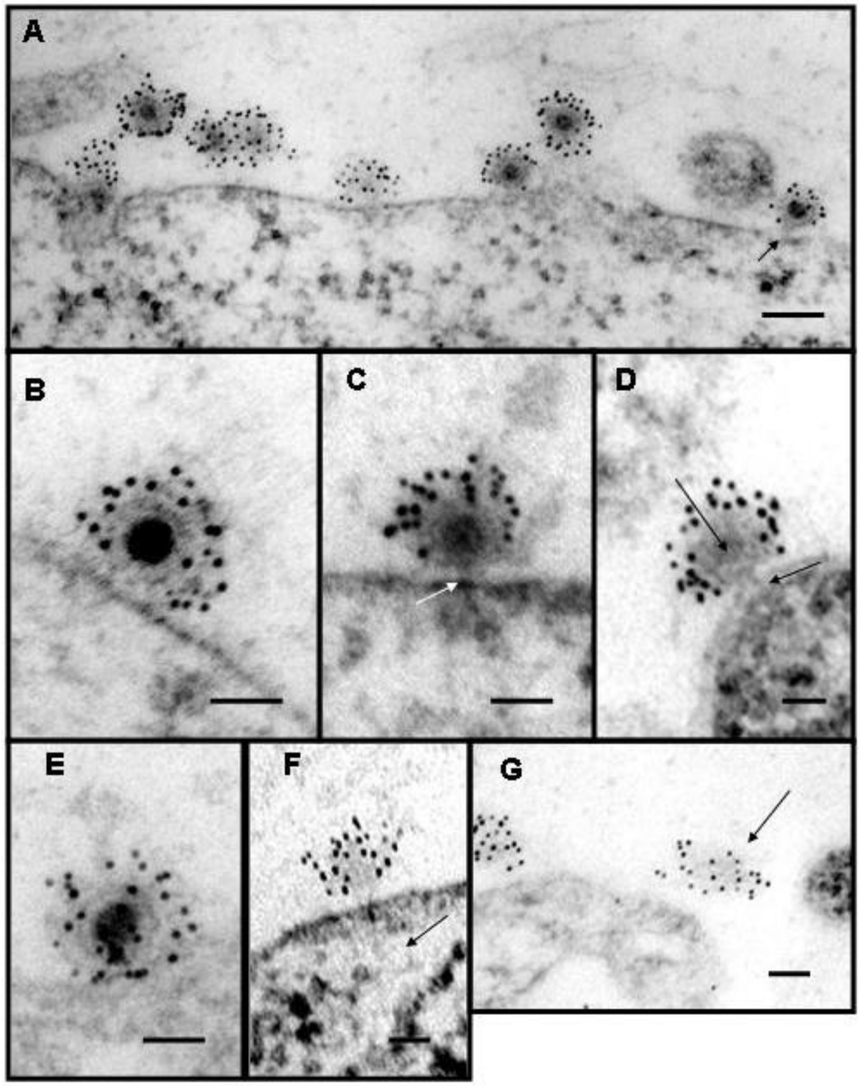

Figure 1.2: Electron micrographs of thin sections of Sindbis virus–cell complexes at pH 7.2.

(A) Low magnification showing ''full'' and ''empty'' particles and a particle attached by a pore to the cell surface (arrow). (B) A virion attached to the cell surface before pore formation. (C) A virion with an electron dense core attached to the cell surface by a pore structure (arrow). (D) The pore at the vertex (V) of the protein shell penetrates the cell membrane (arrow). The virion has reduced electron density in the core region. (E) Reorganization of virus RNA into the developing pore. (F) An empty particle with a possible RNA molecule entering the cell (arrow). (B) An empty virion that has lost structure. Magnification scale bar (A) = 1000 A °, all others = 500 A °.

Reprinted by permission from Elsevier from: *Paredes, A. M., Ferreira, D., Horton, M., Saad, A., Tsuruta, H., Johnston, R., Klimstra, W., Ryman, K., Hernandez, R., Chiu, W., and Brown, D. T. (2004). Conformational changes in Sindbis virions resulting from exposure to low pH and interactions with cells suggest that cell penetration may occur at the cell surface in the absence of membrane fusion. Virology* ***324****(2)***,** *373-86.*

plasma membrane correlate well with a recent publication showing SINV replication complexes at the plasma membrane (Frolova et al., 2010) as it would be easiest to explain the complexes here if the mechanism of entry were at the plasma membrane.

Entry without membrane fusion

An alternative mechanism of entry that is gaining supporting evidence is virus entry at the plasma membrane by pore formation. This mode of entry uses a pore complex made from virus and host proteins that connects the interior of the virus to the cytoplasm of the host cell cytoplasm via a protein channel. Using this type of mechanism the RNA can be delivered to the cell and the rest of the infection process can begin in the absence of membrane fusion. Supporting this mechanism of infection is that infection by alphaviruses has been shown to be a leaky process allowing passage of ions and small molecules across the compromised plasma membrane (Koschinski, Wengler, and Repp, 2005; Madan, Sanz, and Carrasco, 2005; Wengler, Koschinski, and Dreyer, 2003; Wengler, Koschinski, and Repp, 2004). Membrane fusion is a non-leaky process and thus does not reflect the normal response of living cells (Smit et al., 2002a). Were the viruses merely to bind to its receptor and then be enveloped into the cell, as with the low pH endocytosis mechanism, there would be no loss of continuity in the plasma membrane. It was later shown that these virus induced pores could be blocked with rare earth ions which allowed investigators to assign a size to the pores (Koschinski, Wengler, and Repp, 2005). In 2004, Paredes *et al.* were able to show full and empty particles (Figure 2) on the surface of mammalian cells using thin-sections of BHK cells infected with SVHR at a particle/pfu ratio of 1. Empty particles were identified by using anti-SINV antibodies with secondary antibodies conjugated to gold beads, as they would have been easily missed otherwise (Figures 2A, D, F). From the thin-sections, multiple particles with varying electron dense cores were shown and suggested that the virus was losing its RNA to the cell cytoplasm through a proteinaceous connection between the virus and the cell. The virus subsequently appeared to lose structural stability and be released from the cell leaving the proteinaceous pore behind. (Figure 2B, E, F, G). Two sets of pores have been identified to develop during an alphavirus infection, early and late. The size of the late pores was investigated by an experiment that examined alpha sarcin uptake during alphavirus infection (Madan, Sanz, and Carrasco, 2005). Here the 17kDa, 150 amino acid protein was shown to co-enter during infection. Further still, the pores were persistent for a small amount of time, whereas smaller pores were persistent for 6 hours post infection. Alphavirus entry in the absence of endocytosis was shown definitively by infecting cells at low temperature a condition under which membranes cannot fuse (Wang et al., 2007). A GFP reporter carrying SINV was able to infect cells that were incubated at 4C indefinitely until they were assayed for infection by looking for GFP production. While GFP signal increased with temperature and time, the cells at low temperature were still able to become infected. By reducing endocytosis and membrane fusion, these data support the mechanism proposed in Paredes *et al.* which show physical evidence that alphaviruses use a proteinaceous pore to infect cells.

Additional evidence supporting alphavirus entry via a pore at the plasma membrane was obtained using freeze-fracture (Kononchik, Vancinci and Brown, to be published). In these experiments, high MOI of SVHR was adsorbed onto mosquito cells for half an hour then the virus was cross-linked to cell surface proteins with gluteraldehyde. These samples were then processed via the freeze-fracture method to examine the plasma membrane and its components. The technique was a modification of the FRIL (freeze-replicate-immunolabel) technique developed by Fujimoto (Fujimoto, 1995; Fujimoto, 1997). In brief, the cross-linked samples were flash frozen in liquid ethane, fractured at low temperature and pressure. The fracture plane that goes through the sample follows the path of least resistance, which is the middle of lipid bilayers making two replicas: the inner leaflet, or P-face, and the outer leaflet, the E-face. As a result, when the fracture hits a cell, it tends to follow the plasma membrane. This makes it ideal for examining proteins and interactions that occur on the cell surface. In the case of this experiment, the replicas had cross-linked virus proteins attached to the outside of the E-face. Using immunolabeling, these proteins were labeled, and the organization of the proteins was examined by electron microscopy. The data collected showed labeled virus particles adsorbed to the cells' surface. These particles were observed as discrete rings of gold bead tags around the remnants of the virus particles after a cleaning treatment to remove most of the unwanted biological debris. Matching thin-sections of these samples confirmed the observation that the virus particles were on the surface of the cell. What makes this more interesting, is that some of the particles on the cell were empty, as with the previous observations, and the particle protein staining suggested that the particles have gone through a conformational change similar to the one described with vertebrate cells (Flynn et al., 1990).

Summary and Future Directions

Direct observation of alphavirus-cell interaction by electron microscopy has created seemingly conflicting data. In many observations, virus can be seen in endosomes inside the cell (Marsh, Bolzau, and Helenius, 1983). These data suggest the virus particles enter through an endocytic pathway. Coupled with the conformational changes that occur upon exposure to low pH and the fusion capabilities shown by SINV, the suggested route of entry is similar to that of influenza. However, other observations including thin-sections and freeze-fracture have shown that SINV can infect without endocytosis and acidification. These studies also found that as the particle to PFU ratio of the virus employed improved to unity no virus was seen in endosomes and empty particles were seen on the cell surface. These data suggest that the mechanism for virus entry is at the cell surface and involves direct release of the virus genome into the cytoplasm by a pore-like structure.

Indirect observations have not been able to elucidate the mechanism of entry either. The use of downstream reporters has been problematic as there are many steps between virus entry and the expression of the reporter. Treatment of cells with Cab-O-Sil has resulted in data that suggest cholesterol is required for infection. Other chemical treatments of BafA1, chloroquine and ammonium sulfate have suggested an acidic, endocytic pathway. All of these chemical treatments however have been shown to be unreliable, and that they suffer from unwanted secondary effects that inhibit events other than infection, and thus the reporters themselves, lead to false negatives.

The conflict between the two proposed mechanisms of alphavirus infection must be addressed. Whether SINV enters via an endocytic pathway, or directly at the cell surface, the subsequent experiments need to take into consideration the proper controls, especially with regards to secondary reporters, and the relative infectivity of the virus population as it pertains to both direct and indirect observations. The identification of the receptor complex of the alphaviruses is another very important step in dissecting virus entry. While there are proteins that may be receptors, it should be unambiguously shown that alphaviruses either use multiple receptors or that they use one specific receptor.

Acknowledgements

The authors are supported by a grant from The Foundation for Research, Carson City NV and by the North Carolina Agricultural Research Service.

Chapter 1.5

Sindbis Virus Nonstructural Proteins and Pseudo-Atomic Reconstruction Analysis

Sindbis genome organization, polyprotein processing and envelopment

The genome of SINV is a positive sense single-stranded RNA. It has a 5' methyl cap and a poly-A tail at the 3' end. The first two thirds of the genome are coded for the non-structural proteins, while the last third encodes the structural proteins (Strauss, Rice, and Strauss, 1984). Upon genome release into the cytoplasm, the non-structural proteins are readily transcribed from the genome. The synthesis of the structural polyprotein and full-length genomes are not synthesized from the initial genome copy, but are made from other plus strand RNAs that come from an antisense template. This antisense copy has been shown to be regulated by the uncleaved precursor P123 and nsP4 whereas plus-strand synthesis requires the cleavage of P123 (Shirako and Strauss, 1994). From the negative strand RNA, the 49S genome for packaging and the 26S subgenomic RNA template are synthesized. The structural proteins are then translated from the 26S subgenomic RNA (Strauss and Strauss, 1986).

The processing of the structural proteins begins with autoproteolysis of the capsid protein from the polyprotein as it is being synthesized. The cleavage and release of capsid exposes a signal peptide that moves translation to the ER for the rest of the translation (Garoff et al., 1990). Here, the remaining structural proteins are translated as a seven transmembrane polyprotein with the protein order as pE2-6K-E1. Mature proteins result from cleavage of E2 and E1 from the polyprotein and heterodimerization of E1 and E2 followed by trimerization of these complexes (Mulvey and Brown, 1996). E3, the cleaved portion of pE2 and 6K are not present in mature virions though there is evidence that suggests small amount of 6K may be present (Lusa, Garoff, and Liljestrom, 1991). During the maturation process, complex folding and disulfide shuffling occurs to result with a metastable heterodimers complex that is presented on the surface of the cell (Anthony, Paredes, and Brown, 1992; Carleton and Brown, 1996a; Mulvey and Brown, 1994). Envelopment, or budding, of SINV is a result of nucleocapsids which contain a capsid protein shell surrounding the 49S genome associating with the endodomain of E2 at the cell membrane (Hernandez et al., 2005; Hernandez et al., 2000; West et al., 2006; Whitehurst et al., 2006). This interaction is thought to drive the envelopment of the nucleocapsid with the E1/E2 heterodimers and is the form determining factor of the final shape of the virion (Ferreira et al., 2003a; Kononchik et al., 2009).

Structural Proteins Crystallography and Cryo-reconstruction Fit

Structures of E1* (PDB code:1I9W) and an E1-E2 ectodomain fusion protein (PDB codes:3MUU;3MUW) have been solved using x-ray crystallography (Lescar et al., 2001; Li et al., 2010). These proteins were expressed as a soluble protein that lacked the transmembrane domain of their respective full-length proteins. The resulting x-ray structures were then fit into a cryo-reconstruction of Sindbis (PDB code:1Z8Y) along with the C-terminus of the capsid protein (PDB code:1VCQ) (Choi et al., 1997) also solved by x-ray crystallography (Zhang et al., 2002). Ideally, this would give a pseudo atomic-level structure of Sindbis and show how the proteins are organized on the surface of the virus. This would then lead to understanding how the conformational changes occur when the virus is entering the cell, or when it is exposed to low pH. Unfortunately, the crystal structure has problems that are not addressed and cast doubt that it is the correctly folded mature form. First, the structure of the E1* soluble protein was shown to not be in the native conformation that was seen in the virus (Whitehurst et al., 2007). To summarize the study, E1 and E2 generate a complex network of disulfide bonds while maturing through the ER. The data presented examined the disulfide bridges present in the mature virus particles' glycoprotein. The authors found that the disulfide bridges present in the mature particle were not present in the crystal structure. This suggests that, while the overall shape of E1* may be similar to the ectodomain of E1 seen in the virus particle, it should certainly not be expected to be the atomic structure of the native protein in its metastable conformation. This alone should preclude this structure from being fit into the cryo-reconstruction of the virus. The E1/E2 fusion protein, while acknowledging that the two glycoproteins mature, fold and express together, is similar to the E1* structure in that it is lacking transmembrane domains. This fusion protein also discounts the effect 6k and E3 on the maturation of the glycoproteins. Overall, the crystal structure of E1* and the E1/E2 fusion protein may result in a conformation that is similar to that present in the mature particle (i.e. domains, etc.), however the specific conformation of each domain will likely differ from the crystal structure.

The missing transmembrane domains have been shown to be essential in virus production and infectivity (Sjoberg and Garoff, 2003). Deletion mutants of the E1TMD result in a lack of virus budding due to ineffective envelopment or multi-capsid budding from the cell. The authors conclude that the interaction between the E1TMD and E2TMD are essential for creating mature virus. From these data, it can be concluded that E1*, and likely the E1/E2 fusion protein are not structures of functional glycoproteins. As the purpose of determining the atomic structure of any protein is to correlate structure and function, it is misleading to use structures of non-functional proteins in an attempt to solve this problem. Doing so does not facilitate advancement of knowledge, but rather illustrates the authors' lack of understanding the limits of each technique.

In figure 3 of (Li et al., 2010), the comparison is made between earlier E2 mapping with the new E1-E2 fusion protein. The authors state, "The Ca backbone of E2 corresponded well with an earlier tracing obtained by connecting known markers such as glycolsylation and antibody-binding sites." However, examining their own cryo density and the crystal structure, it becomes all too apparent that the antigenic sites, while some are near the corresponding cryo sites, are not in good agreement. Additionally, based on the published figure, the extended E2 cryo density would not fit the crystal structure without gross changes. As a side note about the crystal structures that have been deposited, it is important to state that there are no water molecules in any of the structures. All protein, soluble or membrane associated, has water as an integral part of the structure of the molecule. The apparent lack of water in these reconstructions is of concern, as even protein TMDs can have water molecules in their structure.

Ignoring the inaccuracies of a pseudo-atomic structure of Sindbis Virus using these soluble protein structures, the last remaining unknown piece of the puzzle would be the transmembrane domains. As stated previously, there have been studies showing the importance of the transmembrane domains, and that there are interactions made between the TMDs of E1 and E2 (Sjoberg and Garoff, 2003). The current pseudo-atomic structure of

SINV includes modeled transmembrane domains. The build does take into consideration where the TMDs enter and exit the membrane. There is also reason behind the positioning of E1 with regards to the bend in the TMD. The point at which the TMD bends would allow the hydrophilic hydroxyl of E1-S418 and E1-S419 to bury into the helix. It also takes into consideration the bulky side-chains at the transition between the membrane and the ectodomains. The TMDs, however, as they are constructed, are missing some putative interactions. The data presented in (Ribeiro, *et al.* to be published) suggests that there is interaction between E1 and E2 near E2-M379-M380 and E1-I423-I424. In the reconstruction, the side chains of E2-M379 and E2-M380 are facing into the aliphatic tails of the membrane lipids. This conformation is inconsistent with an interaction between the TMDs involving these residues. There are also a number of other side-chains that are positioned in such a way that is not thermodynamically ideal for a transmembrane such as E2-T376, and E1-R438 and E1-R439 which have their charged tails turned into the hydrophobic membrane. A simple rotation of E2 would accommodate many of these problems, however to fit this data the EMfit program was used to fit ideal helices into the density and allowed a computer to try and best fit the side-chains into the density. While this is acceptable as a starting point, the end result should always be examined for accuracy and logic. These inconsistencies are examples of errors with this modeling and building de novo structures into cryo data.

It is interesting that the TMDs were modeled with side-chains as the resolution of the cryo-reconstruction is not high enough to resolve even large aromatic side-chains. Therefore, to suggest a possible conformation of the TMD and resulting interactions based on the cryo-reconstruction is merely speculation. Using only the beginning and end of the TMDs, and the density for the reconstruction, the best model at this time is a carbon-backbone going through the membrane or none at all. It is neither reasonable nor appropriate to create data from where there is none. It is satisfying that the crystal structure of the E1/E2 fusion protein was deposited as a c-α backbone and does not include side chains. Using the data presented here, and previously described, the interactions between E1 and E2 in the membrane can be added to the c-α backbone to arrive at a putative structure until higher resolution data is available.

Sindbis Virus Non-structural Proteins

The SINV nonstructural proteins are synthesized as the polyproteins P123 and P1234. P1234 is a result of a read-through of an opal codon between nsp3 and nsp4 resulting in the inclusion of nsp4. The processing of the polyprotein has been shown to be a function of nsp2 alone (Ding and Schlesinger, 1989; Hardy and Strauss, 1989). Presented below is a brief summary of the functions of each nonstructural protein with respect to virus replications and host manipulation.

nsP1

NsP1 has been implicated as a promoter protein for minus strand synthesis. This was discovered when a single amino acid mutation A348T resulted in a temperature sensitive (*ts*) mutant that was deficient in minus strand synthesis at non-permissive temperatures (Hahn, Strauss, and Strauss, 1989; Wang, Sawicki, and Sawicki, 1991). It has also been implicated as the capping enzyme of the genomic and subgenomic RNA (Durbin and Stollar, 1985). It has been shown to have methyltransferase activity as a singly expressed protein in E. coli, and mutants of SINV able to grow in methionine-free media (Durbin and Stollar, 1985). With regards to genome capping, nsP1 also has been shown to have guanyltransferase activity. Experiments that chemically lowered the GTP in SINV infected cells resulted in substitution mutations that seemingly enhanced the ability of nsP1 to efficiently bind guanidine triphosphate at its lower concentration (Scheidel, Durbin, and Stollar, 1987).

As a modifier protein, in addition to its modulation of minus strand synthesis, nsP1 has been show to alter the protease activity of nsP2 (de Groot et al., 1990). Here, nsP2 polyproteins containing nsP1 have a decreased ability to cleave the bond between nsP2 and nsP3.

nsP2

As implied above, one of the activities accredited to this protein is the protease activity required for cleavage of the nonstructural polyproteins. Temperature sensitive mutants with mutations nsP2 were all located in the C-terminal half and it was concluded that this was the protease domain of nsP2 (Hahn, Strauss, and Strauss, 1989; Sawicki and Sawicki, 1985; Sawicki and Sawicki, 1993). Further analysis showed that C477 and H546 were the catalytic dyad of this papain-like protease (Hardy and Strauss, 1989). There is no primary sequence alignment that suggests a papain-like protease other than the analysis showing the requirement of a cystines and a downstream histidine for catalytic activity. This lack of alignment to other papain-like proteases is understandable when looking at the crystal structure of the C-terminus nsP2 protease domain (PDB code: 2HWK) (Russo, White, and

Watowich, 2006). The structure of nsP2pro domain is a novel fold inconsistent with other papain proteases. The catalytic dyad is clearly defined, and using peptides from other cystines proteases, the S1, S2 and S3 binding pockets are clearly defined. Using this structure, nsP2 can be an effective target of antiviral therapeutics against alphaviruses. It is interesting that there is a supposedly nonfunctional domain of nsP2 that is fold is similar to a methyltransferase. Perhaps this was functional and originally used to add methyl caps to the viral RNA but when nsP1aquired this enzymatic activity selective pressure to maintain this domain diminished to a point where it lost its function.

In addition to the protease domain nsP2 has another domain that functions as the viral RNA helicase. Two motifs, 189-GSGKS-193 and 252-DEAF-255, are part of a nucleotide (NTP) binding motif in a NTP-binding superfamily (Glanville and Ulmanen, 1976; Gorbalenya et al., 1989; Hodgman, 1988). The crystal structure does not show this domain. Lastly, nsP2 is found in the nucleus. There are multiple nuclear localization and one nucleolus localization sequence in nsP2 (Peranen et al., 1988). The function in the nucleus is still unknown as all of the genome replication and protein processing is a cytoplasmic process. There has been implication that nsP2 also has a part in 26S RNA synthesis (Hahn, Strauss, and Strauss, 1989; Sawicki and Sawicki, 1985; Sawicki and Sawicki, 1993) though there is nothing in the homology of the protein that suggests an additional domain or motif.

nsP3

The function of nsP3 is not well understood. The protein has two domains, a highly conserved N-terminal domain and a non-conserved C-terminal domain (Kinney et al., 1986;

Strauss et al., 1988). There is evidence that it plays a role in RNA synthesis, as a temperature sensitive mutant of SINV contains a mutation in nsP3 of F312S (Hahn, Strauss, and Strauss, 1989). This mutation results in no RNA replication at non-permissive temperatures. Additionally, nsP3 is required in the polyprotein P123 for minus strand synthesis (Lemm and Rice, 1993; Lemm et al., 1994; Shirako and Strauss, 1994). It is interesting that nsP3 is highly phosphorylated by cellular factors, and also localizes to vesicular structures (Li et al., 1990; Peranen, 1991). The fact that highly phosphorylated nsP3 is found in replication complexes (Barton, Sawicki, and Sawicki, 1991) and that these replication complexes are membrane associated (Frolova et al., 2010) it is easy to think of nsP3 as some form of scaffold protein for the replication complex. A less understood mechanism of nsP3 is the modulation of the non-structural polyprotein cleavage between nsP3 and nsP4. When present as part of the nsP2 polyprotein (as in P123 or P1234), nsP3 enhances the cleavage of nsP4 from nsP3 (de Groot et al., 1990). As with nsP2, the soluble macro domain of two alphavirus nsP3 have been solved with ADP and RNA bound as well as an apo form (CHIKV PDB codes: 3GPG, 3GPO, 3GPQ; VEEV 3GQE, 3GQO) (Malet et al., 2009). The structure is consistent with other viral macro domains, insomuch that they all bind ADP-ribose and have phosphatase activity. The homology of these particular macro domains however have more in common with *E. coli* macro domains as opposed to other viral domains, such as that from coronavirus. The authors suggest that macro domains may have been acquired in two separate accounts and that determining the function of one macro domain does not illuminate the function of other macro domains (Neuvonen and Ahola, 2009). Certainly more structural analysis needs to be done on this domain before its elusive function is determined.

nsP4

nsP4 is the RNA dependent RNA polymerase (RdRp) (Hahn et al., 1989; Kamer and Argos, 1984) as it carries the classic GDD motif characteristic of these polymerases. Several mutations in nsP4 have shown that it has RdRp enzyme activity. Four temperature sensitive mutants of SINV have mutations in nsP4, one of which (G153E) results in a complete stop of RNA synthesis at non-permissive temperatures (Barton, Sawicki, and Sawicki, 1988; Keranen and Kaariainen, 1979; Sawicki et al., 1981). Other *ts* mutations in nsP4 have resulted in host range phenotypes that grow well in mosquito but not chicken cells (Lemm et al., 1990). Finally, mutations in nsP4 have been shown to make minus strand synthesis constitutively active (Sawicki et al., 1990). Taken together, these data indicate that nsP4 is the RdRp of alphaviruses. More recently, the catalytic core of nsP4 has been characterized and shown to have adenylyltransferase activity; consistent with other RNA viruses with polyA tailed genomes (Neufeld et al., 1994; Tomar et al., 2006).

CHAPTER 2

Helical virus particles formed from morphological subunits of a membrane containing icosahedral virus

Joseph P. Kononchik Jr., Steevenson Nelson, Raquel Hernandez and Dennis T. Brown

Published in:

Virology. 2009 Mar 15;385(2):285-93

Summary

The classic publication by Caspar and Klug in 1962 (Physical principles in the construction of regular viruses. Cold Spring Harbor Symp. Quant. Biol. **27:**1-24.) has formed the basis of much research on virus assembly. Caspar and Klug predicted that a single virus morphological unit could form a two dimensional lattice composed of 6-fold arrays (primitive plane), a family of icosahedra of increasing triangulation numbers (T) and helical arrays of varying length. We have shown that icosahedral viruses of varying T numbers can be produced using Sindbis virus (Ferreira, D. F. et al. 2003. Morphological variants of Sindbis virus produced by a mutation in the capsid protein. Virology **307:**54-66) Other studies have shown that Sindbis glycoproteins can also form a 2-dimensional lattice confirming Caspar and Klug's prediction of the primitive plane as a biologically relevant structure (VonBonsdorff, C. H., and S. C. Harrison**.** 1978. Sindbis virus glycoproteins form a regular icosahedral surface lattice. J. Virol. **28:**578). In this study we have used mutations in the glycoproteins of membrane containing Sindbis virus to create helical-virus-like particles from the morphological subunits of a virus of icosahedral geometry. The resulting virus particles were examined for subunit organization and were determined to be constructed of only 6-fold rotational arrays of the virus glycoproteins. A model of the tubular virus particles created from the 6-fold rotational arrays of Sindbis virus confirmed the observed structure. These experiments show that a common morphological unit (the Sindbis E1-E2 heterodimer) can produce three different morphological entities of varying dimensions in a membrane-containing virus system.

Introduction

In 1962 Caspar and Klug presented a groundbreaking theory which explained how the assembly of virus particles could be accomplished using as few as one morphological unit (protein); a significant advantage for the limited size of virus genomes (Caspar and Klug, 1962). At its simplest, Caspar and Klug hypothesized that the most energetically favorable construction of virus particles would be organized similar to a primitive plane of subunits sharing identical bonds in identical environments. They proposed that the icosahedron was the only 3-dimensional structure which allowed such an assembly mechanism. With the exception of T=1 particles, the geometry of the icosahedral particle requires that morphological subunits create 3-fold, 5-fold and 2-fold centers of symmetry. This, in addition to the subtriangulation environments on each facet, means the bonds and environments around the bonds are not always identical. The theory still applies, though, as long as the bonds and environments are similar enough to each other. This was termed quasi-equivalence. Much of the structural studies support the quasi-equivalence theory and is traditionally assumed correct until proven false.

Sindbis Virus (SV) is a membrane enclosed positive single-stranded RNA virus and is the prototype for the *Alphaviruses* in the *Togaviridae* family. Sindbis virus particles are 70nm in diameter and consist of two T=4 icosahedral protein shells sandwiching a host-derived membrane bilayer (Paredes et al., 1993). The inner icosahedral shell, made from the capsid protein, surrounds the 49S (+) ssRNA forming the nucleocapsid. The construction of both protein shells is consistent with the predictions of Caspar and Klug (Caspar and Klug, 1962).

The Sindbis virus genome encodes four non-structural proteins nsP1-nsP4 and three structural proteins capsid (C), E1 and E2. The structural proteins are present in the mature virion in a 1:1:1 stoichiometric ratio. The structural proteins are synthesized as a polyprotein, which after the autoproteolytic cleavage of the capsid protein at the amino terminus, is directed to the endoplasmic reticulum (ER) for integration into the membrane. Subsequent step-wise folding (Mulvey and Brown, 1994) and cleavage by signal peptidase (Liljestrom and Garoff, 1991) into pE2, 6k and E1 occurs prior to assembly of E1 and pE2 heterodimers and successive trimerization to form the subunit of the Sindbis virus outer protein shell. The folding of the E1 glycoprotein in the ER results in a compact, energy rich, metastable configuration which is delivered into the mature virion (Carleton et al., 1997; Mulvey and Brown, 1994). The energy stored in E1 is likely used to breach the cell membrane during infection (Paredes et al., 2004). PE2/E1 continues its maturation in the Golgi apparatus with cleavage by furin endoprotease at the sequence Arg-X-Arg/Lys-Arg (de Curtis and Simons, 1988) yielding mature E2. The heterotrimer is then presented to the surface of the cell for association with the independently formed nucleocapsid. Budding of Sindbis virus from the cell surface is the result of a nucleocapsid recruiting E1/E2 heterotrimers to the point of budding and directing the formation of the icosahedral structure (Ferreira et al., 2003b).

Subsequent to Caspar and Klug’s theory of virus assembly, the primitive plane was proved to be a biologically relevant structure for the membrane containing Sindbis virus when the glycoproteins from the icosahedral SV particles were partially dissolved and allowed to reassemble on a 2-dimensional plane. This procedure resulted in a 2-dimensional lattice of the glycoproteins with only 6-fold rotational arrays in the precise configuration predicted by Caspar and Klug's theory (VonBonsdorff and Harrison, 1978). The results of this experiment confirm the bond similarity between the primitive plane and the initial assembly of virus particles as icosahedra.

To further illustrate the similarities between the primitive plane and the icosahedral viruses, a primitive plane can be used to construct icosahedral particles by postulating a quasi-equivalent nature of the interactions between the subunits. By introducing 5-fold rotational arrays at regularly spaced intervals into the primitive plane of 6-fold rotational symmetry, the plane can be bent in such a way that the bonds remain within their quasi-equivalent constraints and still allow full enclosure of 3-dimensional space. The introduction of 5-fold rotational arrays into the primitive plane can generate geometric classes of icosahedrons. There are three icosahedral classes, P=1, P=3 and the skewed classes. Virus particles have been seen in all of the icosahedral classes though only a few species are seen in the skew classes.

SV particles fall into the P=1 class of icosahedral symmetry. This class contains the triangulation numbers of 1, 4, 9, 16, 25 and on following the equation $T=Pf^2$ where T is the triangulation number, f is any integer and $P=h^2+hk+k^2$ where h and k are any pair of integers that do not have a common factor (Caspar and Klug, 1962). For the P=1 class, the latter equation is solved to 1. In 2003 a study of a mutated SV capsid protein was reported. In that study the introduction of specific mutations in the capsid protein resulted in the formation of morphological variants (Ferreira et al., 2003b). These morphological variants were found to have increased diameters in specific size classes and were shown to have icosahedral symmetry and triangulation numbers ranging from 4 to 36. All of these T numbers followed the P=1 class progression of size and follow the predictions of Caspar and Klug. The fact that the mutation producing these variants was in C suggests that the capsid is the determining factor of the final particle size.

In their description of the primitive plane Caspar and Klug predicted that such a structure could also explain the assembly of helical viruses. Rolling the primitive plane into a cylindrical shape results in a reproduction of the pattern seen in some helical virus protein shells. What is important to note is that there is no mixture of 6-fold and 5-fold arrays in the model helical structure, which would create curvature of the relatively ridged structure. This also suggests that the formation of helical-like particles from subunits which normally form icosahedra is possible. It should also be noted that the creation of icosahedral particles from the alfalfa mosaic virus (a helical virus) subunits has been accomplished, but this was not done under physiological conditions (Fukuyama, Abdel-Meguid, and Rossmann, 1981).

Recently, tubular shaped particles have been generated from Rous Sarcoma Virus (RSV) by modifying the spacer between the capsid and nucleocapsid of its Gag polyprotein (Keller, Johnson, and Vogt, 2008). The insertions, deletions and substitutions presented in the study illustrate the importance of the spacer protein (SP) in the envelopment and release of RSV from the membrane. The authors further suggest that the interactions of SP in a cyro-EM model of immature HIV-1 particles may not fully explain the role of SP in the assembly and maturation of RSV. These data support the conclusions presented herein, which attempt to reveal the importance of the capsid-glycoprotein interactions to the envelopment of virus particles. SV, as compared to RSV, is released as a fully matured, strict T=4 enveloped virus resulting from envelopment of a pre-formed nucleocapsid. RSV has particles with varying core structures and sizes that result from release of particles that are assembled from Gag polyproteins that are protyolytically cleaved after assembly. The lack of SP in SV also means that the modified interactions result from changes in the environment around the capsid protein with respect to the glycoproteins. Even though these differences suggest that the assembly of the tubular structures might differ, the similar phenotype may be a result of a fundamental requirement for envelopment between RSV and SV.

In the present study we have found that the basic morphological unit of the membrane-containing Sindbis virus icosahedral outer shell can assemble into a tubular structure. This study supports the predictions of Caspar and Klug that a single morphological unit from an icosahedral virus can form the primitive plane, a family of icosahedral shells and a helical structure of varying length and expands similar assembly studies with bacteriophages into a membrane-containing virus system.

Results

We have previously shown that the Sindbis virus glycoprotein E1 is folded through a complex, multi-step, disulfide stabilized pathway into a compact energy rich structure in the

ER (Carleton et al., 1997; Mulvey and Brown, 1994). In order to make mutations in the E1 protein, which allowed dimerization with E2 and native folding of the complex, it was necessary to find a way to introduce mutations into the membrane proteins that would allow correct folding and assembly in the ER. Proper folding and oligomerization of E1 and E2 is a prerequisite for export from the ER (Carleton et al., 1997). We have found, as have others that the introduction of deletions and insertions in the ectodomains of the membrane glycoproteins can either have no phenotype or result in a failure to correctly fold and export the membrane proteins. Traditional clonal mutagenesis and reverse genetics become difficult tools to use as they rely on creating truncated or elongated proteins from truncated or elongated nucleotides. To overcome these problems we have developed a protocol for the introduction of furin sensitive cleavage sites in the membrane proteins. Furin is a protease which resides in the Golgi apparatus. We have previously shown that these mutations can allow correct folding of the virus proteins in the ER and introduction of alteration in protein structure after export (Nelson et al., 2005).

Production and Growth of Furin Mutants

Sindbis virus synthesizes a polyprotein that contains all of the structural proteins needed for virus assembly. As the polyprotein is synthesized, it undergoes autoproteolytic cleavage of the capsid protein resulting in exposure of a signal sequence and translocation to the ER. The fully synthesized polyprotein is integrated into the membrane as a multi-pass membrane spanning protein with 6 transmembrane domains. The protein undergoes a complex pathway of folding and proteolytic processing that eventually leads to the high energy conformations found in mature SV (Mulvey and Brown, 1994). A furin protease located in the Golgi network is responsible for the final processing event in the maturation of the virus E2 protein. We have shown that the introduction of additional furin recognition sequences (Arg-X-Arg/Lys-Arg) by introduction of amino acid substitutions in the E1 glycoprotein allowed natural folding and processing to occur while the proteins reside in the ER (Nelson et al., 2005). Once transported from the ER to the Golgi some, but not all, of the glycoproteins are cleaved at the new furin recognition sequences altering the ectodomains of E1 and E2. Growth in furin deficient cells confirmed that the mutations were not deleterious and produced a wild-type-like phenotype (Nelson et al., 2005). This method of protein alteration eliminated the possible improper processing that might occur if the primary structure of the polyprotein was changed by insertion or deletion of amino acids. Mutations which affect protein processing and dimerization lead to improper folding and failure to export from the ER (Carleton and Brown, 1996b).

We produced a mutant containing amino acid changes at E1-392 and E2-341 (E1-392/E2-341). This mutant created two glycoprotein sequences sensitive to the enzyme furin. We found that during export to the cell surface the processing of the additional furin sites was incomplete resulting in a mixture of cleaved and uncleaved proteins. The product of this incomplete processing is seen in PAGE of filtered supernatant from infected cells (Figure 2.1). The double mutant shows the presence of E1, E2, capsid (C) and an additional band between 30 and 40 kDa. The double mutant also showed the presence of a slower migrating band with a size consistent with pE2, whereas this band is missing in the wild-type. The appearance of pE2 suggests a conformational change that may occur when E1 is cleaved and bound to pE2.

The individual mutants (E1-392 and E2-341) produced morphological variants similar to the double mutant (described below) but in numbers too low to be useful for

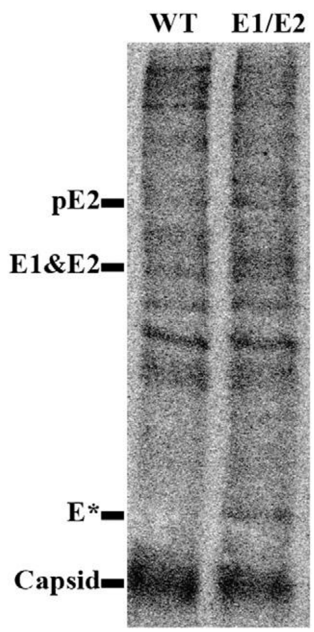

Figure 2.1: SDS-PAGE Autoradiograph of Supernatant

SDS-PAGE autoradiograph of ^{35}S metabolically labeled virus proteins from filtered supernatant of cells infected with wild-type (lane 1) and E1-392/E2-341 (lanes 2). The double furin mutant shows bands consistent with the cleaved ectodomain, labeled as E*, and pE2 . The wild-type sample does not contain the truncated E* band or pE2.

morphological studies. Since we have previously shown that the E1-E2 proteins are exported to the cell surface as a heterotrimer (Carleton and Brown, 1996a), the double mutant was chosen for this study to increase the probability that a trimer of heterodimers might reach the cell surface with one or more furin sites processed. The protocol for the production of this mutant is described in Nelson et al (Nelson et al., 2005).

Expression of furin sensitive variants in CHO RPE.40 cells, which lack the furin protease, show normal morphology suggesting that the cleavage of one or both glycoproteins is the cause of the variant morphologies (Nelson et al., 2005).

Scanning electron microscopy of furin substituted Sindbis Virus infected cells

BHK-21 cells transfected with the furin mutant illustrate the elongation of the virus particles as they mature (Figure 2.2). The tubes vary in size, but remain near the average of 73nm, consistent with normal virus particle diameter. The mock and wild-type transfected cells also exhibit membrane extensions, but these are significantly larger, 95nm in size and are consistent with microvilli produced by BHK-21 cells (Follett and Goldman, 1970; O'Neill and Follett, 1970).

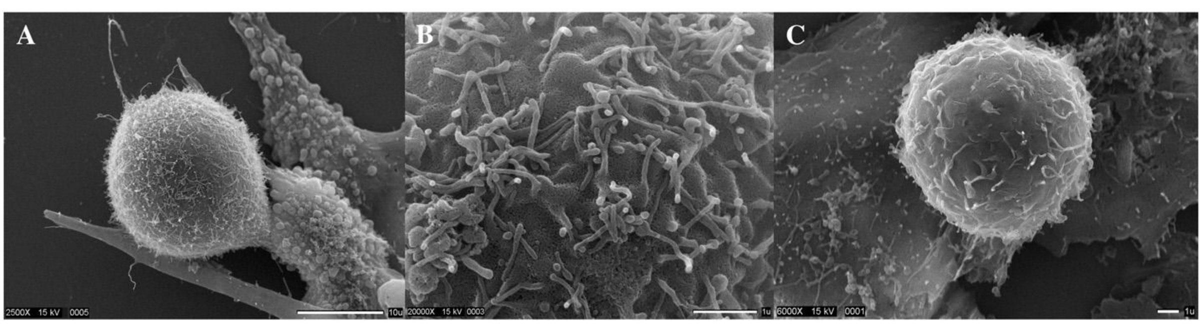

Figure 2.2: Scanning Electron Micrographs of furin mutant infected BHK-21 cells
(A), a higher magnification of an infected BHK-21 cell (B), and uninfected BHK-21 cells (C). Magnifications and measure bar values are as indicated on the images.

Thin-section electron microscopy of furin substituted Sindbis Virus maturation

Maturation of the furin mutants was unique compared to wild-type virus. Thin-section micrographs of mutant infected cells show tubular protrusions (Figure 2.3). The protrusions have electron dense material present within the tube (possibly RNA) and circular-shaped density at the end of the tubes. Some budding particles also show several distinct electron densities within the tubular structure, similar to the density seen at the enclosed end. The distinct electron densities are round in shape and have a diameter varying between 30 and 40nm that suggests these structures are capsids

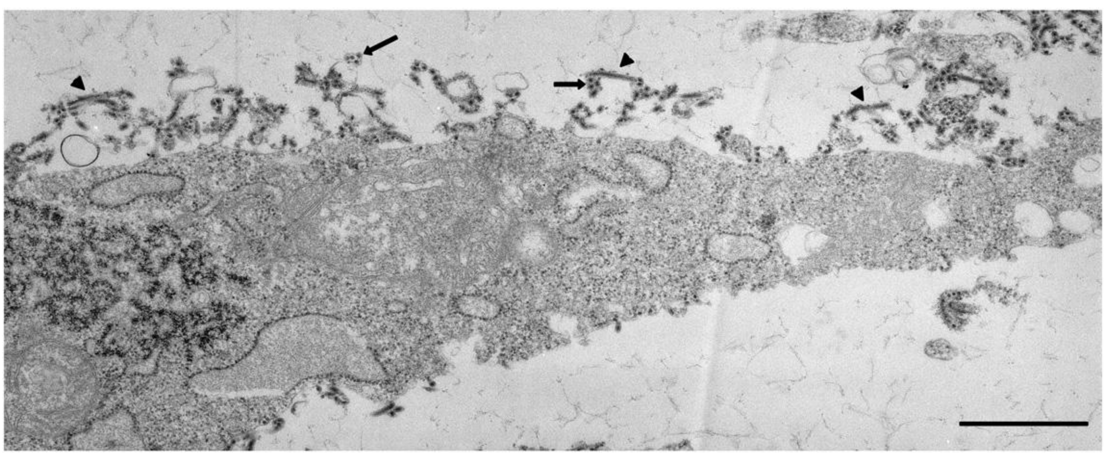

Figure 2.3: Transmission Electron Micrographs of furin mutant infected BHK-21 cells
Electron micrographs of thin sections of a BHK-21 monolayer transfected with furin sensitive double mutant E2-341/E1-392. Tubular formations can be seen budding from the cell with multiple cores (arrows) as well as undefined electron density (arrowheads).

Purification of the Furin Variants

Supernatant collected from the furin E1-392/E2-341 infected BHK-21 cells purified over potassium tartrate density gradients produced two distinct bands of particles. The upper band had a density of 1.368g/mL and electron microscopy revealed that it contained primarily wild-type-like virus structures as well as broken particles. The lower band contained primarily mutant phenotype particles (described below) and had a density of 1.374g/mL. The density difference between the two bands is equal to tartrate concentrations of 22 and 28 percent respectively. The titer of the denser band was approximately $2x10^{8}$pfu/mL, which is 4 orders of magnitude lower than the purified wild-type control, heat resistant Sindbis Virus (SVHR), with a titer of ~$2x10^{12}$pfu/mL. This infectivity is most likely from the wild-type-like particles that co-purified with the tubular variants.

Negative Contrast Staining of the Furin Variants

Electron micrographs of negative stains of the lower band show a mixture of some wild-type structures and mutant phenotype particles. The composition of these particles regarding the incorporation of cleaved and intact glycoprotein is unknown. It is possible there are cleaved proteins present in the wild-type-like particles of both bands. The position of the cleaved proteins in the three dimensional structure of the virus or the number of cleaved proteins in the incorporated trimer, however, may not alter critical protein-protein interactions enough to affect the assembly of the particle. As a result, normal budding could occur and wild-type morphology is seen although infectivity of a particular particle is not known. We found that many of the mutant particles were long structures of varying length with large, spherical structures capping one end and smaller closed spherical shapes on the opposite end (Figure 2.4). The tubular structures ranged in length from 50nm to 921nm probably reflecting a random termination of the assembly process. The smaller closed end of the tubular structure varied in size from 55nm to 100nm in diameter. The large spherical end ranged from 132nm to 293nm in diameter. The size of the small, capped end is large enough to enclose a capsid, which supports the hypothesis that budding is initiated by interaction of the capsid with the virus glycoproteins in the modified membrane and that a subsequent failure in capsid protein envelope protein interaction results in the formation of the tubes. Despite the varying particle diameters, the width of the tubular structure was consistent within each particular particle.

Some particles show a disruption in the formation of the tubular structure followed by a reinitiation of the formation of the particle in a new direction with a shift in the organization of the protein arrays (Figures 2.4D, 2.4G).

Using negative staining of purified virus and counting the number of wild-type-like particles as well as variants in a sample of the lower density band, the ratio of wild-type to variant is approximately 0.8. This would account for the infectivity of this fraction even if the contamination of wild-type-like particles is only 1% of the total population, assuming a titer of approximately 1×10^{12} pfu/mL for 100% wild-type.

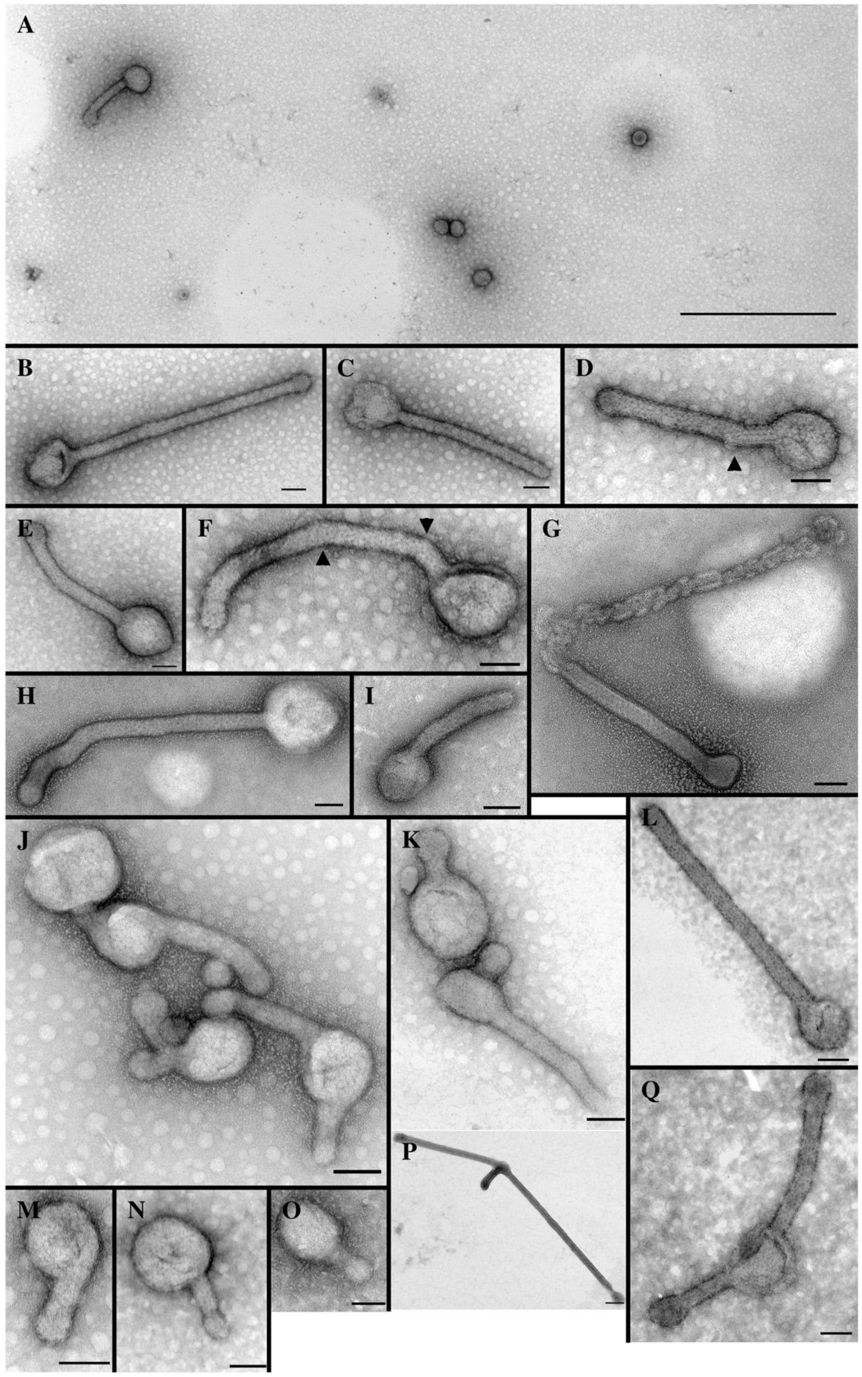

Figure 2.4: Electron micrographs of negatively stained furin mutants

Electron micrographs of negatively stained furin sensitive double mutant E1-392/E2-341 containing virus recovered from the supernatant of transfected BHK-21 cells. A) Low magnification of a typical sample of double mutant E1-392/E2-341. Bar, 1 µm. B-Q) Selected particles demonstrating the variations seen in one preparation of E1-392/E2-341. Arrowheads show points of helical disruption and reinitiation. (see text for explanation. Bars, 100nm.

Organization of virus glycoproteins in the tubular morphological variants

Some of the negative stained particles exhibited a definite regularity to the organization of the glycoproteins on the surface of the tube. Of the particles suggesting an organizational pattern, a few were detailed enough to display full 6-fold rotational arrays (Figure 2.5). To determine the structure of the tubular particles, a technique similar to the Markham rotation technique (Markham, Frey, and Hills, 1963), which is used to determine 5-

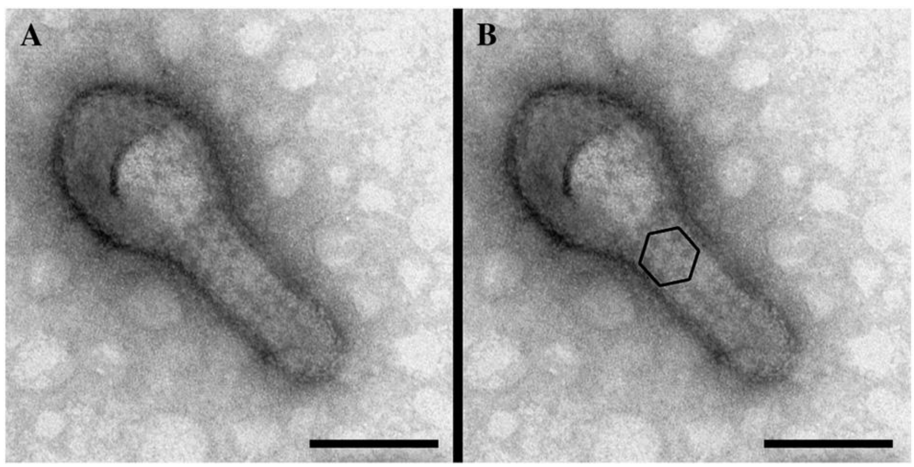

Figure 2.5: Negative Stain of furin double mutant
Electron micrograph of a negatively stained furin double mutant E1-392/E2-341. A) A normal E1-392/E2-341 particle that shows surface detail. B) The same particle (A) highlighting a hexagonal array clearly visible on the tubular structure. Bars, 100nm.

fold and 6-fold rotational symmetry, was used to determine repeating patterns present in the length of the tubular structure. The principle is the same, but instead of rotational superposition, linear translational superposition was used. We applied this technique to tubular structures with discernable structure. We measured the distances required to produce optical reinforcement in the image and the pattern of distance repeat are presented in Table

2.1. The helical angle was determined to be 30 degrees. Measurements of glycoprotein distances on a cryoEM-reconstruction of wild-type Sindbis virus were taken to determine the relevance of the patterns. The repeats were determined to be equivalent to the distance between the center of two opposite trimers in a six fold rotational array of trimers and the diameter of the 6-fold rotational array itself producing repeat lengths of 16nm and 20nm respectively. From the data collected, a model using only 6-fold rotational arrays of protein trimers taken from a cryoEM-reconstruction was created by hand to illustrate the possible organization of glycoproteins on the surface of the tubes (Figure 2.6). The 6-fold arrays were organized to maintain unskewed symmetry and incorporate the 30 degree pitch seen in the negative stains.

Table 2.1: Digital transition reinforcements

Translation of Negative (mm)	Translation of particle (nm)	Distance between reinforcements (nm)
0.6	20	20
1.1	36.67	16.67
1.7	56.67	20
2.2	73.33	16.67
2.8	93.33	20
3.3	110	16.67

The 2-dimensional model demonstrates how a primitive plane containing 6-fold rotational arrays using morphological subunits from an enveloped icosahedral virus can create helical-like particles. The model (Figure 2.6) has the same pitch as the tubular structures and resolves the repeating pattern as indicated, seen in the digital transition overlay

(Table 2.1). Matching the optical reinforcement spacing to the spacing of spike trimers in wild-type virus particle was important because it showed that the distances were relevant to the SV particles and their interactions are probably similar. It also demonstrated that the associations among the 6-fold rotational arrays are the only interactions needed for the assembly of the helical structure as no other measurement on the virus particle correlates with the distances determined from the transitional overlay (Figure 2.6 insert). Interestingly, the 16nm repeat was previously seen in 1978 on a primitive plane produced by association of solubilized virus spikes (VonBonsdorff and Harrison, 1978).

Discussion

The production and characterization of multiple morphological variants in SV illustrate protein-protein interactions that are critical for virus assembly. Previous studies using SV show that capsid-E2 interactions are responsible and required for proper assembly (Hernandez et al., 2000). Additionally, mutations in capsid where the putative binding site for the E2-tail create aberrant particles that suggest alternative budding patterns suggesting that the capsid drives the formation of the icosahedral particle (Ferreira et al., 2003b). Alterations that make the capsid more pliable result in the ability to alter the capsid-capsid protein interactions to accommodate the formation of nucleocapsids with larger T sizes in the same P class (Ferreira et al., 2003b). These results underscored the role of protein-protein interactions within the developing capsid in virus assembly.

The assembly of these morphological variants is likely the result of the incorporation of cleaved E1 and/or E2 proteins into the developing particles as envelopment proceeds. The

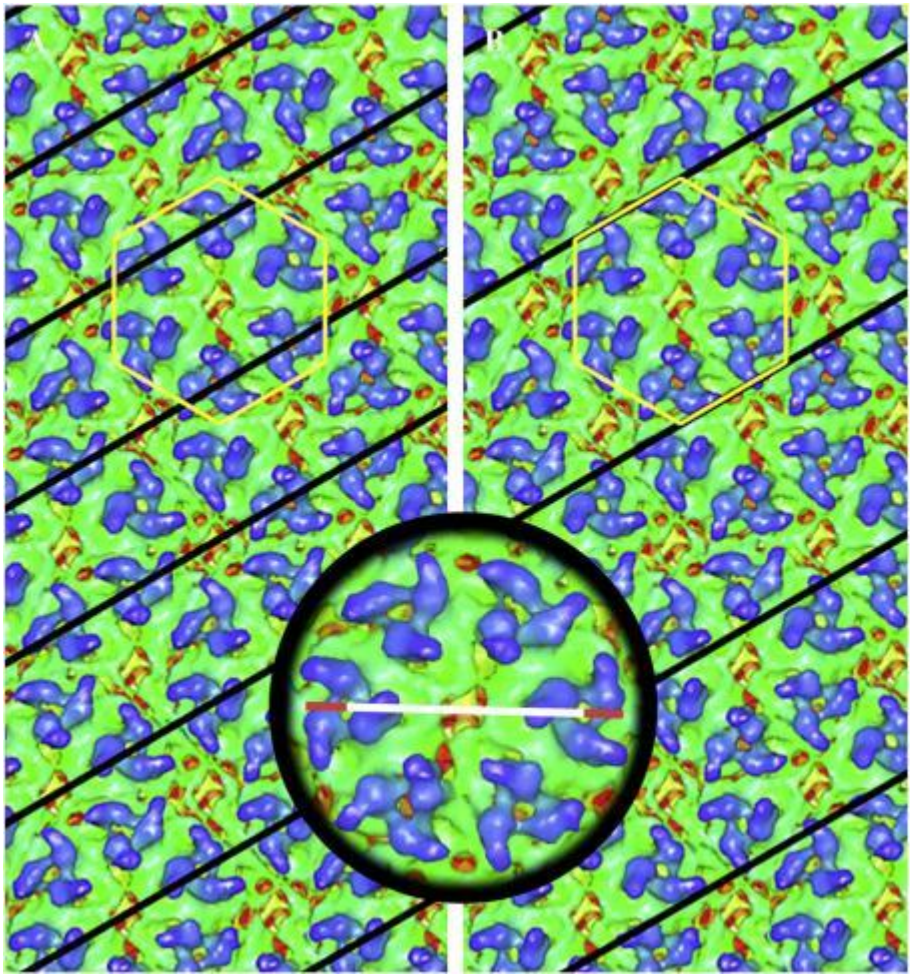

Figure 2.6: Reconstruction of tubular section of furin double mutant

Helical reconstruction of the tubular section of the furin sensitive E1-392/E2-341 created by 6-fold rotational arrays (highlighted). Black lines illustrate the 16nm repeat (A) and the 20nm repeat (B) registers seen on the tubular section of the mutants. Illustrations are drawn to scale with the average width of the tubular structures. The insert illustrates the distances taken from a cryo-electron microscopy reconstruction of wild type Sindbis virus. Measuring across a strict 2-fold axis of a hexagonal array white is 16nm and white with red is 20nm.

cleaved envelope proteins may perturb the interaction between the capsid and the glycoproteins after initiation and result in a failure to close fully around the capsid; transitioning from icosahedral geometry to the tubular structures of the mutant particles. One possible scenario that may result in the transition is that the cleaved glycoprotein trimer is mis-configured such that the E2 endodomain cannot properly interact with the capsid. It is also possible that the mutant glycoproteins can interact with the capsid but cannot interact with each other on the surface of the developing particle. With a loss of correct interaction with the capsid, which serves as scaffold for organization of the outer protein shell (Ferreira et al., 2003b), the glycoproteins are no longer able to form the 5-fold rotational arrays that are essential for the completion of an icosahedral structure. The only structure the glycoproteins can form without interaction with the capsid is a primitive plane of 6-fold rotational arrays. Therefore the virus tubes may form from the initial formation of the icosahedron that produces a regular interaction of the glycoprotein trimers followed by additional trimers forming a long tubular structure. The tube formation continues uninterrupted, unlike that seen in helical viruses such as tobacco mosaic virus, due to the lack of regulation of the length of the helix by the length of the genome. This supports the theory that the envelopment of SV is driven by capsid-glycoprotein interactions.

Uninterrupted growth of the tubular structure may slow the release of particles from the cell as indicated by a significant number of tubular particles still present on the cell surface as seen by scanning electron microscopy and thin-sections. Negative stains of the released virus particles support the hypothesis that the particles are released from the cell by mechanical agitation and are ripped from the cell with an attached fragment of the cell membrane. This is consistent with the observations using scanning electron microscopy and thin-sections.

Additionally, the size of the particles is large enough to encompass multiple cores, indicating that particles may contain multiple cores as well as more distributed RNA and capsid protein. This is supported by the thin-sectioning of infected cells, showing multiple capsid-like densities in a single protrusion. While the exact ratio of protein and RNA in the mutant particles is unknown, the difference in the densities between the wild-type-like particles and the mutants indicate that there may be additional RNA in the mutants. The difference in densities may also be an inherent result of the tubular particle structure. These particles are denser by accommodating more protein contained in more closely knit glycoproteins due to entropic forces creating the smallest size helix. The cylindrical shape also has a smaller surface to volume ratio, which would mean the amount of membrane present in the particle is less than that present in the spherical particles, increasing the relative amount of RNA and protein. The actual protein and RNA content will need to be further investigated to determine the specific effects that create the density change from wild-type particles.

The furin containing variants presented in this study indicate the importance of glycoprotein-glycoprotein on top of glycoprotein-capsid interactions in the formation of mature SV particles. Negative staining shows disorder in some of the tubular particles away from the putative initiation site and suggest that the loss of correct association may be between the glycoproteins on the virus surface. The incorporation of multiple copies of cleaved proteins disrupting the normal assembly of the particle can explain this partial loss of interaction between glycoproteins, creating the unstructured and flexible joints. Once formed, however, the tube continues to form normally as glycoprotein trimers having wild type properties are incorporated into the helix. This suggests formation of the tube is driven by lateral associations between the glycoproteins and that the glycoprotein interactions have a larger role in virus budding than originally anticipated.

The biochemical analysis of the proteins present in the virus particles and in the infected cells shows a few notable features that are unique to the furin mutants, especially E1-392/E2-341. The introduction of the furin recognition sequences alter the cleavage pattern of the glycoproteins. pE2 is present in the mutant particles and cleaved E is present at a molecular weight consistent with the ectodomain of one of the glycoproteins. These changes are likely due to an interaction between E1 and E2 that inhibits E2 cleavage by the furin protease at the endogenous recognition sequence, resulting in pE2 incorporation by the virus. We have shown that pE2 cleavage is not required for successful maturation of SV (Presely and Brown, 1989).

We did not see the incorporation of cleaved products into mature virions. This may result from the possibility that the cleaved ectodomains of the membrane proteins are released and do not co-purify with the virus. In this case, the remaining membrane associated domains may not be resolved on these gels. It is also possible that the incorporation of cleaved E1 and E2 into the mature virions is in numbers too small to be detected in this assay.

Other non-enveloped viruses having icosahedra geometry, such as polyoma and T4 have been shown to create helical-like particles (Finch and Klug, 1965; Klug and Finch, 1965; Onorato, Stirmer, and Showe, 1978; Showe and Onorato, 1978). T4 ‘polyheads’ have a similar elongated structure and tend to have multiple shells within each particle. T4 particles have a complicated host cell membrane-associated step-wise assembly process that assembles the capsid shell and inserts the genome into the head near the end of the assembly process. The data from the T4 polyheads suggest that the growth of these particles is a result of a loss of interaction between gp23 and gp24, the distal vertex protein (Onorato, Stirmer, and Showe, 1978). It is suggested that this loss allows the continued assembly of the core with the shell to create the elongated structure. The uniqueness of the SV tubular particles, when compared to the polyheads and giantheads of T4 is due to the fact that they are not required to have growth of both the core (capsid) and the shell (E1 and E2) to elongate the particle because the capsid is preformed prior to interaction with the glycoprotein modified membrane. Polyoma virus also assembles tubular structures, which have been shown to be made of paired pentamers in a P2 pentamer tessellation (Kiselev and Klug, 1969). These structures are particularly interesting because original observations presumed that the larger particles contained hexamers and the smaller particles contained only pentamers. The tubular particles of SV proteins presented in this study, while similar in overall morphology, have enough identifiable features to rule out the incorporation of pentamers into these structures. Other non-enveloped icosahedral viruses which have been shown to assemble tubular particles either within or secreted from the cell include Tribec, Blue Tongue, and Infectious Bursal Disease (Harkness et al., 1975; Murphy et al., 1971; Oellermann, Els, and Erasmus, 1970). The tubular structures described here for SV are unique in that they demonstrate such an assembly event in a strict T=4 membrane containing virus and add evidence that SV behaves unlike traditional membrane containing viruses.

With the production of this tubular virus variant, the third piece of Caspar and Klug's prediction is satisfied in a membrane containing virus system. Firstly, the aggregation of virus proteins into hexagonal arrays producing a two dimensional primitive plane was demonstrated using Sindbis virus glycoproteins (VonBonsdorff and Harrison, 1978). Next, the icosahedral Sindbis virus, known to assemble by envelopment in a membrane that is a primitive plane, was shown to produce families of icosahedra following specific classes of symmetry (Ferreira et al., 2003b). Finally, helical-like virus structures containing Sindbis virus proteins have been shown to be a result of interactions that are made in the same manner as a primitive plane is created (this study), (VonBonsdorff and Harrison, 1978).

CHAPTER 3

Alphavirus adsorption to mosquito cells as viewed by freeze fracture immunolabeling

Joseph P. Kononchik Jr. Ricardo Vancini and Dennis T. Brown

Submitted to:

Virology. 2010 Dec 15

Summary

Sindbis Virus (SV), the prototype alphavirus in the family togaviridae, infects both mammalian and insect cells. The ability of SV to infect cells possessing significantly different biochemical environments suggests there may be a common mode of entry into each cell type. Previous studies have shown that up to 4 hours post infection cells are permeable to ions and small molecules suggesting that the plasma membrane is compromised as infection takes place. Thin-section electron microscopy has also shown SV to bind to the plasma membrane and lose its electron dense core through a pore like structure developed upon interaction of the virus with the cell surface. Using freeze-fracture replicas, thin-sections and antibody labeling the data presented here show virus associated with intramembrane particles of mosquito cells. These data suggest that the intramembrane particles associated with SV may be part of a pore structure consisting of virus proteins and cell receptor(s). At the end of the chapter is a gallery of cell structures that are observed using freeze-fracture.

Introduction

The structure and function of Sindbis Virus (SV) has been studied extensively. Currently, there is a cryo-reconstruction of the virus showing the T=4 organization of the outer glycoprotein shell, and its tight interaction with the inner capsid protein shell that surrounds the RNA core (Paredes et al., 1993). Two glycoproteins, E1 and E2, make up the outer protein shell. The inner shell is made of only capsid (C) protein and the geometry of the inner shell determines the structure of the mature infectious virus particle (Ferreira et al., 2003a). E1, E2 and C are present in the mature virus particle in a 1:1:1 stoichiometric ratio. The lipid contained in SV is derived from the host plasma membrane (Hafer et al., 2009). SV envelopment occurs as the nucleocapsid associates with the trimers of heterodimers of glycoproteins E1 & E2 at the cell surface and organizes the membrane associated glycoproteins around the nucleocapsid incorporating the host membrane into the mature virion.

Virus entry into animal cells is proposed to occur by three possible mechanisms. In one model the virion is taken up by endocytosis and subsequent acidification of the endosome results in fusion of the virus membrane with the cell membrane releasing the virus genome into the cell cytoplasm (Lakadamyali, Rust, and Zhuang, 2004; Pelkmans and Helenius, 2003; Perez and Carrasco, 1994; Sieczkarski and Whittaker, 2002). In a second mechanism fusion occurs at the cell surface facilitated by interaction with a cell receptor (Akhtar and Shukla, 2009; Lehmann et al., 2005; Melikyan, 2008). A third mechanism proposes that the virus genome is delivered through a pore in the cell membrane created by virus and cellular proteins (Belnap et al., 2000; Hogle, 2002; Ivanovic et al., 2008; Paredes et al., 2004). There is evidence that supports an endocytosis pathway for the entry of alphaviruses (DeTulleo and Kirchhausen, 1998; Kielian and Jungerwirth, 1990; Kielian, Marsh, and Helenius, 1986) and evidence that supports an alternative mechanism which does not invoke endocytosis or exposure to an acidic environment.(Edwards and Brown, 1991;

Paredes et al., 2004; Wang et al., 2007). This latter model is supported by direct observation of virus-cell interaction by electron microscopy (Paredes et al., 2004).

Alphaviruses have been shown to infect cells in culture that come from a variety of insect and vertebrate sources. The identity of SV receptor(s) remains elusive despite many claims of identification. These include the major histocompatibility receptor (Helenius et al., 1978; Maassen and Terhorst, 1981; Oldstone et al., 1980) the major laminin receptor (Wang et al., 1992), DC sign L sign (Klimstra et al., 2003), heparan sulfate (Klimstra, Ryman, and Johnston, 1998), the Heat Shock 70 protein (Ren et al., 2007) and an unidentified 110kDa nerve cell associated protein (Ubol and Griffin, 1991). It is possible that the virus associates non-specifically with various proteins before finding and binding to its specific receptor or receptor complex.

On the assumption that the alphaviruses might employ a common receptor for entry into all cell types, we have examined the role that V-type H^+-ATPase (V-ATPase), a ubiquitous cell surface protein, may play in virus infection. Bafilomycin A1 has been shown to inhibit the activity of V-ATPase in both insect and vertebrate cells at nanomolar concentrations (Bowman et al., 2006; Hanada et al., 1990; Wang, Inoue, and Forgac, 2005; Wieczorek et al., 1991). We have recently shown that this drug does not prevent the passage of virus RNA from the virus into the cell cytoplasm (Hunt, Hernandez, and Brown, 2011a). This does not rule out the possibility that V-ATPase is part of the receptor complex. Based on the recent data collected on the binding of $BafA_1$ and similar inhibitors, the inactivation of the V-ATPase does not suggest that it would interfere with virus protein interaction since the target of $BafA_1$ is the V_0 subunit in the membrane and no gross conformational change seems to occur upon binding (Huss and Wieczorek, 2009). Previous methods that analyze the successful entry of alphaviruses into cells in the presence of inhibitors of endocytosis or endosome acidification were based on secondary reporters. These reporters either determined infection had occurred by synthesis of viral RNA, virus protein synthesis or virus production (DeTulleo and Kirchhausen, 1998; Glomb-Reinmund and Kielian, 1998; Kielian et al., 1984; Perez and Carrasco, 1994). The problem with these assays is the number of steps between the attachment of the virus and RNA, protein or virus production. Each step in the establishment of infection had the potential to be inhibited, and as a result, the assay could report a false negative for infection. It has also been shown that some of these inhibitors have secondary effects on the infection process unrelated to penetration (Hernandez, Luo, and Brown, 2001; Hunt, Hernandez, and Brown, 2011a). Even more important, some of the techniques used previously did not differentiate between infection and internalization of noninfectious particles. This problem of relative infectivity of virus employed in such studies has been overcome by the production of virus preparations having a particle to plaque forming unit (PFU) of near unity (Hernandez et al., 2003; Paredes et al., 2004).

Because of its ability to examine the morphology of cell membranes, freeze-fracture of cells with adsorbed SV may help dissect the interaction between the cell proteins and viral proteins in the initial steps of binding and infection. Freeze-fracture is a technique that gained popularity in the 1970's because of its ability to reveal the structure of membrane surfaces and interiors (see page 78 for a gallery of cellular structures). Since its inception (Steere, 1957; Steere, 1989), the use of freeze-fracture in virology has diminished greatly, though it has continued in the analysis of lipid solutions (Gao, Quinn, and Yu, 2008), and high-order protein complexes in plasma membranes (Fujimoto, 1997; Nicchia et al., 2010). During the peak use of this technique numerous viruses were examined by freeze-fracture both in a purified form and in cell culture; these viruses include tobacco mosaic virus (TMV), poxvirus and others (Brown and Riedel, 1977; Steere, 1989).

Freeze fracture has been successfully used to study the organization of proteins in the capsid of SV and bacteriophages (Brown, Waite, and Pfefferkorn, 1972a; Brown et al., 1975; Lundstrom et al., 1979). It has also been used to study the envelopment of SV, mouse mammary tumor virus (MTV), Herpes Simplex Virus (HSV), vesicular stomatitis virus (VSV) and other membrane containing viruses (Brown and Riedel, 1977; Gliedman, Smith, and Brown, 1975; Hung et al., 1980; Torrisi et al., 1992; Wild et al., 2009). Alphavirus capsid conformations and envelopment processes were also successfully examined by freeze-fracture (Brown, Waite, and Pfefferkorn, 1972b; Gliedman, Smith, and Brown, 1975; Torrisi and Bonatti, 1985; Waite, Brown, and Pfefferkorn, 1972). With the introduction of colloidal gold cytochemistry in the early 1980's, attempts at combining gold labeling and freeze fracture replication were made to bestow compositional information onto the structural information of the replica. Since then, many freeze-fracture techniques have taken advantage of gold labeling. One of the most successful techniques is FRIL, or freeze-fracture replica immunolabeling, which uses a detergent, typically SDS, to remove most of the biological sample from the replica leaving only the leaflet and the proteins attached to the replica or cross-linked to membrane lipids/proteins free for labeling (Fujimoto, 1995; Fujimoto, 1997).

These advancements in cytochemical labeling give freeze-fracture a new role in the identification of cell membrane components by electron microscopy. For a review of current cytochemical techniques in freeze-fracture electron microscopy see (Severs and Robenek, 2008).

In this study we have used the freeze fracture technique together with immunolabeling to examine the interaction of SV with cell membranes and to determine association of the virus with any interior membrane structures. The V-ATPase which is ubiquitous in cell plasma membranes has a morphology described by freeze-fracture (Ratajczak, 2000). If SV associates with this protein complex it should be visualized by this procedure. We have also found a way to purify the HR strain of Sindbis Virus such that it particle to PFU ratio is near unity (Hernandez et al., 2003). This makes studies involving direct morphological observation of virus cell interaction such as we have published previously (Paredes et al., 2004) meaningful.

Results

Freeze-fracture immunolabeling (FRIL)

Freeze-fracture immunolabeling consists of five steps: 1) Rapid freezing of the sample 2) Fracturing of the sample at near liquid nitrogen temperatures 3) Replicating the fractured surface with Pt/C shadowing and carbon support 4) Cleaning the organic material (contaminant) with a detergent, usually SDS 5) Labeling the remaining material that is attached to the replica with antigen specific antibodies. Rapid freezing of the specimen is

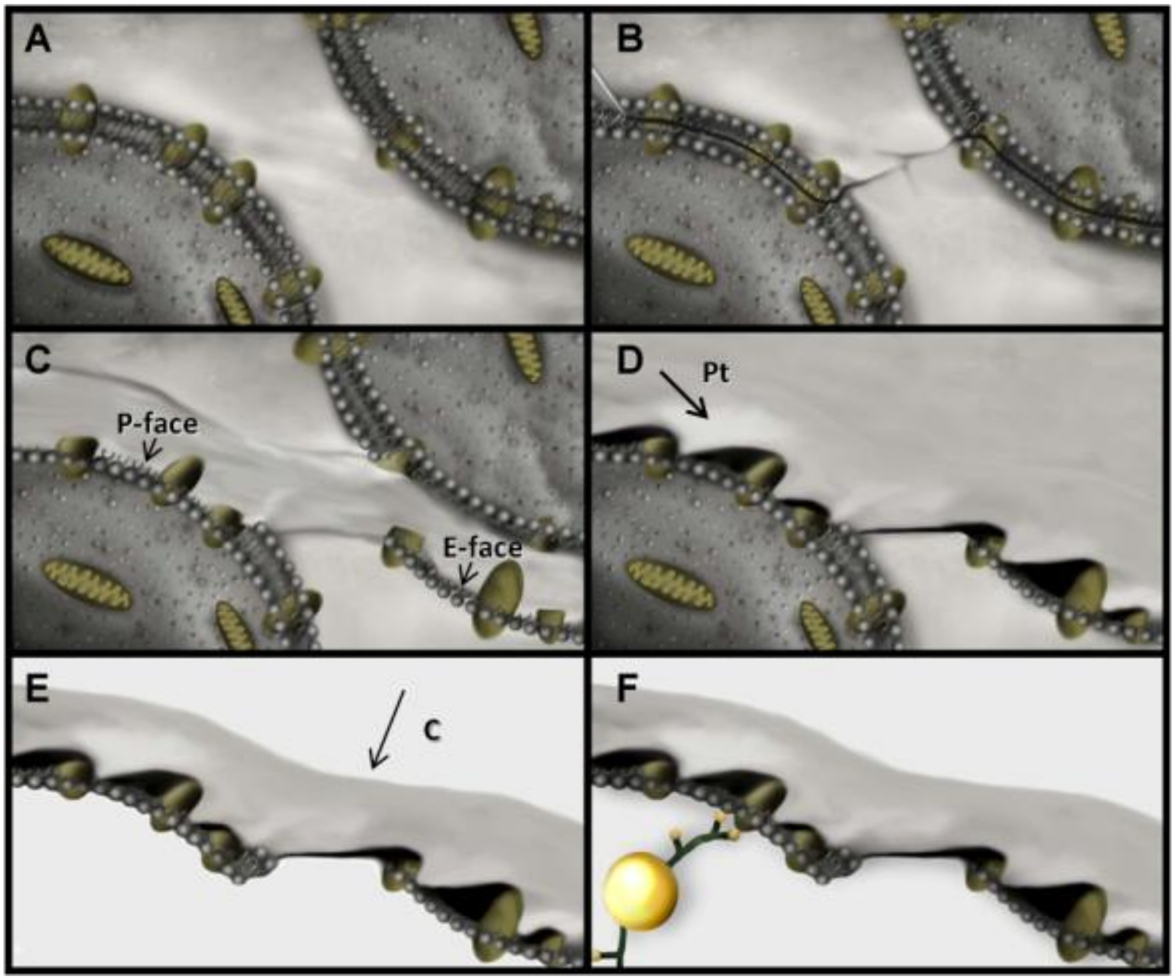

Figure 3.1: Schematic illustration of the freeze-fracture immune-labeling technique

Cell suspension samples are frozen (a) and fractured by hitting them with a cold microtome knife (b). The fracturing exposes the fracture faces E and P for the extracellular leaflet and cytosolic leaflet respectively (c). Replicas are created by shadowing a small amount of Pt/C (1nm) (arrow) on the surface of the fractured surface at 45° and supporting the shadow with a relatively thick layer of carbon (12-15nm) (arrow in E) (d). The resulting replica is cleaned gently with SDS to remove all of the cellular components except for those immediately attached to the replica (e). Molecules still attached can be labeled with antibodies conjugated to colloidal gold beads (f). These gold beads are clearly seen against the replica and can describe the composition of structures seen with the replica.

necessary to prevent ice crystal formation (vitrification) (Figure 3.1A). The addition of a cryoprotectant, usually glycerol, can be used if initial freezing seems too slow and alternative freezing methods are unavailable. Fracturing the sample results in a fracture plane that follows a path of least resistance through the frozen cells; this tends to be the center of lipid bilayers as these are free of water (Figure 3.1B). The splitting of the lipid bilayer results in two faces, the extracellular, or E-face and the periplasmic or cytoplasmic face called the P-face (Figure 3.1C). The resulting faces are shadowed with 1-2nm of Pt/C at an angle near 45° and then the metal shadow (figure 3.1D) is supported by a layer of carbon 12-15nm thick (Figure 3.1E). To avoid artificial changes of intramembrane particle (IMP) measurements due to different amounts of Pt/C deposited, the same amount of Pt/C was deposited onto each sample (~1.1nm). Once replicated, the sample can be brought to room temperature and cleaned to remove the biological material, which is now a contaminant on the replica (Figure 3.1E). Once cleaned sufficiently, the exposed antigens that are bound to the replica can be labeled and resolved in an electron microscope with antibody conjugated to colloidal gold beads (Figure 3.1F). The resulting replica contains both structural and compositional information. In this study the observed face is identified by curvature, where concave is the E-face and convex is the P-face. The size and distribution of IMPs also identifies the face observed. For the P-face, there are significantly more small IMPs, ~610/μm^2 vs 150/μm^2 on the E-face. The P-face also has fewer large IMPs (~65/um^2 vs 260/um^2) as seen in Figure 3.2C. The E-face has the opposite features, where there are more large IMPs and fewer to no small IMPs (Figure 3.2D). Small IMPs are any that are <8nm in width, whereas large IMPs are any ≥8nm. This cut-off was determined by examining the segregation of IMPs to each face and determining the size of IMPs that were primarily on the E-face.

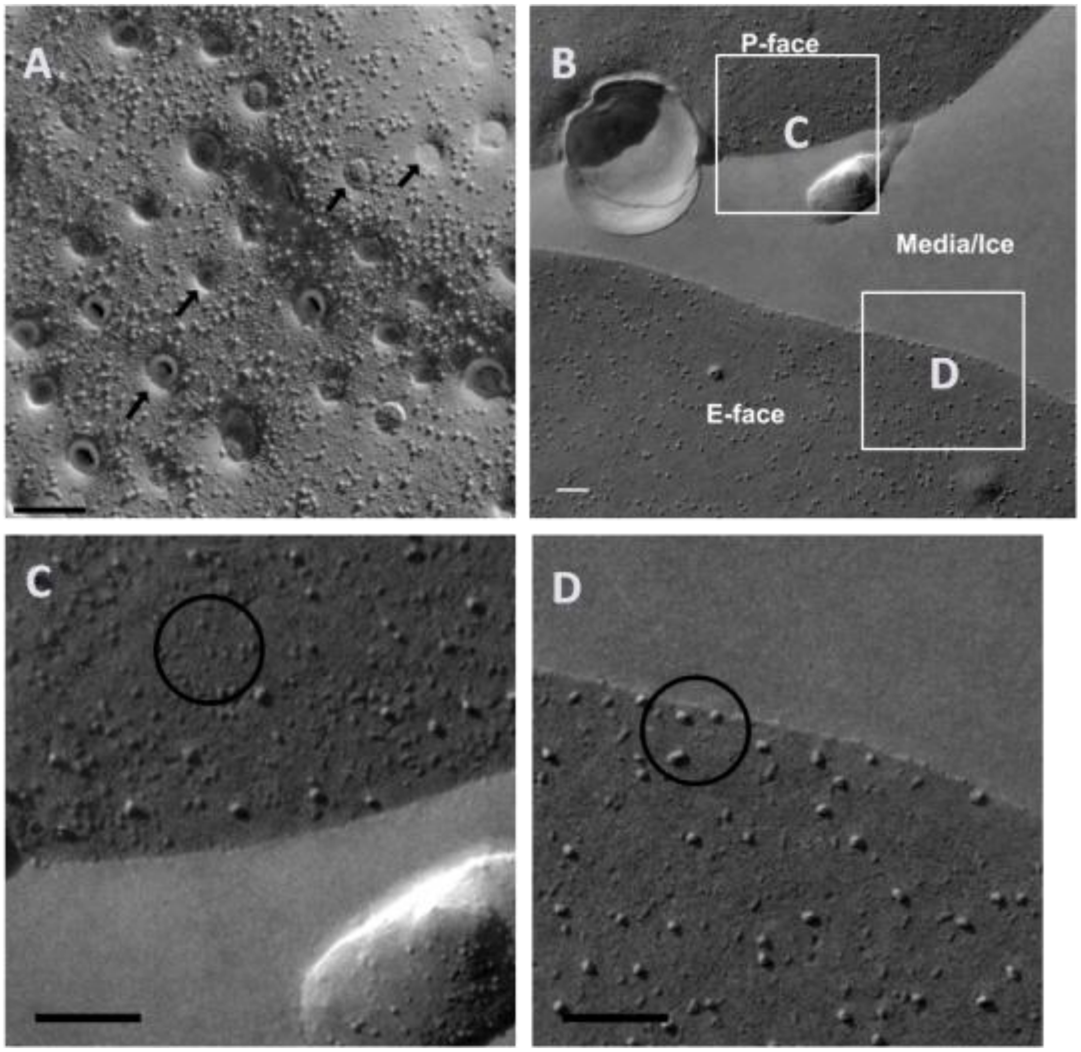

Figure 3.2: Freeze fracture replica of mammalian and insect cell plasma membranes
(A) Mammalian cell replicas show large numbers of caveolae (arrows) when treated with gluteraldehyde and glycerin. (B) The insect cell membranes are free of caveolae, smooth and show curvature. (C & D) Replicas of mosquito cells show segregation of small IMPs to the P-face, while only larger IMPs were seen on the E-face. See text for distribution and quantification of IMP. Magnification bars are 100nm.

Electron microscopy of mosquito cell-virus complexes

In this study, we used mosquito cells that grow in suspension. The benefit of suspension cells include; simple dilution of cells to increase the MOI; easy fixation and removal of biological contaminants without cross-linking neighboring cells, as occurs in a monolayer; recovery of cells without scraping or using lifting buffers that might interfere with virus-cell interactions; smaller diameter and thus greater curvature for easier recognition of E- and P-faces; and finally an even distribution of virus particles across the entire plasma membrane. Initial attempts to analyze mammalian cells for virus structure were not fruitful due to the monolayer cross-linking issue and the complexity of the cell membrane compared to mosquito cells. Mammalian cell membranes, when fixed in gluteraldehyde, create a significant number of caveolae that occlude and distort any structural information at the surface (Figure 3.2A) (McGuire and Twietmeyer, 1983). The artificially created caveolae are nearly the same size as virus particles and as a result add an additional level of complexity to the membrane morphology that is undesirable. Cholesterol is the primary component of these caveolae (Parat, 2009; Sharma, Yu, and Bernatchez, 2010) and therefore moving to a naturally cholesterol deficient cell line (Hafer et al., 2009) eliminates the artificial structures created during the necessary fixing and glycerinating processes.

We have previously shown by thin section analysis that at 4 C only 4-6% of attached particles lost their RNA core indicating that entry had taken place while at room temperature 26-30% became empty. (Paredes et al., 2004) Thus incubation of samples at 4C and room temperature allow us to examine virus adsorption with and without endocytosis (Wang et al., 2007) and controlling the amount of virus that penetrate the cell membrane. Comparing the room temperature and low temperature conditions may allow us to determine changes in structure related to loss of RNA during entry.

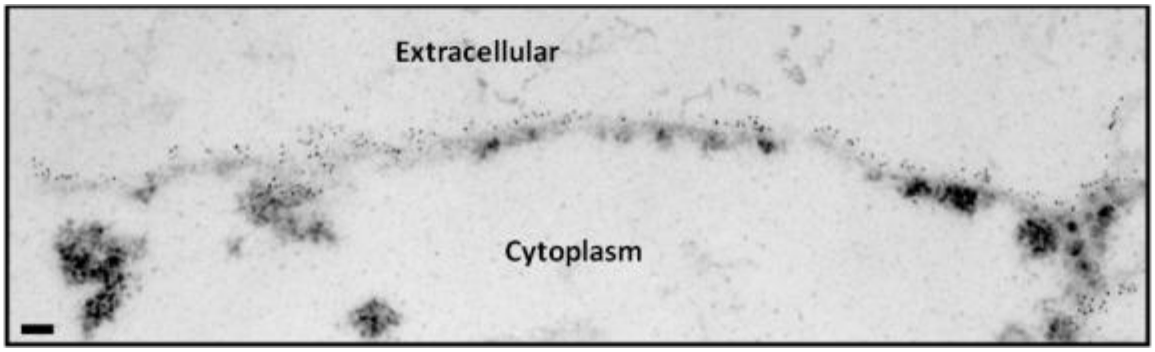

Figure 3.3: Thin-section of SV fused to BHK cells by exposure to low pH environment. Baby hamster kidney cells with adsorbed virus at pH 7.4, exposed to pH 5.3, returned to pH 7.4 and labeled with antibody with bound colloidal gold beads. The gold beads are distributed uniformly on the cell surface indicating that fusion has taken place. Antibody is rabbit anti-whole virus, as used in (Paredes et al., 2004). Magnification bar is 100nm.

Freeze-fracture replica labeling of SV

Replicas of uninfected cells did not bind virus antibody (data not shown). Samples without primary antibody were negative for secondary labeling. Labeling of cells with attached virus was primarily limited to discrete locations on the cell surface (Figure 3.4A-D) suggesting fusion has not occurred, as labeling would be distributed across the membrane as described previously (Paredes et al., 2004) and in Figure 3.3. U4.4 cells that had adsorbed virus at 4C were positive for virus proteins on the extracellular side of the E-face of the plasma membrane (Figures 3.4A-D). Replicas from samples adsorbed with SV at room temperature (Figures 3.4A and 3.4B) also had labeling of virus proteins on the E-face similar to the labeled virus proteins in the low temperature samples (Figures 3.4C and 3.4D). The gold conjugated antibodies were organized in circles outlining the shape of the attached virion. Many were seen to have an intramembrane particle in the center of the circle (figure 3.4D). These outlined virus particles show adsorbed virus on the membrane that is cross-linked to its receptor.

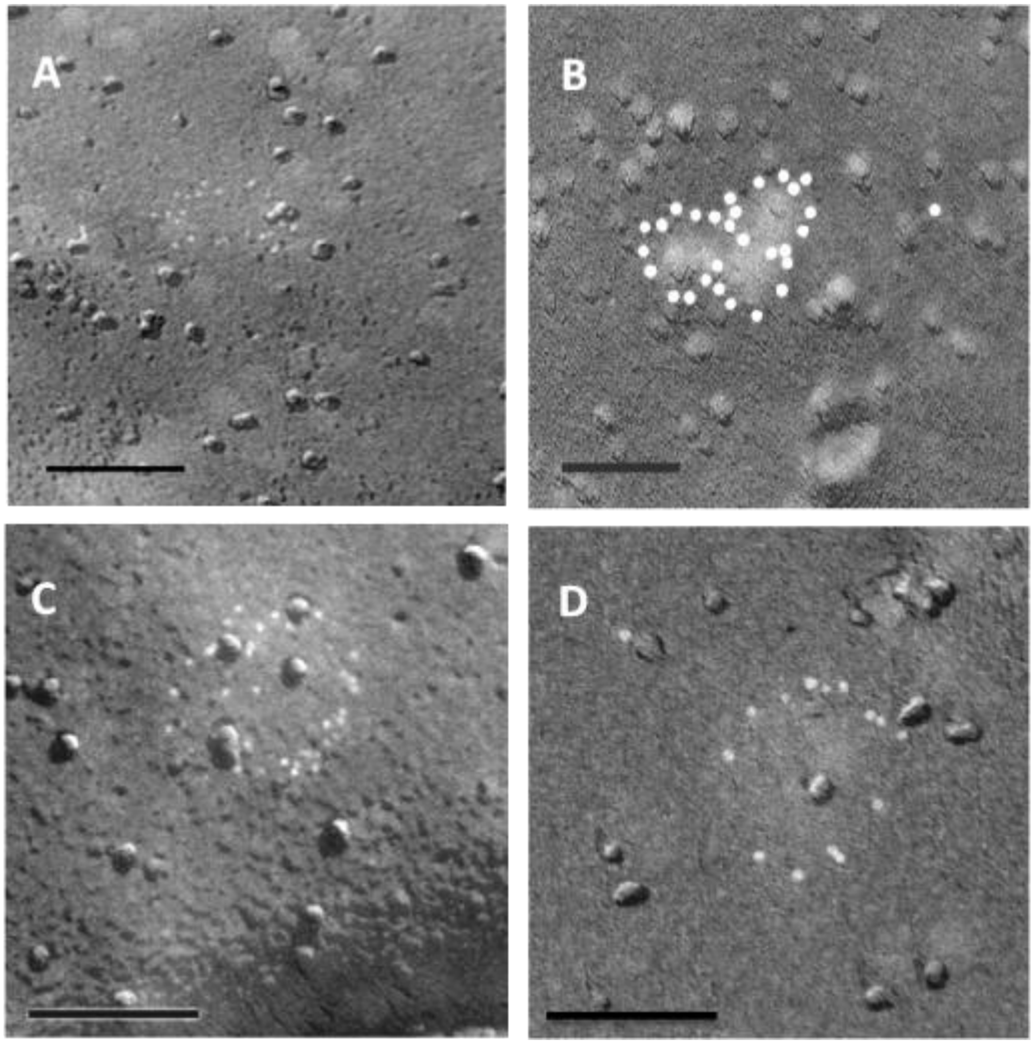

Figure 3.4: Freeze fracture replicas of insect plasma membranes with attached virus.
(A & B). SV adsorbed onto mosquito cells at room temperature labeled with 6 and 12nm colloidal gold beads against SV proteins respectively. (C & D) Replicas of SV adsorbed onto mosquito cells at 4C labeled with 6nm colloidal gold beads. Many virus particles are associated with the intramembrane particles. All magnification bars are 100nm and all panels are E-face replicas.

Non-specific interactions were easily determined using stereo pairs to examine the face on which the labeling occurred (Figure 3.5). With stereo images, the side on which the labeling occurs can be determined. Since the replica covers any antigenic sites on one side of the replica, any labeling that occurs on this side of the replica is non-specific labeling.

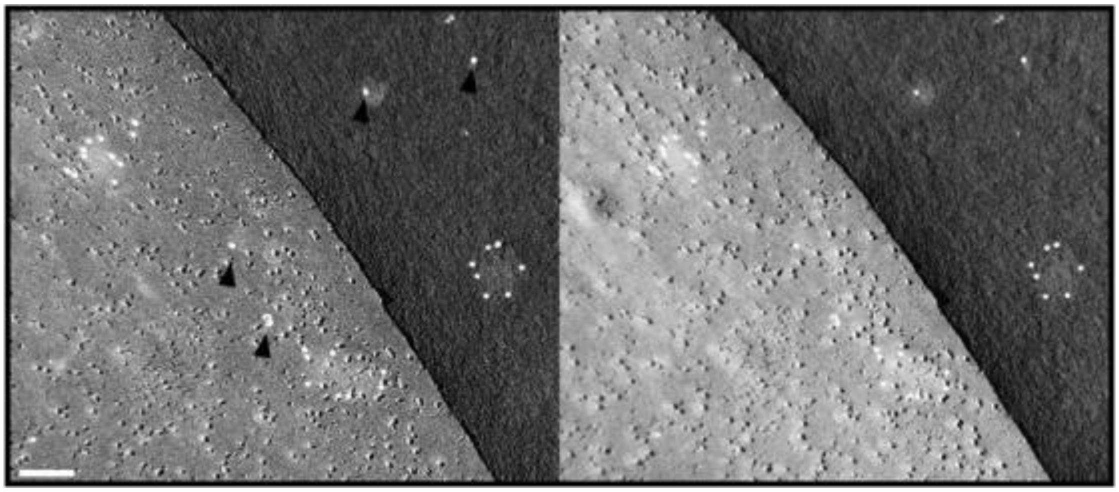

Figure 3.5: A stereo pair image of a freeze fracture replica.

The image shows non-specific binding of some antibody on the cell surface (arrows) and specific binding to a virion located away from the cell surface. Smaller groupings of antibody are fragments of particles that have injected their RNA, lost structural stability and fallen apart. Magnification bar is 100nm.

Approximately 90% of the labeled virus proteins were found near IMPs of approximately 8-10nm (Figure 3.4). Near is defined as an IMP in or on the circle of antibodies labeling SV. The number of IMPs of this size is frequent as the density of large IMPs on the E-face is ~260/μm^2. Assuming an even distribution, this result equates to roughly one IMP for every virus particle area (~3800nm^2), however the uneven distribution of the IMPs on the replica reduce the number of IMPs per virus area to less than one giving the possibility of labeling an entire virus particles outside of IMP. Virus labeling also formed chained circles suggesting multiple virus particles were clumped together before or after adsorption onto the cell (Figure 3.4B); this was seen infrequently.

The use of a high MOI ensures that the receptors on the mosquito cells have been fully saturated. However the number of virus receptors may be limited and virus that is simply "stuck" to the cell may not bind tightly enough to remain attached after the virus cell complexes are processed for the EM. Thus the fact that only a few virus particles are seen is either a testament to the specificity of the binding of the virus to its receptor, the large surface area of the suspended cells and/or a function of removing non-specific interactions by spinning and resuspending the pellet of adsorbed cells in buffer before cross-linking. The particle to pfu ratio of the virus used in this study is less than 2, suggesting that at least half of the virus particles visualized are infectious. The data presented here is therefore more likely to represent the actual infection mechanism as opposed to the noninfectious virus-cell interactions that dominate with virus preparations having higher particle/pfu ratios. The data presented here is in contrast to previous studies, where the particle/pfu ratio is high, over 100, or not calculated at all.

Freeze-fracture replica labeling of the V-type H^+-ATPase

Replicas labeled for C1 subunit of the V-ATPase had gold beads associated with IMPs that were approximately 8-10nm in diameter (Figure 3.6A). This is consistent with the cryo-reconstruction seen previously (Muench et al., 2009) as discussed below. Since the pump is ubiquitous in the cell, normal concentrations of antibody against the V-ATPase complex resulted in a high degree of labeling that obscured the structures labeled. By reducing the concentration of the antibody significantly, and extending the hours of incubation for labeling, we were able to better distinguish the IMPs that were the proton pump (Figure 3.6A). In an attempt to better visualize the association of virus with the V-ATPase we conducted an experiment in which thin sections of cells with attached Sindbis virus were labeled with goat anti V-ATPase antibody followed by anti-goat IgG conjugated to 12nm gold beads and with rabbit anti Sindbis IGG followed by anti-rabbit IgG conjugated to 6 nm gold beads. A result is shown in figure 3.6B. The labeled virus particle is associated with a place on the cell membrane that labeled with the anti V-ATPase antibody. Attempting to label the replica with both anti V-ATPase and SV antibody is impossible, as the virus

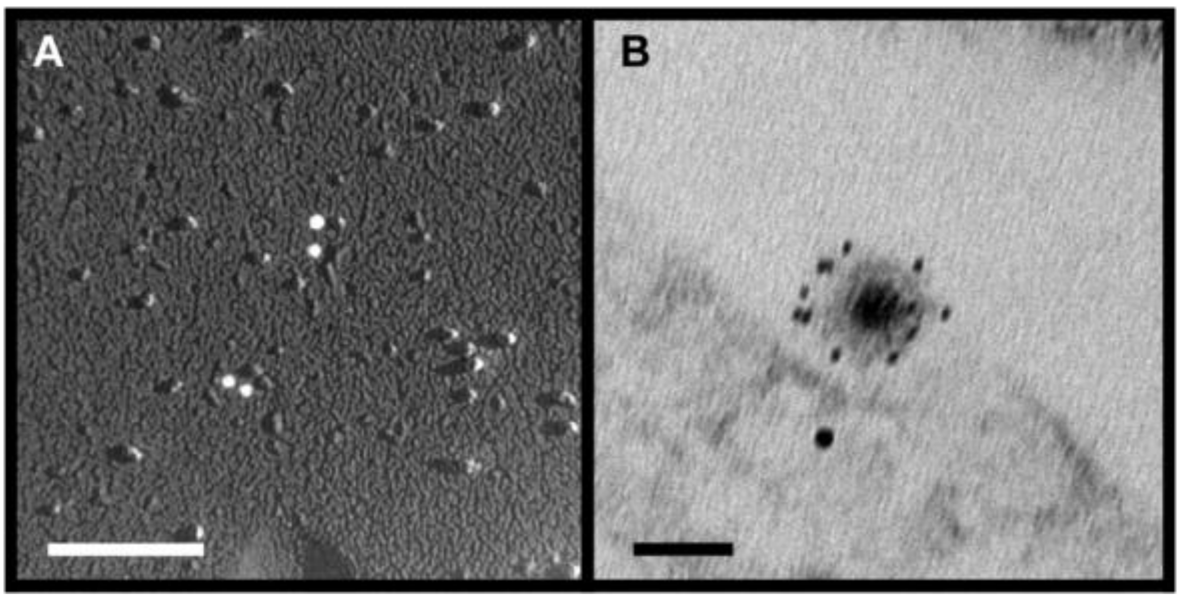

Figure 3.6: Replica and thin-section labeled for the C subunit of the V-Type ATPase
(A) Replica of uninfected mosquito cell plasma membrane labeled for the ATPase showing individual IMPs labeled as part of the V-type H^+-ATPase complex. (B)Thin-section of infected BHK cells labeled for the ATPase visualized with 12nm gold beads and for whole SV visualized with 6nm gold beads. Magnification bars are 100nm.

particle covers and protects the V-ATPase on the outside surface of the cell the shadowing and carbon support are covering the other side of the replica which resolves the IMPs. As a result, the only way to associate the two together is to use thin-sections labeling for both the V-ATPase and SV (Figure 3.6). In this experiment the virus was labeled with antibody linked to 6nm gold beads. This antibody was applied before the cells were embedded for thin sectioning and the completely accessible virus was readily coated with antibody. The V-ATPase was labeled with antibody bound to 12nm gold beads after the thin sections were made. This resulted in few double labels seen as the plane of the section only exposed the V-ATPase infrequently. We have attempted to further implicate the V-ATPase as the receptor by blocking attachment with antibody. This was not possible as all of the antibodies available were to components of the complex not exposed on the cell surface. This fact also rendered some of the double labeling efforts impossible. Despite this pitfall, the data suggest that SV associates with IMPs that are, or are in part, the V-ATPase when adsorbed to cells. Additionally, the IMP may be the proteinaceous pore between the virion and the cell. Based on SV having a conformational change as a result of adsorption to mammalian cells thin-sections of each sample under every condition were prepared to examine any structural change that may have occurred.

Discussion

Dissecting the interaction between virus and cell is important for understanding conditions required for virus entry. Thin-sections have been a common and very productive technique for examining these interactions (Paredes et al., 2004). This technique has assisted in visualizing the overall mechanism of entry for many viruses, but there are other methods to examine virus-cell interactions that can add unique and valuable information about the initial interactions between virus and cell. One such method is freeze-fracture. Using thin-sections and replicas, we have been able to further characterize the adsorption of Sindbis

Virus onto cells. The data collected support previous findings that SV may infect cells by way of a pore complex at the plasma membrane.

Sindbis Virus adsorbed onto mosquito cells show discrete virus protein labeling

Replicas of mosquito cells with adsorbed virus show discrete immune labeling of viral proteins on the cell surface. The implications of this labeling are that the virus is bound to the cell surface, presumably by its receptor. As such, the virus has not undergone endocytosis during adsorption at either room temperature or 4C, nor has it fused with any membrane. Complete fusion would result in viral proteins diffused across the membrane as in Figure 3.3. As for the small patches of labeled viral proteins observed at room temperature (Figure 3.5), they are inconsistent also with fusion, and are likely the result of virus particles that have injected their RNA, broken up and resulting fragments have adhered to the cell surface before fixation. This hypothesis is supported by thin-sections published previously that show empty malformed particles bound to the cell surface indicating they have released their RNA into the cell (Paredes et al., 2004). These data would then suggest that some virus particles were empty and have released their RNA into the cell.

Labeled viral proteins may associate with V-type H^+-ATPase

The labeled virus proteins in the mosquito plasma membrane are associated with IMPs (Figure 3.4). Previous studies (Paredes et al., 2004) have indicated that the virus receptor complex forms a pore in the plasma membrane. These IMPs may be part of the receptor/pore complex on U4.4 cells for SV. Labeling of uninfected cell membranes with anti V-ATPase, together with the labeling of the viral proteins on adsorbed cells labeled for SV, suggests that many of the particles in the membrane may be both the ATPase as well as part of the receptor complex for the virus (Figure 3.6). Based on recent cryo-electron microscopy data of V-ATPase from *Manduca sexta*, the average diameter of the catalytic V_1 domain is approximately 18nm, with the V_0 subunit approximately 16nm wide (Muench et al., 2009). Ideally, these would be approximately the sizes of the IMP seen for this protein complex in the divided membrane. It is unclear whether the fracturing process separates the catalytic domain from the membrane domain when cross-linked. It may be possible that the sheer force from the fracture plane would not only separate the two domains, but pull some of the subunits from the opposing domain with it. As a result, a range of particle sizes could all represent parts of the same V-ATPase complex. Since most of the IMPs were approximately 8-10nm in diameter, and the presence of 15nm or larger IMPs was not seen for any treatment, it is likely that the domains are cleaved from each other during fracturing and the remaining IMP is the decameric ring made of membrane subunit *c*. This is consistent with the hypothesis that the V_1 and V_0 domains are regulated by dissociation (Cipriano et al., 2008) and that the stalk proteins are linkers between the domains. Comparing the replica labeled for the V-ATPase and the replicas labeled for viral proteins, it appears as though the viral proteins are associated with the IMPs of 8-10nm. These are consistent with V-ATPase IMPs from previous freeze-fracture studies (Ratajczak, 2000). This would support the hypothesis that SV binds to a receptor complex that may include the V-ATPase prior to entry.

The possibility that Sindbis virus RNA is delivered directly through the plasma membrane may be supported by a recent report that places the Sindbis virus RNA replication complex at the plasma membrane (Frolova et al., 2010). A model of this mode of infection is shown in Figure 3.7. If the RNA entered through the plasma membrane as opposed to entering into the interior of the cell via an endosome creation of the replication complex at the plasma membrane would be logistically easier to accomplish.

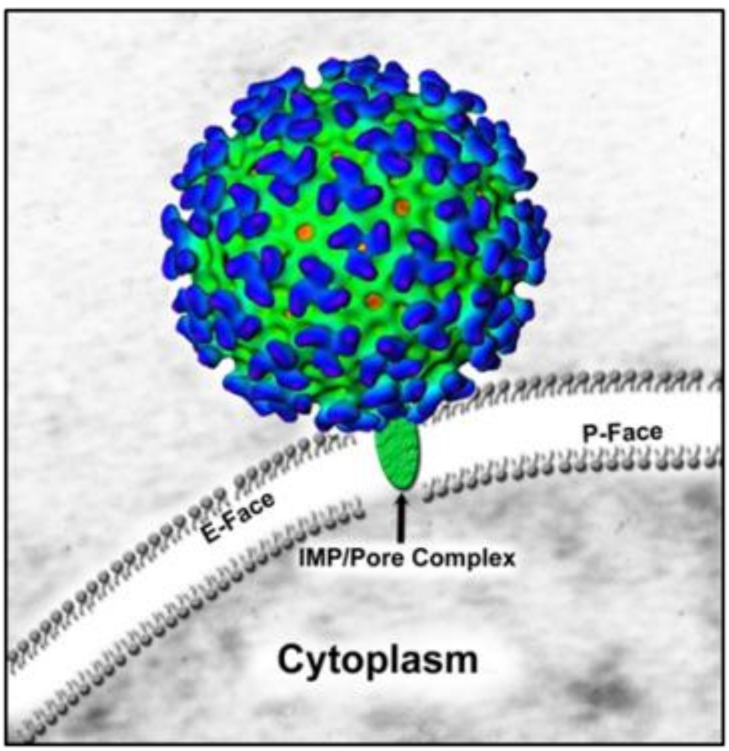

Figure 3.7: Schematic of virus attached to cell surface

Cartoon representation of cross-linked virus attached to 'tissue-side' of E-face replicas. Virus adsorbed onto mosquito cells remains attached to the replica after SDS treatment. The labeling resulting from the remaining proteins (see above) suggests the configuration presented. Here, the virus is bound to its receptor(s) seen as an IMP in freeze-fracture replicas. The E-face and P-face are labeled to convey which leaflet the virus particle is seen. This also shows the virus particle bound to the exterior surface of the replica to orient the reader to the virus position with respect to the replica, where the replica is of the inside of the leaflet.

Acknowledgements

The authors thank Dr. John Mackenzie and the staff of the NCSU EM Center for training and assistance with the electron microscopy. We also thank Amanda Mclamore for producing figure 1. This research was supported by a grant from The Foundation for Research, Carson City NV and by the North Carolina Agricultural Research Service

Freeze-Fracture Gallery

In this chapter, freeze-fracture has shown to be a useful tool in the analysis of virus-cell adsorption and receptor binding. In addition, it also has created replicas of various cell structures. Below is a gallery of images containing plasma membranes, the inner and outer nuclear membranes, virus-cell cross-sections and alterations seen in the plasma membrane as a result of gluteraldehyde fixation and glycerol cryoprotectant. Following each image is a small discussion of the interesting structures seen in the replica, how the replica created the image, and when applicable how the structure was created.

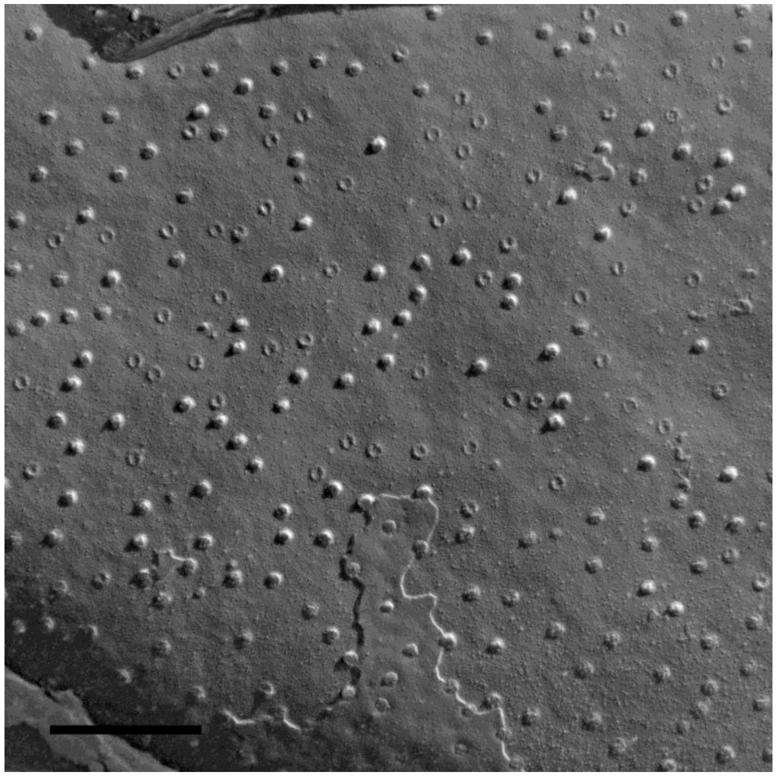

Figure 3.8: Replica of BHK nucleus

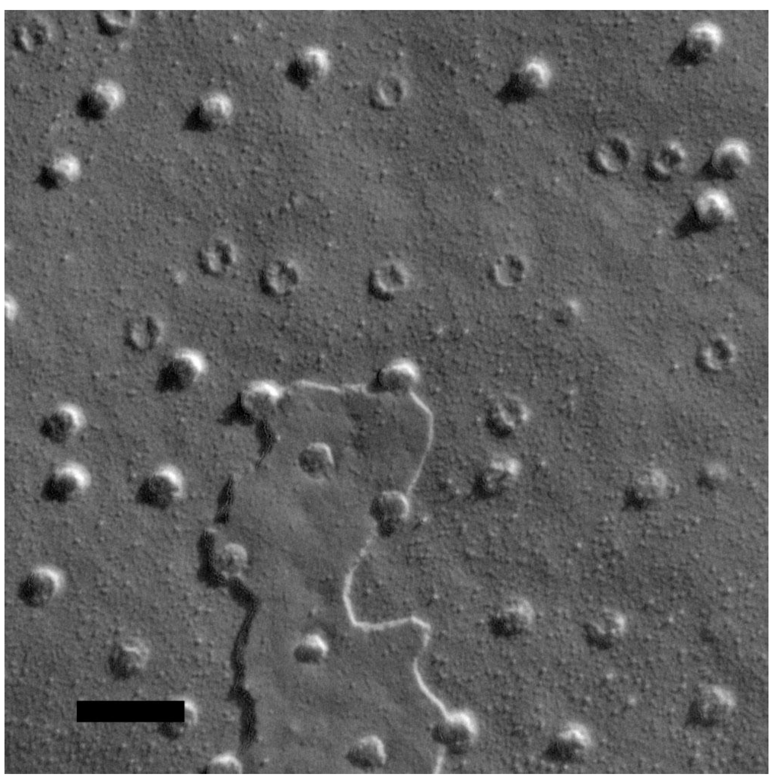

Figure 3.9: Higher magnification of Figure 3.8

Nucleus

In this micrograph a particle replica of the nucleus takes up a majority of the viewing field (Figure 3.8). At this magnification, the nuclear pores look like spheres sitting on the membrane as well as sockets that look as though they accept these spheres. The major membrane this is seen is the P-face of the inner nuclear membrane. Toward the bottom of the nucleus a small section of the outer membrane is seen with nuclear pores embedded into it. There is no evidence of missing nuclear pore complexes in this portion of the replica. The face seen here is likely the P-face of the outer nuclear membrane. Based on a general overview of all the replicated nuclear pores, it seems that their removal is random as to whether they follow the outer or inner membrane. Perhaps the removal of the pore is dependent on whether or not it is in the process of transporting. The major difference seen between the outer and inner membrane is the distribution of the intramembrane particles (IMPs). On the outer membrane, there are either very few IMPs or the majority of the IMPs partition to the outer leaflet. The visualized inner membrane is drastically different in that it looks nearly saturated with IMPs (Figure 3.9). The possible reasons for this partitioning may have to do with functional separation of integral membranes This is merely speculation, but this hypothesis is supported by the fact that the inside of the nuclear membrane is covered with the thick, very small meshed nuclear lumina that contains multiple transmembrane proteins anchoring it to the inner membrane. Each transmembrane complex in the membrane is represented by an IMP. Replicas are of BHK-21 cells processed as normal (see: Chapter 5 for the section on freeze-fracture processing).

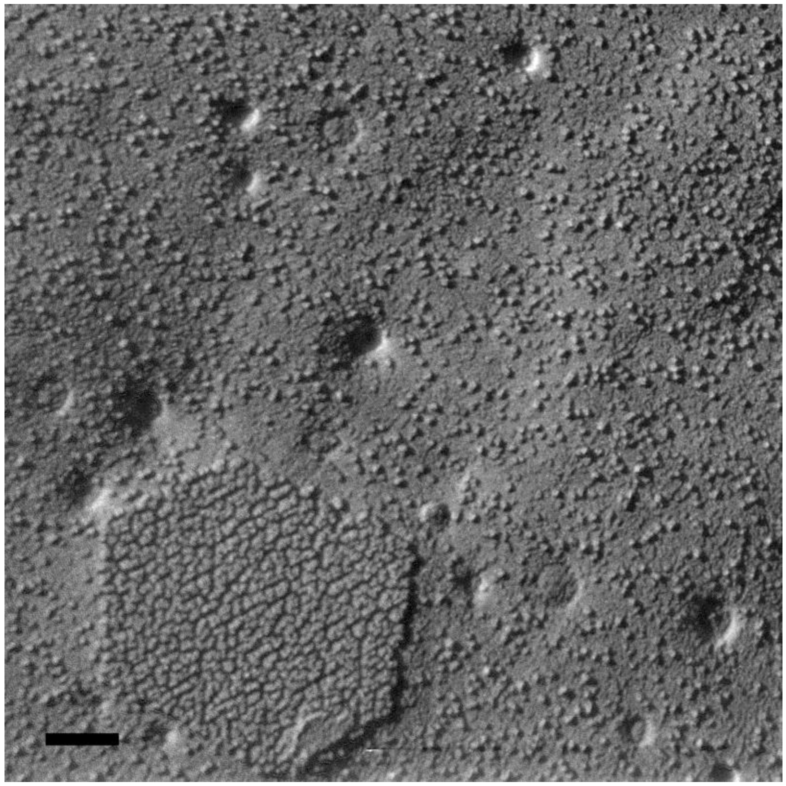

Figure 3.10: Replica of BHK-21 cell showing P-face and gap junction

Gap Junction

BHK-21 fibroblasts form a monolayer when grown *in vitro*. Here, a replica of the P-face between two cells is shown (Figure 3.10). The characteristic high population of IMPs is present, as are the occasional caveolae. What is interesting here is a gap junction plaque that is seen at the bottom of the image. This gap junction is hexagonal in shape, and has a rough appearance. This appearance is a result of connexons aggregating together. Each plateau in the plaque is likely one connexon, or connexin hexamer. The specific details of this plaque are not resolved in these replicas due to the lower limit of resolution of the technique. The replica of this plaque results from the fracture plane cleaving the gap junction channel in half, presumably into the hemichannels from each cell. If this were a double replica, the gap junction from the connected cell would be seen in the crevice left in the E-face by this plaque. It would have a mirrored structure that would fit perfectly with this plaque to complete the gap junction channels.

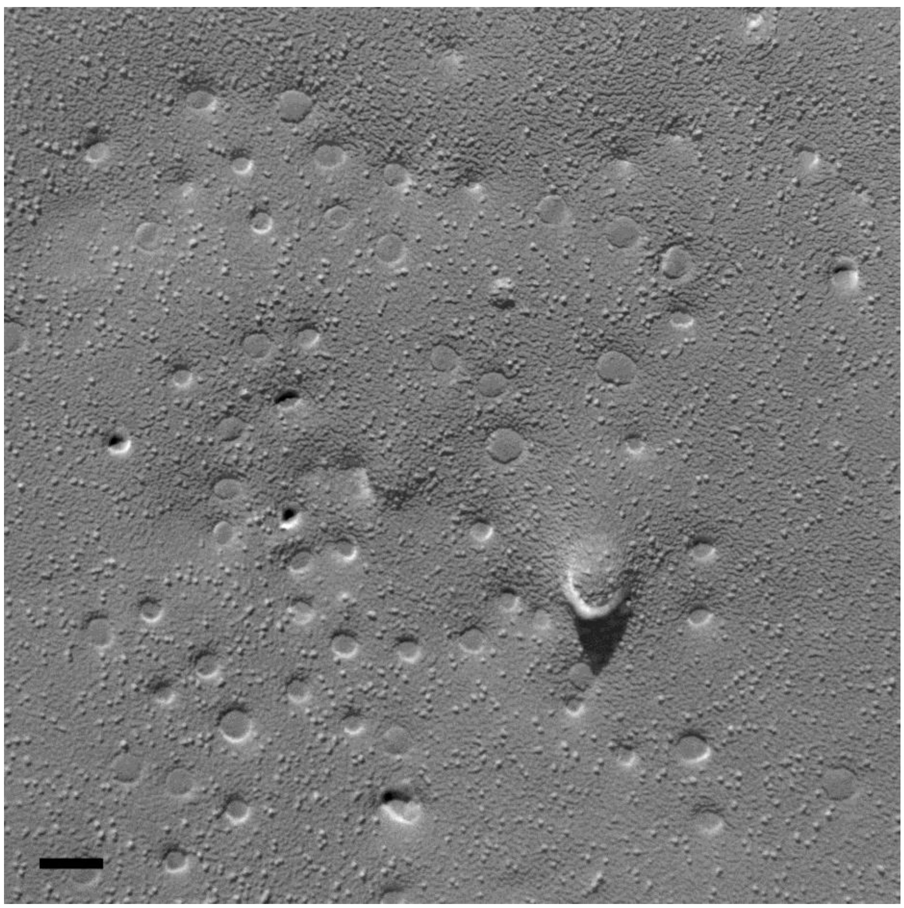

Figure 3.11: P-face of BHK-21 cells with caveolae

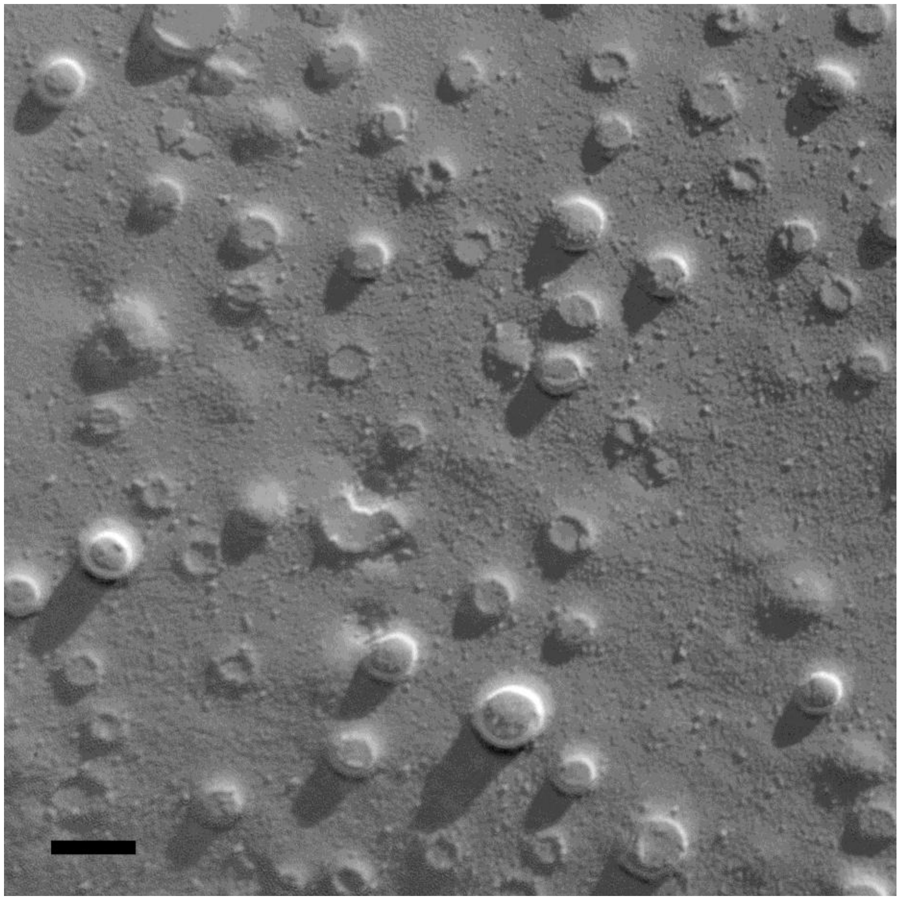

Figure 3.12: E-face of BHK-21 cells with caveolae

BHK-21 & U4.4 Plasma Membranes

The plasma membrane of BHK-21 cells and of mosquito cells has significant biochemical differences. As a result it might be expected to have some difference when examined by freeze-fracture. Due to the method of creating a replica the differences are not readily observable between the two membranes. If the method of freezing and fixing is altered however, the compositional differences between the two membranes can create interesting structures. In the case of mammalian cells, replicas of cells fixed with gluteraldehyde and cryoprotected with glycerol create interspersed structures roughly 40nm in diameter (Figure 3.11 and 3.12). These structures, however, are not of virus particles, but are artifacts of the high cholesterol content in mammalian cells. The cryoprotectant and the

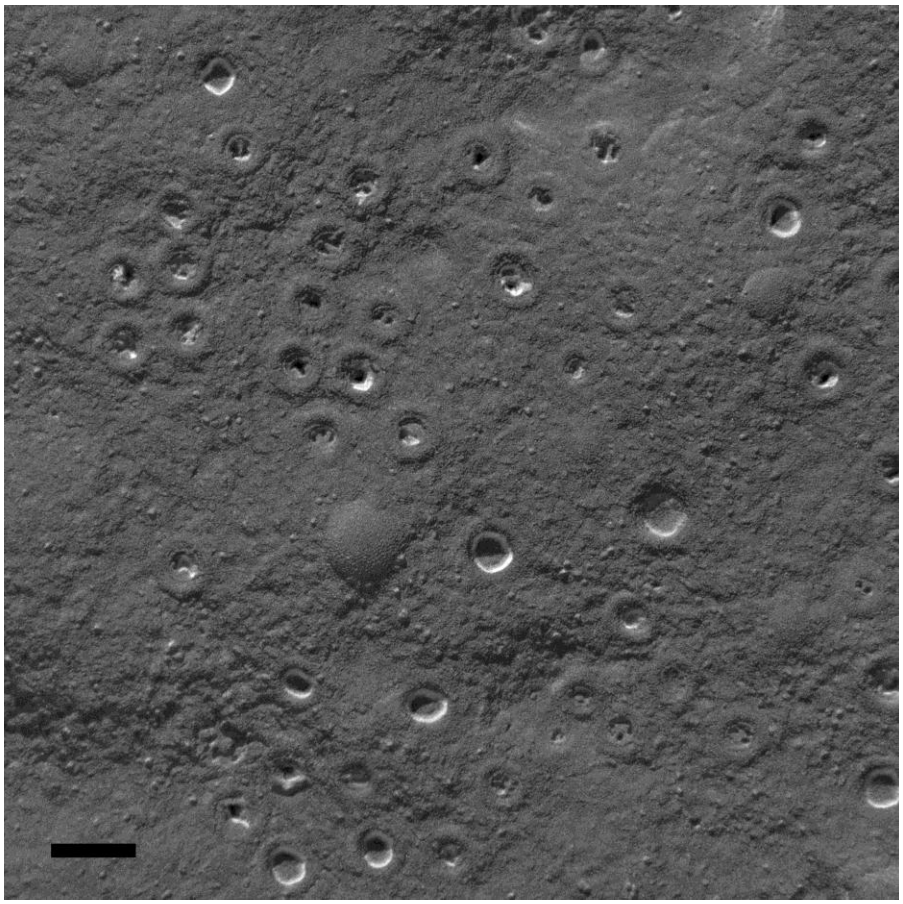

Figure 3.13: Altered caveolae structure in the presence of Bafilomycin A1

fixation method used in the above samples created artificial caveolae in the plasma membrane. The caveolae on the E-face are almost exclusively convex, whereas on the P-face they are almost all concave (compare Figures 3.11 and 3.12). This suggests that these structures are shaped like cups in the plasma membrane, supporting thin-section observations of caveolae. By exposing the cells to Bafilomycin A1, a specific inhibitor of the V-type H^+-ATPase, the caveolae structure seems to change (Figure 3.13). The reason for this change is unknown.

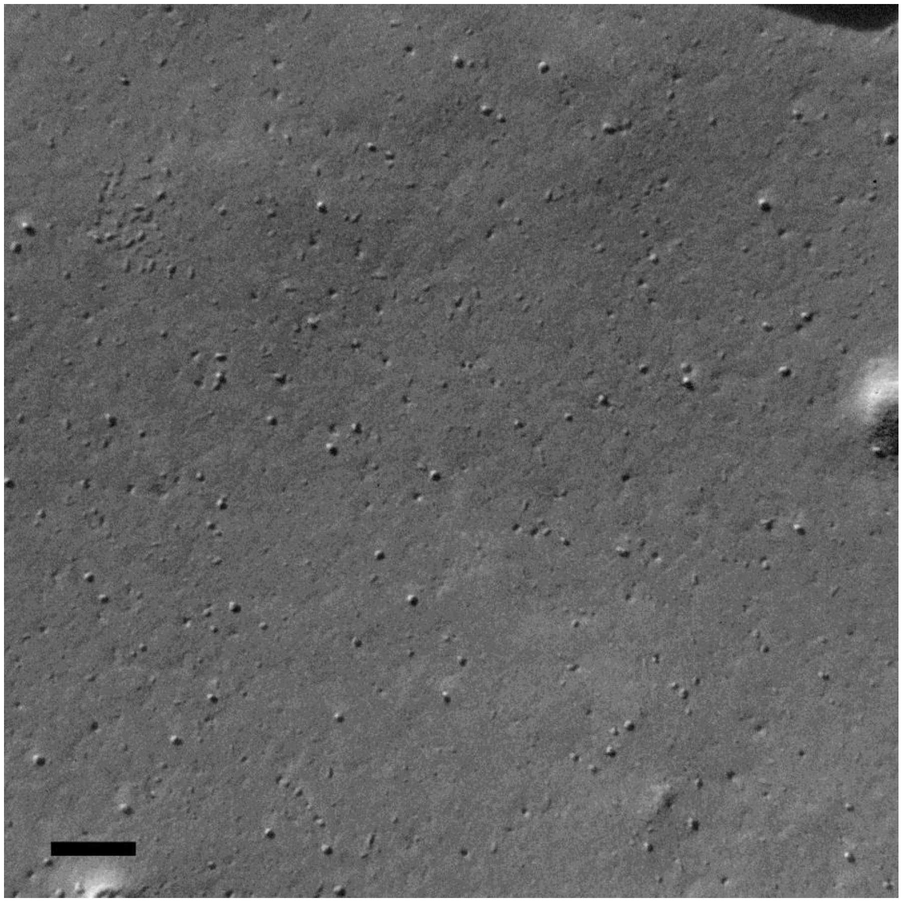

Figure 3.14: Replica of uninfected mosquito cells plasma membrane

Replicas of mosquito cell plasma membranes are not altered in the same manner as mammalian cells' membranes. The reason for this is the extremely low cholesterol content of these cells. Without cholesterol caveolae are unable to form, and a smooth, uniform surface is replicated (Figure 3.14). Uninfected and virus-adsorbed cells exhibit the same structural characteristics on their replicas. Details of these characteristics are summarized earlier in the chapter, but they will be summarized here. The E-face and P-face partition large (>8nm) and small (<8nm) IMPs to the E and P-faces respectively. This is a major factor in determining the faces that are observed. The E-face is concave as a result of the curvature of the cell membrane, whereas the P-face is usually convex. In large cells, and especially in cell monolayers, the E-face and the P-face can appear flat and other factors need to be taken into consideration when determining the observed face. It should be noted here that the partitioning of the IMPs is dependent on the treatment of the cells. Fixatives such as gluteraldehyde have been shown to change the partitioning of IMPs of mammalian cells. Therefore, the partitioning of IMPs needs to be determined for each cell type and condition to ensure that there is proper identification of the faces. In the case of BHK-21 cells and U4.4 mosquito cells the partitioning of IMPs is the same and for the mosquito cells, the curvature of the membrane is easily seen.

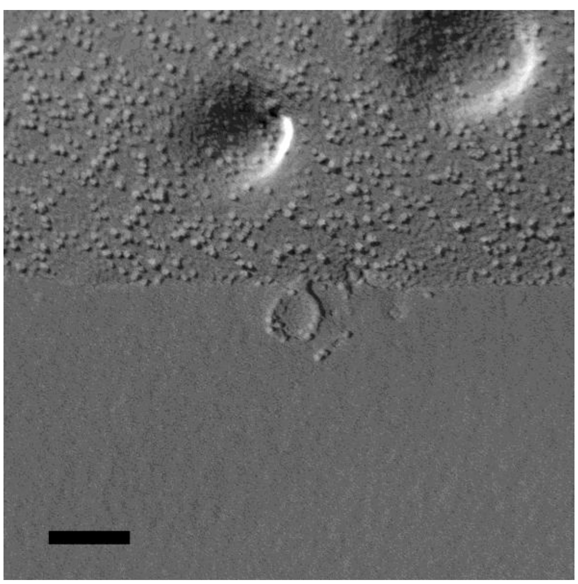

Figure 3.15: Concave replica of adsorbed virus

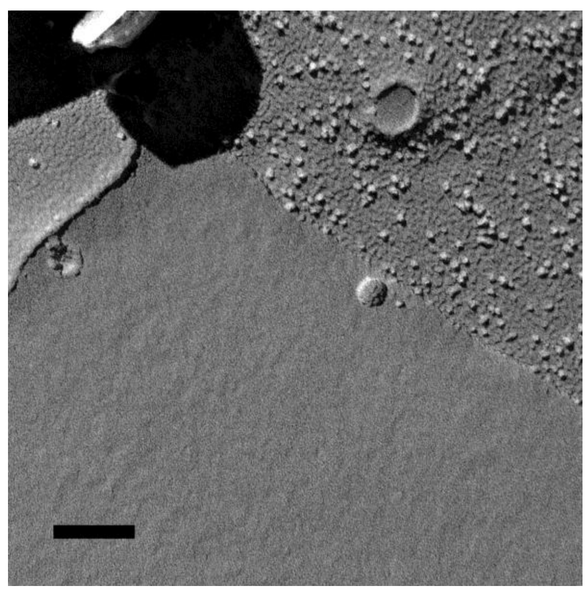

Figure 3.16: Convex replica of adsorbed virus

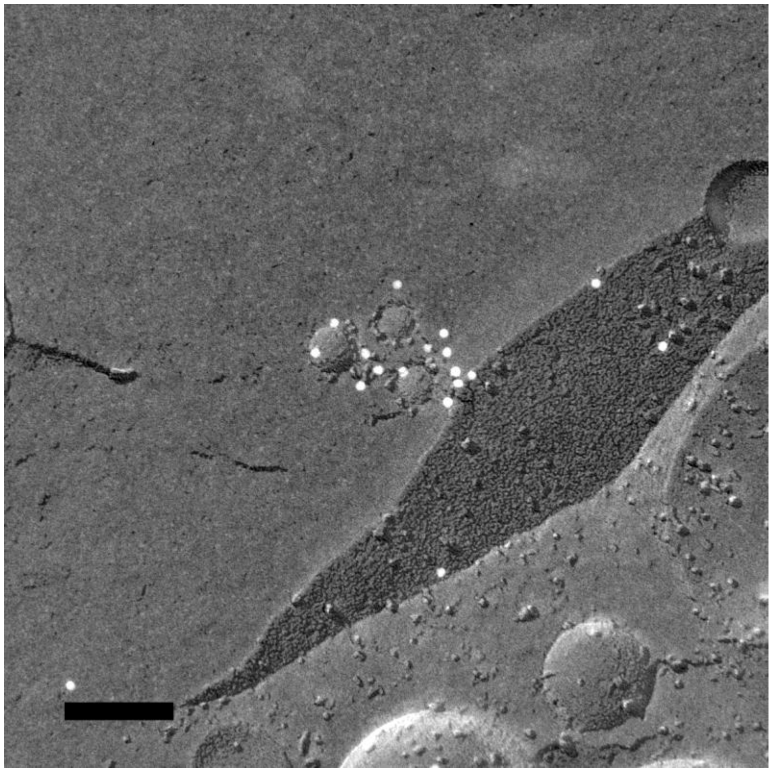

Figure 3.17: Sindbis Virus adsorbed to mosquito cells

Adsorbed Virus

Replicas of virus adsorbed to the cell surface are only obtained by cross section of the cell and the virus adsorbed to its surface. As you can imagine, this is highly unlikely, especially considering the tendency for the fracture-plane to follow membranes laterally and not cut normal to their surface. Extended treatment with fixatives can increase the likelihood of a fracture to cross-section a cell's plasma membrane, but the frequency is still low. Even when the plasma membrane is cross-sectioned, the probability of a virus particle being present at the precise position to get fractured is extremely low as well. Despite these odds, occasionally the fracture plane can result in a cross-sectioned plasma membrane that exposes a virus particle adsorbed to the outer surface (Figures 3.15 and 3.16). Here replicas of cross-sectioned BHK-21 cells have attached virus-like particles attached to their surface. It is impossible to determine whether or not these structures are indeed virus particles without labeling. Figure 3.17 is a cross-section of a mosquito cell labeled with anti-SINV antibody. There are similar structures as seen in the BHK-21 replicas; however they are now labeled with SINV antibodies indicating that they are indeed virus particles.

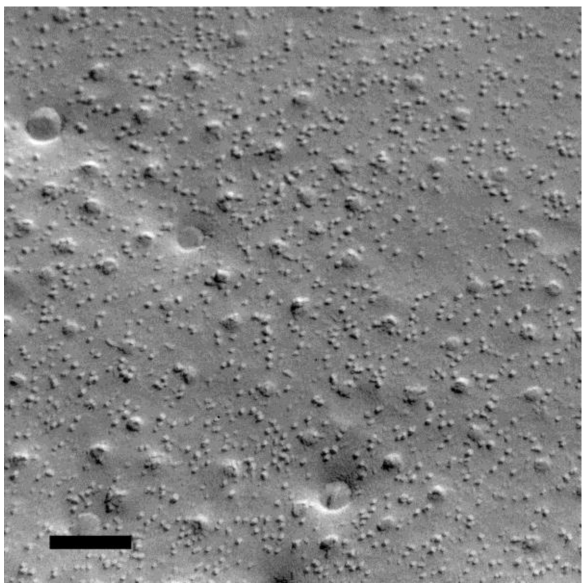

Figure 3.18: SINV induced structures on BHK P-face

BHK cells adsorbed with SINV and incubated for 4 hours have been infected but have not started releasing virus particles. The plasma membrane of these cells have small structures that are not characteristic of caveolae are observed (Figure 3.18). These structures may be created by virus particles binding to the cell surface, releasing their RNA into the cell then falling off into the media. The structure itself may be the remaining viral proteins with the cellular proteins that made the pore used to inject the RNA into the cell. The number of these structures is supported by thin-sections that show multiple virus particles bound to the surface of BHK cells. More evidence is needed however to determine the composition of these structures.

Chapter 4

Random mutagenesis as a method of generating host-range phenotypes in Sindbis Virus

Summary

As an arbovirus, Sindbis Virus (SV) has to mature and propagate in many divergent biochemical environments. One environment is in the mosquito, while the others are mammals and birds. The necessity to mature in each environment requires SV to adapt its genome and proteins so that it is expressed efficiently in both vertebrates and invertebrates. To find these adaptations, we have devised a method in which a cDNA clone of SV is mutagenized to introduce changes throughout the genome. The cDNA was first grown in *E. coli* cells that are deficient in DNA repair mechanisms followed by treatment with a mutagenic compound, N-methyl-N'-nitro-N-nitrosoguanidine. The two treatments allow for deletions, insertions and substitutions throughout the entire genome. The virus grown from these treated clones resulted in a number of host-range phenotypes. Two mutants were enhanced for growth in insect cells in addition to being deficient in growth in mammalian cells. Sequencing these mutants showed a number of mutations which may or may not work in concert to create the host-range phenotype. These data show that this method of random mutagenesis is sufficient to create host-range phenotypes. Further analysis of the mutations created will lead to possible host adaptive sites that are essential for growth in a mosquito biochemical environment but unnecessary for growth in mammalian cells. This study was undertaken with Sindbis virus to develop a new method for the selection of insect cell adapted host range mutants which would be good vaccine candidates for pathogenic Alphaviruses.

Introduction

Arthropod borne viruses (arboviruses) are believed to have originally been strictly invertebrate viruses that have expanded their host range to include vertebrates. Data supporting this hypothesis show that there is vertical infection of mosquito to mosquito via venereal transmission (Mavale et al., 2010; Ovenden and Mahon, 1984; Shroyer, 1990). Additionally, there is data that supports transmission from the female to her eggs (Pelz and Freier, 1990) as well as other evidence of vertical transmission (Dhileepan, Azuolas, and Gibson, 1996; Fulhorst et al., 1994). This transmission cycle is sufficient to maintain the virus; however it is likely due to the hematophagic nature of these insects that transmission from insect to vertebrates occurred. To accomplish this species jump the virus must adapt on both the genomic and protein level to identify and successfully infect new cell-types. Equally important, the virus must be able to replicate its genome and process its proteins in the new biochemical environment all while coping with new antiviral mechanisms fighting the infection. The adaptation of the virus to the new epizootic cycle is likely to include both modification of genome replication (Spotts et al., 1998) and protein expression (Brault, Powers, and Weaver, 2002; Greene et al., 2005a) possibly including antigenic site modifications that would increase evasion from the immune system of the host (Aguilar et al., 2008).

The data presented in this chapter supports the hypothesis that arboviruses, specifically SV, have host adaptive sites that are important in its ability to infect and replicate in mammalian cells. In an attempt to determine these host adaptive sites, random mutagenesis is employed under selective pressure to create host-restricted mutants of SV. These mosquito restricted (MR) mutants ideally contain mutations in host adaptive motifs needed for growth in mammalian cells. Examining the genomes of these mutants and comparing mutations across various randomly generated mutants should highlight the host adaptive sites in addition to giving examples of mutations that cause the MR phenotype.

Materials and Methods

cDNA clone and cell propagation

The cDNA clone of SV used in these experiments was TOTO1101 (Rice et al., 1987). The full sequence of this clone is known, and was therefore used as the template for the mutation. The clone was grown in DH5-alpha *E. coli* (Sigma Aldrich) and a sample supplemented with 30% glycerol was saved at -80C. cDNA from these cells were harvested by miniprep of a 5mL overnight amplification at 37C (this is the kit place). Harvested cDNA was stored in dH_2O at -20C until needed.

BHK-21 cells were propagated in EMEM supplemented with 10% fetal bovine serum, 5% gluteraldehyde, 5% L-glutamine and buffered with HEPES (pH 7.4). Cells were grown in 75cm2 flasks in an incubator set to 100% humidity and 5% CO_2. BHK-21 cells were split every day at a ratio 1:3 as needed. Low passage cells were used to screen for host-range phenotypes. Mosquito C7/10 cells were propagated in EMEM media supplemented as the

BHK-21 cells. These cells however were incubated at 27C and split as needed every two days at a ratio of 3:1.

Random mutagenesis

XL1-Red *E. coli* cells (maker) (described below) were transformed with TOTO1101 cDNA and were grown overnight in LB containing 100ug/mL carbenicillin to select for transformed cells. A sample of this overnight growth was diluted in 10mL to OD_{600} 0.0005 and grown for 96 hours, diluting again in 10mL to OD_{600} 0.0005 after 48 hours. After 25 generations the cDNA from the cells were harvested by miniprep and transformed into XL1-Blue cells (Maker). Generations were calculated by the equation $N_t=N_0*2^n$, where N_t is the OD_{600} at time t, N_0 is the initial absorbance and n is the number of generations. These cells were grown in LB containing 100ug/mL carbenicillin to OD_{600} of 0.2 (~100 Klett units). Once in log phase, the cells were gently pelleted (1000xg for 1 minute) and washed three times with 50mM Citrate buffer (pH 6.0) and resuspended in 1mL of the buffer. Enough freshly prepared N-methyl-N'-nitro-N-nitrosoguanidine (MNNG) in dimethyl sulfoxide (1mg/mL) was added to the cells to make a final concentration of 100ug/mL MNNG. The cells were gently agitated at 37C for 15 minutes in the MNNG buffer. After, the cells were pelleted as above and washed twice with 50mM Citrate buffer. The pellet was resuspended in LB containing 100ug/mL carbenicillin and grown overnight at 37C to recover. cDNA was harvested from the overnight by miniprep and stored in dH_2O at -20C.

Mutagenized virus production

Mutagenized cDNA were linearized with XhoI and used as templates to create full-length RNA transcripts as in (Hernandez, Sinodis, and Brown, 2010). The RNA transcripts were electroporated into C7/10 cells, infecting the cells with the mutant virus. These cells were then incubated as described above at 27C. After two days, the supernatant was harvested from infected cells, clarified by centrifugation and stored at 4C for no less than 16 hours. The titer of the supernatant was assessed at this point by MTT (M-tetrazolium) assay (Heldt et al., 2006). After confirmation that the samples were no more than 1 log lower in titer compared to the wild-type, individual samples from the supernatant were collected by infectious center assay (ICA).

Infectious center assay and host-range screening

Host range mutants restricted to growth in the insect cells were desired. For this reason the primary selection was done in insect C7/10 cells. Additionally, these cells display cytopathic effect which not all insect cells develop. 3-6x10^4 C7/10 cells/mL are infected with an MOI=10 of harvested virus from above. 100uL of these infected cells are mixed with 1 mL 2x10^7 cells/mL and added to 1mL 1.4% soft agar in 1x MEM. This mixture was plated onto 60x15mm plates underlayed with 2mL hard agar in 1xMEM. The plates were incubated at 28C for 48 hours then stained with neutral red. The infectious centers (IC) resolved by staining were picked and eluted in 1mL 3% FBS in PBS-D at 4C overnight. Each IC was amplified in C7/10 cells for 48hours before screening for host-range phenotype.

Screening for host-range phenotype was done in duplicate using 3D cultures of C7/10 and BHK-21 cells. This "spot assay" uses 60 x15 plates of BHK-21 and C7/10 cells prepared as above with the following modifications. For the BHK-21 cells, $2x10^6$ cells/mL

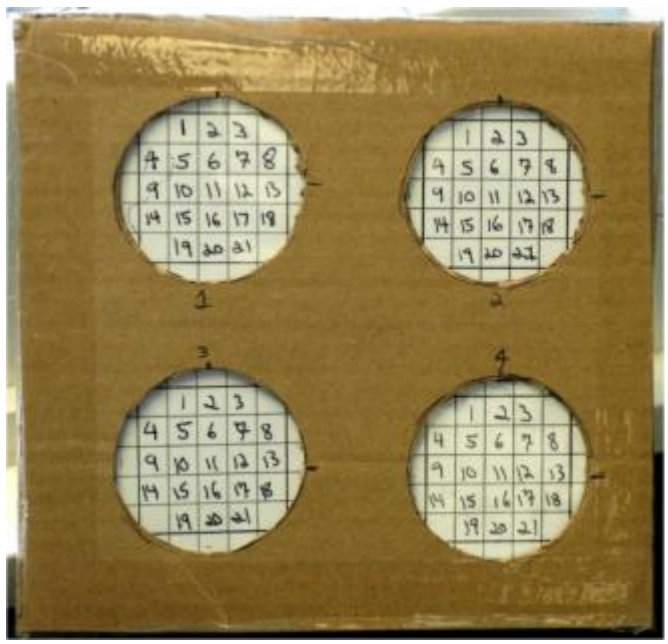

Figure 4.1: Grid Template for Spot Assay

Spot assays were inoculated in a grid fashion to make it easy to locate points of inoculation. Reference marks on the top and right of each plate were used to position each 60 x 15mm plate in the template and to orient plates after staining. This template will hold 4 plates.

were added to soft agar. The C7/10 cells were prepared as previously ($2x10^7$ cells/mL) without the addition of infected cells. Each assay was done in duplicate for each cell line. Inoculation of 2uL amplified IC/spot was in a grid pattern (Figure 4.1) to facilitate identification of inoculation sites for each plate. The infected plates were incubated at 28C for both BHK and C7/10 cells. The plates were stained 24 hours post-infection and spots were graded with a + or – regarding the presence or absence of a plaque. Spots double negative in BHK cells and positive in C7/10 cells were titered by MTT.

Virus genome sequencing

RNA extraction of the mutagenized virus was done under RNAse free conditions. 3mL of amplified virus supernatant was pelleted at 50,000rpm in a Beckman SW 50.1Ti rotor (Beckman Coulter Inc, Brea, CA) in H_2O_2 treated ultracentrifuge tubes. The pellet was resuspended in 100uL TE (1mM Tris-HCl, 20mM EDTA, pH7.0) and solublized with 100uL 2x lysis buffer (100mM Tris-HCl, 20mM EDTA, 1%SDS, pH7.0) for 20 minutes at 37C with occasional agitation. The solution was extracted with three washes of the order: phenol, phenol-chloroform-isoamyl alcohol (25:24:1) and chloroform. The resulting RNA was precipitated with ethanol (2 volumes of 100% ethanol) and potassium acetate (1/10 volume of 3M KAc) at -20C for at least 30 minutes. The pellet was washed twice with ice-cold %70 ethanol before dissolved in 100uL DEPC-treated water. Reverse transcription with MMLV reverse transcriptase (RT) followed under the following conditions. 10uL of extracted RNA was added to PCR buffer (Tris-HCl, 50mM KCl, 5mM $MgCl_2$, pH 8.3) containing 20U RNasin, 200uM each dioxynucleotide, 1uM reverse primer (Table 4.1) and 50U of MMLV RT in a final volume of 20uL. This reaction was incubated at 42C for 20minutes and inactivated at 99C for 5 minutes.   This entire reaction was used in a PCR reaction of 100uL with adjustments to the $MgCl_2$ and dioxynucleotides for the larger volume and the addition of 1uM reverse and forward primers (Table 4.1). 2.5U of Taq polymerase was added to the reaction and the entire reaction was amplified using the following PCR program: 5min95C; (3min95C; 30secT_m-5C; 2min72C) x25; 10min72C; hold4C.

PCR products were added directly to ligation reactions following the standard reaction of the pGEM T-easy vector kit (Promega, Madison, WI) and incubated at 4C

Table 4.1: RT-PCR Primers for Sindbis Virus Sequencing

	Forward Primer	Reverse Primer	Region Sequence
	Name **Sequence (5'-3')**	**Name** **Sequence (5'-3')**	
1	5'-UTR ATTGACGGCGTAGTACACAC	Sin(nsp1)_973R GCGTATCCCACGGTTTCTCC	5'-UTR and nsP1
2	Sin(nsp1)_854F CCACTTGAATGGAAAGCAGTCG	Sin(nsp2)_1842R CGGAGTGTGTTATGATCTTAACC	nsP1
3	Sin(nsp2)_1680F GCATTAGTTGAAACCCCGCGC	Sin(nsp2)_2644R GCTGTAACTGGCTGTGTGCAAC	nsP2
4	Sin(nsp2)_2501F GGTAGTACTATGCGGAGACCC	Sin(nsp2)_3435R GGAACACCGGAAATCTACGGG	nsP2
5	Sin(nsp2)_3304F GCATCCCACTAACGTACCATCC	Sin(nsp3)_4280R GCACACAGTCATTCTTGCGGTG	nsP2
6	Sin(nsp2)_4076F GGGTACAAGAGATGGAGTTGG	Sin(nsp3)_5056R CGAATGCGGGAGTGTGCGG	nsP2 and nsP3
7	Sin(nsp3)_4113F CGCACCAAAAGGGAGAATATTGC	Sin(nsp3)_5062R GGAACGAATGCGGGAGTGTGC	nsP3
8	Sin(nsp3)_4936F GCAATAACGTCAAAGAAGTTACAG	Sin(nsp4)_5878R GCATGAATTCTTTCCAGGACATTG	nsP3
9	Sin(nsp4)_5737F GGACTGAATACTGACTAACCG	Sin(nsp4)_6685R GGTCTTTCTTCTGTGTGTTTCG	nsP4
10	Sin(nsp4)_6528F GCATATGTAGCTAGATCTGAAAGG	Sin(nsp4)_7506R GTGTAATATTGTCTACCTCATACC	nsP4
11	Sin(nsp4)_7380F GACGACGAGCAAGACGAAGAC	Sin(C)_8267R GCGAGGGATGGTAAATCTACC	nsP4 and C
12	Sin(C)_8200F CCGAAGGATTCTATAACTGGC	Sin(E2)_9168R GGTAGGATGTATAAGCGTGCG	C and E3 and E2
13	Sin(E2)_9036F GGACGGGAAAAATATGATCTACC	Sin(6K)_9979R GCCAAAGGTATGCACAACTGG	E2 and 6K
14	Sin(E2)_9848F CGTAATCCCAACTTCGCTGG	Sin(E1)_10779R CTGATGAGGCCTGCGTGTAC	6K and E1
15	Sin(E1)_10708F CCAGCACAGACATTAGGCTAC	PolyATail TTTTTTTTTTTTTTTTTTTTGAAATG	E1 and 3'-UTR

overnight. Completed ligation reactions were transformed into DH5-alpha *E. coli* cells (Sigma-Aldrich St. Louis, MO) and plated on X-gal/Lac-Z LB plates containing 50ug/mL carbenicillin and incubated at 37C until colonies were visible. Colonies positive for insertions were grown in 5mL LB suspension cultures containing 50ug/mL carbenicillin at 37C overnight. Minipreps and glycerol stocks were prepared from each suspension culture. To check for insert length, the extracted DNA was run on a 1% agarose gel in Modified-TAE (40mM Tris-Acetate, 0.1mM Na_2EDTA, pH8.0). DNA with an insert of 500bp or greater were sent to MWG for sequencing.

Results

Mechanism of mutation

To determine the best route of mutation, various methods were examined. In the end, the best method of mutation was considered to be a two-step process in which *E. coli* deficient in three DNA repair mechanisms would introduce insertions deletions and substitutions followed by a more aggressive mutation process in which the cDNA genome would be exposed to MNNG during replication to increase the rate of substitution mutations. The *E. coli* cells used in this experiment were XL1-Red competent cells (Agilent Technologies). These cells have error-prone mismatch repair (Glickman and Radman, 1980), deficient 3’-5’ exonuclease activity in DNA polymerase III (Scheuermann et al., 1983), and are unable to hydrolyze 8-oxodGTP (Cox, 1976). These alterations in this strain of *E. coli* result in a 5,000-fold increase in mutation over wild-type. A drawback of this strain is that due to its poor repair machinery, it is slow to grow and does not tend to have longevity due to chromosomal damage. Also, even with its significant increase in mutation, there will only be a few mutations (1 mutation/10kb DNA/generation) due to this strain in the relatively small 11kb genome of SV. This is another reason why other mechanisms of mutation were used to create host-restricted mutants.

N-methyl-N'-nitro-N-nitrosoguanidine, more commonly known as nitrosoguanidine or MNNG, is well suited to create random mutagenesis in cDNA clones. MNNG is a class 2A carcinogen and is a strong alkylating chemical. DNA exposed to MNNG results in methylated bases, such as O6-methylguanidine (m^6G), 7-methylguanidine and 3-methyladenine (Lawley and Orr, 1970) though m^6G is thought to be the reason for the high mutation frequency of MNNG as *E. coli* over-expressing a methyltransferase that removes methyl groups from m^6G are resistant to mutations when exposed to MNNG (Olsson and Lindahl, 1980; Samson and Cairns, 1977; Schendel and Robins, 1978). Sequences that m^6G can pair with both cytosine and thymine (Loveless, 1969). The latter pairing results in a GC-AT conversion. As a result, the primary mutation as a result of MNNG exposure is substitutions or early termination due to new stop codon creation (Lucchesi, Carraway, and Marinus, 1986). Together with the repair deficient *E. coli*, a broad spectrum of mutations across the entire genome are generated.

Host-range mutant characterization

From the infectious center assay, 63 plaques were harvested. Of these plaques, only 21 were positive for the host-range phenotype as tested for by the spot assay. These 21 resulting host-range mutants are summarized in Figure 4.2. Briefly, all mutants with the exception of 7 and 8 were host restricted by at least one log. Mutants 3, 4, 6, 9, 34 and 53 displayed the greatest host-range phenotype of having more than a 2.5 log difference between growth in mosquito cells and mammalian cells. Mutants 3 and 4 were of particular interest due to their significantly enhanced growth in mosquito cells as compared to the wild-type.

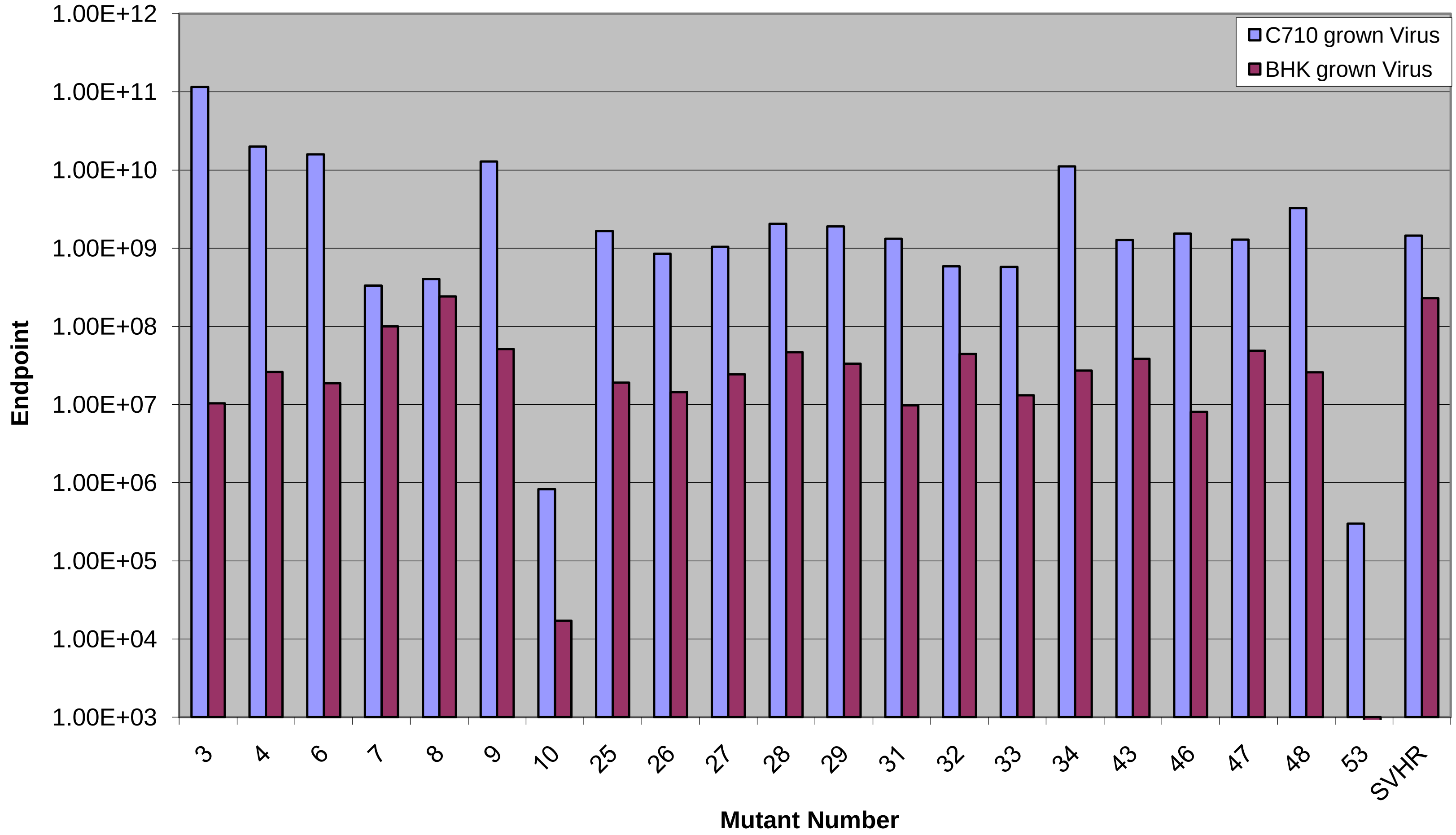

Figure 4.2: MTT Assay of Host-Range Phenotype Mutants

Mutants that were positive for host-range phenotype in the spot assay were tittered by MTT (described in the text).

Table 4.2: MR3 mutations

nt: nucleotide of mutation based on complete genome; Mutation: nucleotide substitution or insertion; Amino-Acid: change in amino acid if any (Silent is no change and N/A is untranslated changes); Amino-Acid#; Amino acid number based on individual protein sequence; Protein: protein in which the mutation occurred.

nt	mutation	Amino-Acid	Amino-Acid#	Protein
121	insert A	Q->TKKLPANstop	21	nsp1
353	C->T	Silent	98	nsp1
391	A->G	N->S	111	nsp1
2066	A->G	Silent	129	nsp2
2992	C->T	P->L	438	nsp2
3326	C->T	Silent	549	nsp2
3631	A->G	E->G	651	nsp2
3664	G->A	W->stop	663	nsp2
3833	T->G	Silent	718	nsp2
4229	G->A	R->H	40	nsp3
5702	A->T	Silent	534	nsp3
6369	G->A	A->T	207	nsp4
8239	A->G	Y->C	198	C
8698	T->A	V->E	23	E2
9090	G->T	V->L	154	E2
9144	A->G	R->G	172	E2
9382	C->T	A->V	251	E2
9536	A->G	Silent	302	E2
9685	C->T	P->L	352	E2
9803	A->T	K->N	391	E2
10288	A->G	D->G	75	E1
11156	C->T	Silent	364	E1
11426	T->G	N/A	N/A	3'UTR
11535	A->G	N/A	N/A	3'UTR
11549	insert A	N/A	N/A	3'UTR

These two were selected for sequencing to determine the mutations involved in these host-range phenotypes. The mutations for mosquito restricted (MR) mutant 3 and MR4 are summarized in Tables 4.2 and 4.3 respectively. MR3 has 25 mutations that spanned all of the viral proteins. Some of the more interesting mutations are a frame shift at nt6543 in

Table 4.3: MR4 mutations

nt: nucleotide of mutation based on complete genome; Mutation: nucleotide substitution or insertion; Amino-Acid: change in amino acid if any (Silent is no change and N/A is untranslated changes); Amino-Acid#; Amino acid number based on individual protein sequence; Protein: protein in which the mutation occurred.

nt	mutation	Amino-Acid	Amino-Acid#	Protein
151	C->T	A->V	31	nsp1
353	C->T	silent	98	nsp1
1113	T->C	S->P	352	nsp1
1756	T->C	V->A	26	nsp2
3579	A->G	K->E	634	nsp2
3743	C->A	D->E	688	nsp2
3799	A->G	E->G	707	nsp2
3833	T->G	silent	728	nsp2
5072	A->T	silent		nsp3
6543	insert T	Lstop	265	nsp4
6727	C->T	A->V	326	nsp4
6971	A->G	E->G	407	nsp4
7177	A->G	H->R	476	nsp4
8009	G->A	silent		capsid
9144	A->G	R->G	172	E2
9249	A->G	K->E	206	E2
9382	C->T	A->V	251	E2
10288	A->G	D->G	75	E1
10511	C->G	N->K	149	E1

NSP4 resulting in a truncation. Additional mutations were also concentrated at the N terminus of E1 and E2 and in the 3’-UTR region as well. MR3 had 19 mutations with similar distribution. Partial sequencing of other MR mutants showed partial overlap of some mutations. MR4 and MR29 have two overlapping mutations, V23E and R172G in E2. Partial sequencing of MR32 shows a D75G mutation in E1, and A11535G nucleotide substitution and an A insertion at 11549 in the 3’-UTR.

Discussion

The hypothesis that SV as with other arboviruses have adapted genetic mutations that increase their fitness in vertebrates suggests that there are host adaptive sequences in the genome of these viruses that can be exploited to determine how these viruses adapted. This method can also be exploited for the selection of vaccine candidates. In support of this hypothesis, we have used random mutagenesis with selective pressure to discover mutations that may be located in these host adaptive sites. The resulting phenotype of these mutations is a host-restricted virus that grows efficiently in mosquito cells, but is less efficient in growing in mammalian cells. The significant level of mutation in the viruses sequenced suggests that there may be multiple sequences that are not necessary for growth in insect cells, and that they are instead important for mammalian growth. Of these mutations, it is possible that some or all of them are required for the host-range phenotype, which would indicate that there is a general genomic sequence that is preferential for growth in vertebrates that is not required for mosquito cells.

For MR3, the 26 mutations observed are dispersed throughout the genome. There are a large number of mutations in E2 and nsP2, where 14/26 mutations are in these two proteins. nsP2 is the protease that cleaves all of the non-structural proteins from the polyprotein precursor. Its' high level of mutation is perplexing as its' functions in the cell do not seem to be host-specific. The mutations here span across both the helicase domain as well as the protease domain. These mutations perhaps suggest that there may be more cellular proteins assisting in the processing of the nonstructural proteins or in the replication of the genome.

E2, as opposed to nsP2, as the glycoprotein responsible for receptor recognition, is an ideal protein to create a host-range phenotype. Mutations here are most likely involved in receptor recognition or polyprotein processing, as alterations in the protein could change the intermediate conformations of the protein as it matures through the ER. This holds especially true for substitution mutations such as P352L, allowing for greater flexibility where none may be desired. Other mutations that cause large charge changes such as V23E and R172G could alter protein-protein interactions with E1 or domain-domain interactions within itself. In Alphaviruses it has been shown that vector infection has much to do with E2 (Brault, Powers, and Weaver, 2002). It has also been shown that the glycoproteins are largely responsible for the virulence of alphaviruses in mammals (Greene et al., 2005b; Paessler et al., 2003). MR4, as with MR3, has mutations across all proteins of SV. The mutations in MR4, however, seem to be focused in the nonstructural proteins. The completely different distribution of mutations between these two mutants suggests that there may be multiple host adaptive motifs in both the structural proteins as well as the nonstructural proteins. Again nsP2 is highlighted in MR4 having 5/13 of the mutations in the nonstructural proteins. nsP4 is also highly mutated and includes an insertion that results in early truncation of the protein. This truncation would eliminate a significant portion of the protein. What is interesting though is that the latter part of nsP4, the RNA-dependent RNA polymerase, has been shown to be functional in mosquito cells even with significant mutation (Lemm et al., 1990). This suggests that nsP4 may interact with cellular proteins, such as enhancers or other regulators, which increase its viability in mammalian cells. It is worth noting that there were no observed truncations of structural proteins in any of the mutants sequenced. Perhaps as the packaging and transport mechanism of the viral RNA, gross alterations in the glycoproteins will significantly degrade viability in either cell type and not lend itself to a host-range phenotype. The effect of alterations of capsid and truncations of E1 and E2 have been seen, all resulting in structurally altered virus particles, which were not all infectious (Ferreira et al., 2003a; Hernandez et al., 2005; Kononchik et al., 2009; Schlesinger, London, and Ryan, 1993; West et al., 2006). There is data from structural protein deletion mutants that show host-range phenotype (Hernandez et al., 2003). These mutations can be summarized by recognizing that the lipid bilayer of mosquitoes and mammals differ significantly in thickness. With the thinner membrane, mosquito viruses can accommodate shorter transmembrane domains, whereas the thicker membranes from mammalian cells are unable to use short transmembranes to properly express the alphavirus glycoproteins. Such fundamental differences between the two cells types are likely to be the cause of other host-restricted mutants.

To test the possibility that one or more of the mutations are required, it would be necessary to reintroduce each mutation into wild-type virus and assay for the host-range phenotype. This is a large and time consuming task. To this extent, it is easier to passage virus in mammalian cells, look for a loss of host-range phenotype and sequence the passaged virus for revertant or compensatory mutations. The hypothesis behind this experiment is that the changes in the genome would indicate where the host adaptive sites were and eliminate mutations that occurred that were not playing a role in the host-range phenotype. This task is currently underway for MR3 and MR4. Of special interest are truncations of nonstructural proteins. Ideally, there will be a few sites that revert, which would make these sites ideal for vaccine studies. On a more basic level, the identification of host adaptive sites would help characterize arboviruses and show how they were able to adapt from purely invertebrate viruses to a combination of invertebrate and vertebrate. These data can be added to other bioinformatics data to possibly locate other host adaptive sites that may be in other vertebrate viruses and possibly determine the mechanism involved in creating the host-range phenotype for each motif.

CHAPTER 5

Materials and Methods

Chapter 2:

Cells, media and virus

Baby Hamster Kidney cells strain 21 (BHK-21) were passaged as described previously (Renz and Brown, 1976) at 37°C with 5% CO_2 in minimum essential medium (MEM) supplemented with 10% fetal bovine serum (FBS), 5% tryptose phosphate broth, 2mM glutamine, 50 µg/mL gentamicin as described previously (Renz and Brown, 1976) and 10mM HEPES at pH 7.4. Mutant virus was produced from the cDNA clone TOTO1101 with a substitution in E2 of a serine to a tyrosine, S420Y and has been studied previously (Liu and Brown, 1993) to show that this modification does not affect virus production or assembly.

Site Directed Mutagenesis, in vitro transcription and RNA transfection

Site directed mutagenesis was generated as described by (Nelson et al., 2005) The following primers were used to generate the mutations: E2 341 (5'-GCACACTCGCGCGCGGAAAGTAGGACTGC-3'), E1 392 (5'-GAGCACCCCGAGACACAAAAGAGACCAAGAATTTC-3'). Infectious RNA was synthesized by in vitro synthesis by combining approximately 1 µg of template with 40 units of SP6 polymerase, 1mM of ATP, UTP and CTP, 0.5mM GTP, 1mM m7GpppG, and 10 units of RNase inhibitor. The mixture was incubated at 40°C for 1 hour. 2µl of the sample was run on a 1% agarose gel to confirm synthesis of the RNA and assess quality. The template was removed by RNase free DNase incubated at 37°C for 30 minutes. Prior to transfection, cells were trypsinzied and washed three times with RNase-free PBS-D (2.7mM

KCl, 1.5mM KH_2PO_4, 137mM NaCl, 8mM Na_2HPO_4) in diethyl pyrocarbonate (DEPC-treated) water, with a final concentration of cells at approximately $2x10^7$ cells/mL. 20µL of the infectious RNA and 400µL of the cell suspension were added to a 0.5cm gap-length cuvette. The RNA was introduced into the BHK-21 cells by electroporation (Liljestrom and Garoff, 1991) under the following conditions: 1.5kV, 25µF and ∞ resistance. Cells were pulsed once and allowed to rest for 10 minutes before transferring them to 10mL MEM and incubated at 37°C and 5% CO_2 until cytopathic effect (CPE) was visible. The supernatant was collected, quick-frozen in liquid nitrogen and stored at -80°C until needed.

Production and purification of furin sensitive virus

90% confluent BHK-21 monolayers were infected with 200µL of the tranfection supernatant and incubated at 25°C for 1 hour. 4.8mL of MEM was added to the cells and the cells were incubated at 37C and 5% CO_2 until CPE was visible. Supernatant of cells showing CPE was harvested and centrifuged at low speed in a clinical centrifuge to remove large cell debris. The remaining supernatant was purified by isopycnic tartrate gradient centrifugation as described previously (Coombs and Brown, 1987a).

Metabolic Labeling, Immunoprecipitation and SDS-PAGE

Metabolic labeling and immunoprecipitation using anti-whole-virus rabbit IgG were done as described previously (Nelson et al., 2005). Briefly, 85-90% confluent monolayers of BHK-21 were infected with 1mL of virus diluted with 1X PBS-D supplemented with 3% FBS to a MOI of 0.03-0.3 pfu/mL. The monolayers were incubated with the virus for one hour at room temperature followed by incubation at 37°C and 5% CO_2. 6.5 hours post-infection, 5mL of media containing 4ug/mL Actinomycin-D was added to the washed cells and returned to 37C to incubate for one hour. 50uCi of [35S]methionine-cysteine (Met/Cys)/ml in 5mL of starvation media were added and returned to 37C and 5% CO2 until advanced cytopathic effect was seen. Samples were filtered, where indicated, through a Sephadex G25 column to remove excess label and concentrate the sample. SDS-PAGE was carried out under denaturing conditions (0.1% SDS) in 10.8% or 12.5% polyacrylamide gels as described previously (Liu and Brown, 1993). Autoradiographs of labeled proteins were processed as described previously (Liu and Brown, 1993).

Titration of furin sensitive virus

Titration of the E1-392/E2-341 double mutant was done on BHK-21 cells. BHK-21 cells were grown in 25cm^2 flasks to 90% confluence for the titration. Virus was stored in tartrate at 4°C for no more than one day before dilutions were made. Dilutions from 1x10^{-1} to 1x10^{-10} were made of both stock wild-type virus and the double mutant and kept on ice until used. 200µL of each dilution was overlayed onto the monolayers and allowed to adsorb for 1 hour at room temperature. After adsorption, the dilution was removed from the flask and the cells were overlayed with 2% agarose in 1X MEM and incubated at 37°C with 5% CO_2 for two days. After two days, the cells were stained with 2% neutral red in 1% agarose in 1X PBS-D until plaques were visible; approximately 4 hours.

Scanning electron microscopy

BHK-21 cells were transfected by electroporation with wild-type and furin mutants and incubated for 16-18 hours on 12mm glass coverslips treated for 5 minutes with a 1% poly-D-lysine solution. Incubated cells were fixed over night at 4°C with 3% glutaraldehyde in 0.1M cacodylic acid buffer (pH 7.4). Fixed cells were washed three times and subjected to ethanol dehydration before dried in a Tousimis Sandri 795 (Tousimis Research, Rockville, MD) critical point dryer and coated with 25Å of gold-palladium using a Hummer 6.2 Sputter Coater (Anatech USA, Hayward, CA). Coated samples were imaged on a JEOL JSM5900LV scanning electron microscope (JEOL USA, Peabody, MA).

Transmission electron microscopy

Thin-sections

BHK-21 cells were infected by virus from transfections and incubated for 16-18 hours, after which the cells were removed from the flask by versine (0.1M EDTA and 0.5% phenol Red in 1X PBS-D), pelleted by low-speed centrifugation and fixed with 3% glutaraldehyde in 0.1M cacodylic acid buffer (pH 7.4). Fixed cells were washed with 0.1M cacodylic acid three times and then embedded into 1% agarose and cut into 1mm squares. The samples were then pre-stained with 1% uranyl acetate overnight at 4°C. The samples were then washed and ethanol dehydrated by a series of soaks in higher percentage ethanol. SPURR compound (LADD Research Industries, Williston, VT) was used to infiltrate the samples after dehydration, following a step gradient from mostly ethanol to only SPURR.

The blocks were trimmed on an LKB NOVA Ultotome and thin sections were stained with 5% uranyl acetate for 1 hour and lead citrate (pH12) for 4 minutes. Samples were then examined on a JEOL JEM 100S transmission electron microscope.

Negative contrast staining

Purified virus from tartrate gradients were attached to carbon-coated copper grids, washed three times with distilled water and stained with 1% uranyl acetate before viewing on a JEOL JEM 100s transmission electron microscope.

Chapter 3:

Cells, media and virus production

Mosquito (U4.4) cells were maintained as described in (Hernandez, Sinodis, and Brown, 2010) at 28C with 20% FBS supplemented Mitsuhashi and Maramorosch (M&M) media. Virus was produced from the cDNA clone TOTO1101. Virus was harvested from the supernatant of infected C7/10 cells two days post infection and purified using isopycnic tartrate gradient centrifugation as described in (Coombs and Brown, 1987b). Purified virus was stored at 4C until needed.

Titration and protein concentration of purified virus

Titration of purified virus was done on BHK-21 cells as described in (Hernandez, Sinodis, and Brown, 2010). Briefly, BHK-21 cells were grown in 25 cm^2 flasks to 90% confluence for the titration. Dilutions from 1 x 10^{-1} to 1 x 10^{-14} were made of both stock wild-type and the purified virus and kept on ice until used. 200uL of each dilution was overlayed onto the monolayers and allowed to adsorb for 1 h at room temperature followed by removal from the flask and overlay with 2% agarose in 1x MEM. The flasks were incubated at 37 C with 5% CO2 for 2 days, after which cells were stained with 2% neutral red in 1% agarose in 1x PBS-D until plaques were visible. Virus protein concentration was determined using the BCA Protein Assay Kit (Pierce Biotechnology, Rockford, Il).

Virus adsorption and Bafilomycin A_1 ($BafA_1$) treatment

Uninfected U4.4 cells and U4.4 cells incubated with $BafA_1$ for 1 h at 4C were fixed with 3% glutaraldehyde in 0.1M cacodylic acid buffer (pH 7.4). SV, with a particle/pfu ratio of 2, was adsorbed onto untreated U4.4 cells at an MOI $\geq$100,000 for 0.5 h at 4C. SV was also adsorbed onto $BafA_1$ treated U4.4 cells at 4C and room temperature using the same MOI. Samples were then washed with 1x PBS-D, pelleted by low-speed centrifugation and fixed with 3% glutaraldehyde in 0.1M cacodylic acid buffer. The samples were split in half for thin-sections and freeze fracture.

Transmission Electron Microscopy

<u>Thin-sections</u>

Samples were washed with 0.1M cacodylic acid buffer three times, and then fixed in 2% OsO_4 for 1 h on ice. Fixed samples were washed three times in 0.1M cacodylic buffer, embedded into 1% agarose and cut into 1mm cubes. The samples were then pre-stained in 1% uranyl acetate overnight at 4C. Pre-stained samples were washed then ethanol dehydrated by a series of soaks in increasing percentages of ethanol. Samples were then infiltrated by SPURR compound (LADD Research Industries, Williston, VT) stepwise from mostly ethanol to only SPURR. Blocks were trimmed on an LKB NOVA Ultotome and thin sections were stained with 5% Uranyl Acetate for 1 h and lead citrate (pH 12) for 4 min. Samples were examined on a Philips 400T transmission electron microscope.

Freeze-fracture replication, cleaning and labeling

Samples used for freeze-fracture were glycerinated overnight at 4C in 1x PBS-D containing 30% glycerol (v/v). These samples were pelleted using low-speed centrifugation and the supernatant most completely removed. The remaining cell pellet was resuspended in the remaining supernatant and frozen on Balzer gold specimen holders (Leica Microsystems, Bannockburn, Il) by plunge-freezing into liquid nitrogen cooled ethane in a custom built plunge-freezer. Samples were stored under liquid nitrogen until fractured. Samples were fractured in a Cressington CFE-60 (Cressington Scientific Instruments, Watford WD19 4BX, England) at a vacuum of approximately 1 x 10^{-7} mbar and a temperature of 111K. Samples were unidirectionally shadowed at 45° using 1nm Pt/C and supported with 12nm of carbon deposited normal to the sample. The sample was rotated while coating with carbon.

Replicas were cleaned as in (Suzuki et al., 2008) by floating onto SDS-digestion buffer (15mM Tris-HCl, 2.5% SDS, 20% Sucrose, pH 8.3) and incubated at 121C for 30min. After cooling, the replicas were washed three times in wash buffer (25 mM Tris–HCl, 0.1% Tween-20, 137 mM NaCl, 2.7 mM KCl, 0.05% BSA, 0.05% NaN_3, pH 7.4) and blocked in blocking buffer (5% BSA in wash buffer) for 30min. After blocking, replicas were transferred to rabbit anti-SV antibody NCSU66 (1:200 dilution) in blocking buffer overnight at 4C. Rabbit anti-V-type H^+-ATPase antibody against the C1 subunit was also used at a dilution of 1:1000 and left for 22 hours at 4C to adsorb. Replicas were then washed three times in wash buffer, blocked for 30min in blocking buffer and incubated with goat anti-rabbit IgG secondary antibody conjugated to 6 or 12nm colloidal gold beads (Jackson ImmunoResearch, West Grove, PA) for 1h at room temperature. Labeled replicas were washed again three times in wash buffer, twice in distilled water and collected on Butvar coated 200-mesh or uncoated 400-mesh copper grids. Images of replicas were collected on a Philips 400T transmission electron microscope. Stereo images were collected by tilting the stage ±4°.

Chapter 6

References

(2007). Update: chikungunya fever diagnosed among international travelers--United States, 2006. *MMWR Morb Mortal Wkly Rep* **56**(12)**,** 276-7.

Abell, B. A., and Brown, D. T. (1993). Sindbis virus membrane fusion is mediated by reduction of glycoprotein disulfide bridges at the cell surface. *J Virol* **67**(9)**,** 5496-501.

Aguilar, P. V., Adams, A. P., Wang, E., Kang, W., Carrara, A. S., Anishchenko, M., Frolov, I., and Weaver, S. C. (2008). Structural and nonstructural protein genome regions of eastern equine encephalitis virus are determinants of interferon sensitivity and murine virulence. *J Virol* **82**(10)**,** 4920-30.

Ahn, A., Klimjack, M. R., Chatterjee, P. K., and Kielian, M. (1999). An epitope of the Semliki Forest virus fusion protein exposed during virus-membrane fusion. *J Virol* **73**(12)**,** 10029-39.

Akhtar, J., and Shukla, D. (2009). Viral entry mechanisms: cellular and viral mediators of herpes simplex virus entry. *FEBS J* **276**(24)**,** 7228-36.

Angelini, R., Finarelli, A. C., Angelini, P., Po, C., Petropulacos, K., Macini, P., Fiorentini, C., Fortuna, C., Venturi, G., Romi, R., Majori, G., Nicoletti, L., Rezza, G., and Cassone, A. (2007). An outbreak of chikungunya fever in the province of Ravenna, Italy. *Euro Surveill* **12**(9)**,** E070906 1.

Anthony, R. P., Paredes, A. M., and Brown, D. T. (1992). Disulfide bonds are essential for the stability of the Sindbis virus envelope. *Virology* **190**(1)**,** 330-6.

Barton, D. J., Sawicki, S. G., and Sawicki, D. L. (1988). Demonstration in vitro of temperature-sensitive elongation of RNA in Sindbis virus mutant ts6. *J Virol* **62**(10)**,** 3597-602.

Barton, D. J., Sawicki, S. G., and Sawicki, D. L. (1991). Solubilization and immunoprecipitation of alphavirus replication complexes. *J Virol* **65**(3)**,** 1496-506.

Belnap, D. M., Filman, D. J., Trus, B. L., Cheng, N., Booy, F. P., Conway, J. F., Curry, S., Hiremath, C. N., Tsang, S. K., Steven, A. C., and Hogle, J. M. (2000). Molecular tectonic model of virus structural transitions: the putative cell entry states of poliovirus. *J Virol* **74**(3)**,** 1342-54.

Bowman, B. J., McCall, M. E., Baertsch, R., and Bowman, E. J. (2006). A model for the proteolipid ring and bafilomycin/concanamycin-binding site in the vacuolar ATPase of Neurospora crassa. *J Biol Chem* **281**(42)**,** 31885-93.

Brault, A. C., Powers, A. M., and Weaver, S. C. (2002). Vector infection determinants of Venezuelan equine encephalitis virus reside within the E2 envelope glycoprotein. *J Virol* **76**(12)**,** 6387-92.

Brown, D. T., and Condreay, L. D. (1986). Replication of Alphaviruses in Mosquito Cells. *In* "The Togaveriridae and Flaviviridae" (M. J. Schlesinger, Ed.), pp. 171-207. Plenum Publishing Corporation.

Brown, D. T., and Riedel, B. (1977). Morphogenesis of vesicular stomatitis virus: electron microscope observations with freeze-fracture techniques. *J Virol* **21**(2)**,** 601-9.

Brown, D. T., Waite, M. R., and Pfefferkorn, E. R. (1972a). Morphology and morphogenesis of Sindbis virus as seen with freeze-etching techniques. *J Virol* **10**(3)**,** 524-36.

Brown, D. T., Waite, M. R. F., and Pfefferkorn, E. R. (1972b). Morphology and Morphogenesis of Sindbis virus as seen with freeze-etching techniques. *J. Virol.* **10,** 534-536.

Brown, D. T., Westphal, M., Burlingham, B. T., Winterhoff, U., and Doerfler, W. (1975). Structure and composition of the adenovirus type 2 core. *J Virol* **16**(2)**,** 366-87.

Byrnes, A. P., and Griffin, D. E. (1998). Binding of Sindbis virus to cell surface heparan sulfate. *J Virol* **72**(9)**,** 7349-56.

Carleton, M., and Brown, D. T. (1996a). Disulfide bridge-mediated folding of Sindbis virus glycoproteins. *J Virol* **70**(8)**,** 5541-7.

Carleton, M., and Brown, D. T. (1996b). Events in the endoplasmic reticulum abrogate the temperature sensitivity of Sindbis virus mutant ts23. *J Virol* **70**(2)**,** 952-9.

Carleton, M., Lee, H., Mulvey, M., and Brown, D. T. (1997). Role of glycoprotein PE2 in formation and maturation of the Sindbis virus spike. *J Virol* **71**(2)**,** 1558-66.

Caspar, D. L. D., and Klug, A. (1962). Physical principles in the construction of regular viruses. *Cold Spring Harbor Symp. Quant. Biol.* **27,** 1-24.

Choi, H. K., Lu, G., Lee, S., Wengler, G., and Rossmann, M. G. (1997). Structure of Semliki Forest virus core protein. *Proteins* **27**(3)**,** 345-59.

Cipriano, D. J., Wang, Y., Bond, S., Hinton, A., Jefferies, K. C., Qi, J., and Forgac, M. (2008). Structure and regulation of the vacuolar ATPases. *Biochim Biophys Acta* **1777**(7-8)**,** 599-604.

Coombs, K., and Brown, D. T. (1987a). Organization of the Sindbis virus nucleocapsid as revealed by bifunctional cross-linking agents. *J Mol Biol* **195**(2)**,** 359-71.

Coombs, K., and Brown, D. T. (1987b). Topological organization of Sindbis virus capsid protein in isolated nucleocapsids. *Virus Res* **7**(2)**,** 131-49.

Coombs, K., Mann, E., Edwards, J., and Brown, D. T. (1981). Effects of chloroquine and cytochalasin B on the infection of cells by Sindbis virus and vesicular stomatitis virus. *J Virol* **37**(3)**,** 1060-5.

Cox, E. C. (1976). Bacterial mutator genes and the control of spontaneous mutation. *Annu Rev Genet* **10,** 135-56.

de Curtis, I., and Simons, K. (1988). Dissection of Semliki Forest virus glycoprotein delivery from the trans-Golgi network to the cell surface in permeabilized BHK cells. *Proc Natl Acad Sci U S A* **85**(21)**,** 8052-6.

de Groot, R. J., Hardy, W. R., Shirako, Y., and Strauss, J. H. (1990). Cleavage-site preferences of Sindbis virus polyproteins containing the non-structural proteinase. Evidence for temporal regulation of polyprotein processing in vivo. *Embo J* **9**(8)**,** 2631-8.

DeTulleo, L., and Kirchhausen, T. (1998). The clathrin endocytic pathway in viral infection. *Embo J* **17**(16)**,** 4585-93.

Dhileepan, K., Azuolas, J. K., and Gibson, C. A. (1996). Evidence of vertical transmission of Ross River and Sindbis viruses (Togaviridae: Alphavirus) by mosquitoes (Diptera: Culicidae) in southeastern Australia. *J Med Entomol* **33**(1)**,** 180-2.

Ding, M. X., and Schlesinger, M. J. (1989). Evidence that Sindbis virus NSP2 is an autoprotease which processes the virus nonstructural polyprotein. *Virology* **171**(1)**,** 280-4.

Durbin, R. K., and Stollar, V. (1985). Sindbis virus mutants able to replicate in methionine-deprived Aedes albopictus cells. *Virology* **144**(2)**,** 529-33.

Edwards, J., and Brown, D. T. (1986). Sindbis virus-mediated cell fusion from without is a two-step event. *J Gen Virol* **67**(Pt 2)**,** 377-80.

Edwards, J., and Brown, D. T. (1991). Sindbis virus infection of a Chinese hamster ovary cell mutant defective in the acidification of endosomes. *Virology* **182**(1)**,** 28-33.

Ferreira, D., Hernandez, R., Horton, M., and Brown, D. T. (2003a). Morphological variants of Sindbis virus produced by a mutation in the capsid protein. *Virology* **307**(1)**,** 54-66.

Ferreira, D. F., Hernandez, R., Horton, M., and Brown, D. T. (2003b). Morphological variants of Sindbis virus produced by a mutation in the capsid protein. *Virology* **307**(1)**,** 54-66.

Finch, J. T., and Klug, A. (1965). The structure of viruses of the papilloma-polyoma type 3. Structure of rabbit papilloma virus, with an appendix on the topography of contrast in negative-staining for electron-microscopy. *J Mol Biol* **13**(1)**,** 1-12.

Flynn, D. C., Meyer, W. J., Mackenzie, J. M., Jr., and Johnston, R. E. (1990). A conformational change in Sindbis virus glycoproteins E1 and E2 is detected at the plasma membrane as a consequence of early virus-cell interaction. *J Virol* **64**(8)**,** 3643-53.

Follett, E. A., and Goldman, R. D. (1970). The occurrence of microvilli during spreading and growth of BHK21-C13 fibroblasts. *Exp Cell Res* **59**(1)**,** 124-36.

Frolova, E. I., Gorchakov, R., Pereboeva, L., Atasheva, S., and Frolov, I. (2010). Functional Sindbis virus replicative complexes are formed at the plasma membrane. *J Virol* **84**(22)**,** 11679-95.

Fujimoto, K. (1995). Freeze-fracture replica electron microscopy combined with SDS digestion for cytochemical labeling of integral membrane proteins. Application to the immunogold labeling of intercellular junctional complexes. *J Cell Sci* **108 (Pt 11),** 3443-9.

Fujimoto, K. (1997). SDS-digested freeze-fracture replica labeling electron microscopy to study the two-dimensional distribution of integral membrane proteins and phospholipids in biomembranes: practical procedure, interpretation and application. *Histochem Cell Biol* **107**(2)**,** 87-96.

Fukuyama, K., Abdel-Meguid, S. S., and Rossmann, M. G. (1981). Crystallization of alfalfa mosaic virus coat protein as a T = 1 aggregate. *J Mol Biol* **150**(1)**,** 33-41.

Fulhorst, C. F., Hardy, J. L., Eldridge, B. F., Presser, S. B., and Reeves, W. C. (1994). Natural vertical transmission of western equine encephalomyelitis virus in mosquitoes. *Science* **263**(5147)**,** 676-8.

Gao, W. Y., Quinn, P. J., and Yu, Z. W. (2008). The role of sterol rings and side chain on the structure and phase behaviour of sphingomyelin bilayers. *Mol Membr Biol* **25**(6-7)**,** 485-97.

Garoff, H., Huylebroeck, D., Robinson, A., Tillman, U., and Liljestrom, P. (1990). The signal sequence of the p62 protein of Semliki Forest virus is involved in initiation but not in completing chain translocation. *J Cell Biol* **111**(3)**,** 867-76.

Gibbons, D. L., Reilly, B., Ahn, A., Vaney, M. C., Vigouroux, A., Rey, F. A., and Kielian, M. (2004a). Purification and crystallization reveal two types of interactions of the fusion protein homotrimer of Semliki Forest virus. *J Virol* **78**(7)**,** 3514-23.

Gibbons, D. L., Vaney, M. C., Roussel, A., Vigouroux, A., Reilly, B., Lepault, J., Kielian, M., and Rey, F. A. (2004b). Conformational change and protein-protein interactions of the fusion protein of Semliki Forest virus. *Nature* **427**(6972)**,** 320-5.

Glanville, N., and Ulmanen, I. (1976). Biological activity of in vitro synthesised protein: binding of Semliki Forest virus capsid protein to the large ribosomal subunit. *Biochem Biophys Res Commun* **71**(1)**,** 393-9.

Glickman, B. W., and Radman, M. (1980). Escherichia coli mutator mutants deficient in methylation-instructed DNA mismatch correction. *Proc Natl Acad Sci U S A* **77**(2)**,** 1063-7.

Gliedman, J. B., Smith, J. F., and Brown, D. T. (1975). Morphogenesis of Sindbis virus in cultured Aedes albopictus cells. *J Virol* **16**(4)**,** 913-26.

Glomb-Reinmund, S., and Kielian, M. (1998). fus-1, a pH shift mutant of Semliki Forest virus, acts by altering spike subunit interactions via a mutation in the E2 subunit. *J Virol* **72**(5)**,** 4281-7.

Gorbalenya, A. E., Koonin, E. V., Donchenko, A. P., and Blinov, V. M. (1989). Two related superfamilies of putative helicases involved in replication, recombination, repair and expression of DNA and RNA genomes. *Nucleic Acids Res* **17**(12)**,** 4713-30.

Greene, I. P., Paessler, S., Austgen, L., Anishchenko, M., Brault, A. C., Bowen, R. A., and Weaver, S. C. (2005a). Envelope glycoprotein mutations mediate equine amplification and virulence of epizootic venezuelan equine encephalitis virus. *J Virol* **79**(14)**,** 9128-33.

Greene, I. P., Wang, E., Deardorff, E. R., Milleron, R., Domingo, E., and Weaver, S. C. (2005b). Effect of alternating passage on adaptation of sindbis virus to vertebrate and invertebrate cells. *J Virol* **79**(22)**,** 14253-60.

Hafer, A., Whittlesey, R., Brown, D. T., and Hernandez, R. (2009). Differential incorporation of cholesterol by Sindbis virus grown in mammalian or insect cells. *J Virol* **83**(18)**,** 9113-21.

Hahn, Y. S., Grakoui, A., Rice, C. M., Strauss, E. G., and Strauss, J. H. (1989). Mapping of RNA- temperature-sensitive mutants of Sindbis virus: complementation group F mutants have lesions in nsP4. *J Virol* **63**(3)**,** 1194-202.

Hahn, Y. S., Strauss, E. G., and Strauss, J. H. (1989). Mapping of RNA- temperature-sensitive mutants of Sindbis virus: assignment of complementation groups A, B, and G to nonstructural proteins. *J Virol* **63**(7)**,** 3142-50.

Hanada, H., Moriyama, Y., Maeda, M., and Futai, M. (1990). Kinetic studies of chromaffin granule H+-ATPase and effects of bafilomycin A1. *Biochem Biophys Res Commun* **170**(2)**,** 873-8.

Hardy, W. R., and Strauss, J. H. (1989). Processing the nonstructural polyproteins of sindbis virus: nonstructural proteinase is in the C-terminal half of nsP2 and functions both in cis and in trans. *J Virol* **63**(11)**,** 4653-64.

Harkness, J. W., Alexander, D. J., Pattison, M., and Scott, A. C. (1975). Infectious bursal disease agent: morphology by negative stain electron microscopy. *Arch Virol* **48**(1)**,** 63-73.

Harrison, S. C. (2008). Viral membrane fusion. *Nat Struct Mol Biol* **15**(7)**,** 690-8.

He, L., Piper, A., Meilleur, F., Myles, D. A., Hernandez, R., Brown, D. T., and Heller, W. T. The structure of Sindbis virus produced from vertebrate and invertebrate hosts as determined by small-angle neutron scattering. *J Virol* **84**(10)**,** 5270-6.

Heldt, C. L., Hernandez, R., Mudiganti, U., Gurgel, P. V., Brown, D. T., and Carbonell, R. G. (2006). A colorimetric assay for viral agents that produce cytopathic effects. *J Virol Methods*.

Helenius, A., Marsh, M., and White, J. (1982). Inhibition of Semliki forest virus penetration by lysosomotropic weak bases. *J Gen Virol* **58 Pt 1,** 47-61.

Helenius, A., Morein, B., Fries, E., Simons, K., Robinson, P., Schirrmacher, V., Terhorst, C., and Strominger, J. L. (1978). Human (HLA-A and HLA-B) and murine (H-2K and H-2D) histocompatibility antigens are cell surface receptors for Semliki Forest virus. *Proc Natl Acad Sci U S A* **75**(8)**,** 3846-50.

Hernandez, R., Ferreira, D., Sinodis, C., Litton, K., and Brown, D. T. (2005). Single amino acid insertions at the junction of the sindbis virus E2 transmembrane domain and endodomain disrupt virus envelopment and alter infectivity. *J Virol* **79**(12)**,** 7682-97.

Hernandez, R., Lee, H., Nelson, C., and Brown, D. T. (2000). A single deletion in the membrane-proximal region of the Sindbis virus glycoprotein E2 endodomain blocks virus assembly. *J Virol* **74**(9)**,** 4220-8.

Hernandez, R., Luo, T., and Brown, D. T. (2001). Exposure to low pH is not required for penetration of mosquito cells by Sindbis virus. *J Virol* **75**(4)**,** 2010-3.

Hernandez, R., Sinodis, C., and Brown, D. T. (2010). Sindbis virus: propagation, quantification, and storage. *Curr Protoc Microbiol* **Chapter 15,** Unit15B 1.

Hernandez, R., Sinodis, C., Horton, M., Ferreira, D., Yang, C., and Brown, D. T. (2003). Deletions in the transmembrane domain of a sindbis virus glycoprotein alter virus infectivity, stability, and host range. *J Virol* **77**(23)**,** 12710-9.

Hodgman, T. C. (1988). A new superfamily of replicative proteins. *Nature* **333**(6168)**,** 22-3.

Hogle, J. M. (2002). Poliovirus cell entry: common structural themes in viral cell entry pathways. *Annu Rev Microbiol* **56,** 677-702.

Hung, T., Chou, C., Fang, C., and Chang, Z. (1980). Morphogenesis of vaccinia virus in the process of envelopment as observed by freeze-etching electron microscopy. *Intervirology* **14**(2)**,** 91-100.

Hunt, S. R., Hernandez, R., and Brown, D. T. (2011a). Role of the vacuolar-ATPase in Sindbis virus infection. *J Virol* **85**(3)**,** 1257-66.

Hunt, S. R., Hernandez, R., and Brown, D. T. (2011b). The Role of the Vacuolar-ATPase in Sindbis Virus Infection. *J Virol*.

Huss, M., and Wieczorek, H. (2009). Inhibitors of V-ATPases: old and new players. *J Exp Biol* **212**(Pt 3)**,** 341-6.

Ivanovic, T., Agosto, M. A., Zhang, L., Chandran, K., Harrison, S. C., and Nibert, M. L. (2008). Peptides released from reovirus outer capsid form membrane pores that recruit virus particles. *EMBO J* **27**(8)**,** 1289-98.

Johnston, R. E., Wan, K., and Bose, H. R. (1974). Homologous interference induced by Sindbis virus. *Journal of Virology* **14**(5)**,** 1076-1082.

Kamer, G., and Argos, P. (1984). Primary structural comparison of RNA-dependent polymerases from plant, animal and bacterial viruses. *Nucleic Acids Res* **12**(18)**,** 7269-82.

Karpf, A. R., Lenches, E., Strauss, E. G., Strauss, J. H., and Brown, D. T. (1997). Superinfection exclusion of alphaviruses in three mosquito cell lines persistently infected with Sindbis virus. *J Virol* **71**(9)**,** 7119-23.

Keller, P. W., Johnson, M. C., and Vogt, V. M. (2008). Mutations in the spacer peptide and adjoining sequences in Rous sarcoma virus Gag lead to tubular budding. *J Virol* **82**(14)**,** 6788-97.

Keranen, S., and Kaariainen, L. (1979). Functional defects of RNA-negative temperature-sensitive mutants of Sindbis and Semliki Forest viruses. *J Virol* **32**(1)**,** 19-29.

Kielian, M., and Jungerwirth, S. (1990). Mechanisms of enveloped virus entry into cells. *Mol Biol Med* **7**(1)**,** 17-31.

Kielian, M. C., and Helenius, A. (1984). Role of cholesterol in fusion of Semliki Forest virus with membranes. *J Virol* **52**(1)**,** 281-3.

Kielian, M. C., Keranen, S., Kaariainen, L., and Helenius, A. (1984). Membrane fusion mutants of Semliki Forest virus. *J Cell Biol* **98**(1)**,** 139-45.

Kielian, M. C., Marsh, M., and Helenius, A. (1986). Kinetics of endosome acidification detected by mutant and wild-type Semliki Forest virus. *Embo J* **5**(12)**,** 3103-9.

Kinney, R. M., Johnson, B. J., Brown, V. L., and Trent, D. W. (1986). Nucleotide sequence of the 26 S mRNA of the virulent Trinidad donkey strain of Venezuelan equine encephalitis virus and deduced sequence of the encoded structural proteins. *Virology* **152**(2)**,** 400-13.

Kiselev, N. A., and Klug, A. (1969). The structure of viruses of the papilloma-polyoma type. V. Tubular variants built of pentamers. *J Mol Biol* **40**(2)**,** 155-71.

Klimstra, W. B., Nangle, E. M., Smith, M. S., Yurochko, A. D., and Ryman, K. D. (2003). DC-SIGN and L-SIGN can act as attachment receptors for alphaviruses and distinguish between mosquito cell- and mammalian cell-derived viruses. *J Virol* **77**(22)**,** 12022-32.

Klimstra, W. B., Ryman, K. D., and Johnston, R. E. (1998). Adaptation of sindbis virus to BHK cells selects for use of heparan sulfate as an attachment receptor. *J Virol* **72**(9)**,** 7357-66.

Klug, A., and Finch, J. T. (1965). Structure of Viruses of the Papilloma-Polyoma Type. I. Human Wart Virus. *J Mol Biol* **11,** 403-23.

Kononchik, J. P., Jr., Nelson, S., Hernandez, R., and Brown, D. T. (2009). Helical virus particles formed from morphological subunits of a membrane containing icosahedral virus. *Virology* **385**(2)**,** 285-93.

Koschinski, A., Wengler, G., and Repp, H. (2005). Rare earth ions block the ion pores generated by the class II fusion proteins of alphaviruses and allow analysis of the biological functions of these pores. *J Gen Virol* **86**(Pt 12)**,** 3311-20.

Lakadamyali, M., Rust, M. J., and Zhuang, X. (2004). Endocytosis of influenza viruses. *Microbes Infect* **6**(10)**,** 929-36.

Lawley, P. D., and Orr, D. J. (1970). Specific excision of methylation products from DNA of Escherichia coli treated with N-methyl-N'-nitro-N-nitrosoguanidine. *Chem Biol Interact* **2**(2)**,** 154-7.

Ledrans, M., Quatresous, I., Renault, P., and Pierre, V. (2007). Outbreak of chikungunya in the French Territories, 2006: lessons learned. *Euro Surveill* **12**(9)**,** E070906 3.

Lehmann, M. J., Sherer, N. M., Marks, C. B., Pypaert, M., and Mothes, W. (2005). Actin- and myosin-driven movement of viruses along filopodia precedes their entry into cells. *J Cell Biol* **170**(2)**,** 317-25.

Lemm, J. A., Durbin, R. K., Stollar, V., and Rice, C. M. (1990). Mutations which alter the level or structure of nsP4 can affect the efficiency of Sindbis virus replication in a host-dependent manner. *J Virol* **64**(6)**,** 3001-11.

Lemm, J. A., and Rice, C. M. (1993). Roles of nonstructural polyproteins and cleavage products in regulating Sindbis virus RNA replication and transcription. *J Virol* **67**(4)**,** 1916-26.

Lemm, J. A., Rumenapf, T., Strauss, E. G., Strauss, J. H., and Rice, C. M. (1994). Polypeptide requirements for assembly of functional Sindbis virus replication complexes: a model for the temporal regulation of minus- and plus-strand RNA synthesis. *Embo J* **13**(12)**,** 2925-34.

Lescar, J., Roussel, A., Wien, M. W., Navaza, J., Fuller, S. D., Wengler, G., and Rey, F. A. (2001). The Fusion glycoprotein shell of Semliki Forest virus: an icosahedral assembly primed for fusogenic activation at endosomal pH. *Cell* **105**(1)**,** 137-48.

Li, G. P., La Starza, M. W., Hardy, W. R., Strauss, J. H., and Rice, C. M. (1990). Phosphorylation of Sindbis virus nsP3 in vivo and in vitro. *Virology* **179**(1)**,** 416-27.

Li, L., Jose, J., Xiang, Y., Kuhn, R. J., and Rossmann, M. G. (2010). Structural changes of envelope proteins during alphavirus fusion. *Nature* **468**(7324)**,** 705-8.

Liljestrom, P., and Garoff, H. (1991). Internally located cleavable signal sequences direct the formation of Semliki Forest virus membrane proteins from a polyprotein precursor. *J Virol* **65**(1)**,** 147-54.

Liu, N., and Brown, D. T. (1993). Transient translocation of the cytoplasmic (endo) domain of a type I membrane glycoprotein into cellular membranes. *J Cell Biol* **120**(4)**,** 877-83.

Loveless, A. (1969). Possible relevance of O-6 alkylation of deoxyguanosine to the mutagenicity and carcinogenicity of nitrosamines and nitrosamides. *Nature* **223**(5202)**,** 206-7.

Lu, Y. E., Cassese, T., and Kielian, M. (1999). The cholesterol requirement for sindbis virus entry and exit and characterization of a spike protein region involved in cholesterol dependence. *J Virol* **73**(5)**,** 4272-8.

Lucchesi, P., Carraway, M., and Marinus, M. G. (1986). Analysis of forward mutations induced by N-methyl-N'-nitro-N-nitrosoguanidine in the bacteriophage P22 mnt repressor gene. *J Bacteriol* **166**(1)**,** 34-7.

Lundstrom, K. H., Bamford, D. H., Palva, E. T., and Lounatmaa, K. (1979). Lipid-containing bacteriophage PR4: structure and life cycle. *J Gen Virol* **43**(3)**,** 583-92.

Lusa, S., Garoff, H., and Liljestrom, P. (1991). Fate of the 6K membrane protein of Semliki Forest virus during virus assembly. *Virology* **185**(2)**,** 843-6.

Maassen, J. A., and Terhorst, C. (1981). Identification of a cell-surface protein involved in the binding site of Sindbis virus on human lymphoblastic cell lines using a heterobifunctional cross-linker. *Eur J Biochem* **115**(1)**,** 153-8.

Madan, V., Sanz, M. A., and Carrasco, L. (2005). Requirement of the vesicular system for membrane permeabilization by Sindbis virus. *Virology* **332,** 307-315.

Malet, H., Coutard, B., Jamal, S., Dutartre, H., Papageorgiou, N., Neuvonen, M., Ahola, T., Forrester, N., Gould, E. A., Lafitte, D., Ferron, F., Lescar, J., Gorbalenya, A. E., de Lamballerie, X., and Canard, B. (2009). The crystal structures of Chikungunya and Venezuelan equine encephalitis virus nsP3 macro domains define a conserved adenosine binding pocket. *J Virol* **83**(13)**,** 6534-45.

Markham, R., Frey, S., and Hills, G. J. (1963). Methods for Enhancement of Image Detail and Accentuation of Structure in Electron Microscopy. *Virology* **20**(1)**,** 88-&.

Marsh, M., Bolzau, E., and Helenius, A. (1983). Penetration of Semliki Forest virus from acidic prelysosomal vacuoles. *Cell* **32**(3)**,** 931-40.

Marsh, M., Wellsteed, J., Kern, H., Harms, E., and Helenius, A. (1982). Monensin inhibits Semliki Forest virus penetration into culture cells. *Proc Natl Acad Sci U S A* **79**(17)**,** 5297-301.

Mavale, M., Parashar, D., Sudeep, A., Gokhale, M., Ghodke, Y., Geevarghese, G., Arankalle, V., and Mishra, A. C. (2010). Venereal transmission of chikungunya virus by Aedes aegypti mosquitoes (Diptera: Culicidae). *Am J Trop Med Hyg* **83**(6)**,** 1242-4.

McGuire, P. G., and Twietmeyer, T. A. (1983). Morphology of rapidly frozen aortic endothelial cells. Glutaraldehyde fixation increases the number of caveolae. *Circ Res* **53**(3)**,** 424-9.

Melikyan, G. B. (2008). Common principles and intermediates of viral protein-mediated fusion: the HIV-1 paradigm. *Retrovirology* **5,** 111.

Meyer, W. J., Gidwitz, S., Ayers, V. K., Schoepp, R. J., and Johnston, R. E. (1992). Conformational alteration of Sindbis virion glycoproteins induced by heat, reducing agents, or low pH. *J Virol* **66**(6)**,** 3504-13.

Mitsuhashi, J., Nakasone, S., and Horie, Y. (1983). Sterol-free eukaryotic cells from continuous cell lines of insects. *Cell Biol Int Rep* **7**(12)**,** 1057-62.

Muench, S. P., Huss, M., Song, C. F., Phillips, C., Wieczorek, H., Trinick, J., and Harrison, M. A. (2009). Cryo-electron microscopy of the vacuolar ATPase motor reveals its mechanical and regulatory complexity. *J Mol Biol* **386**(4)**,** 989-99.

Mukhopadhyay, S., Zhang, W., Gabler, S., Chipman, P. R., Strauss, E. G., Strauss, J. H., Baker, T. S., Kuhn, R. J., and Rossmann, M. G. (2006). Mapping the structure and function of the E1 and E2 glycoproteins in alphaviruses. *Structure* **14**(1)**,** 63-73.

Mulvey, M., and Brown, D. T. (1994). Formation and rearrangement of disulfide bonds during maturation of the Sindbis virus E1 glycoprotein. *J Virol* **68**(2)**,** 805-12.

Mulvey, M., and Brown, D. T. (1996). Assembly of the Sindbis virus spike protein complex. *Virology* **219**(1)**,** 125-32.

Murphy, F. A., Borden, E. C., Shope, R. E., and Harrison, A. (1971). Physicochemical and morphological relationships of some arthropod-borne viruses to bluetongue virus--a new taxonomic group. Electron microscopic studies. *J Gen Virol* **13**(2)**,** 273-88.

Nelson, S., Hernandez, R., Ferreira, D., and Brown, D. T. (2005). In vivo processing and isolation of furin protease-sensitive alphavirus glycoproteins: a new technique for producing mutations in virus assembly. *Virology* **332**(2)**,** 629-39.

Neufeld, K. L., Galarza, J. M., Richards, O. C., Summers, D. F., and Ehrenfeld, E. (1994). Identification of terminal adenylyl transferase activity of the poliovirus polymerase 3Dpol. *J Virol* **68**(9)**,** 5811-8.

Neuvonen, M., and Ahola, T. (2009). Differential activities of cellular and viral macro domain proteins in binding of ADP-ribose metabolites. *J Mol Biol* **385**(1)**,** 212-25.

Nicchia, G. P., Rossi, A., Mola, M. G., Pisani, F., Stigliano, C., Basco, D., Mastrototaro, M., Svelto, M., and Frigeri, A. (2010). Higher order structure of aquaporin-4. *Neuroscience*.

O'Neill, C. H., and Follett, E. A. (1970). An inverse relation between cell density and the numner of microvilli in cultures of BHK 21 hamster fibroblasts. *J Cell Sci* **7**(3)**,** 695-709.

Oellermann, R. A., Els, H. J., and Erasmus, B. J. (1970). Characterization of African horsesickness virus. *Arch Gesamte Virusforsch* **29**(2)**,** 163-74.

Oldstone, M. B., Tishon, A., Dutko, F. J., Kennedy, S. I., Holland, J. J., and Lampert, P. W. (1980). Does the major histocompatibility complex serve as a specific receptor for Semliki Forest virus? *J Virol* **34**(1)**,** 256-65.

Olmsted, R. A., Meyer, W. J., and Johnston, R. E. (1986). Characterization of Sindbis virus epitopes important for penetration in cell culture and pathogenesis in animals. *Virology* **148**(2)**,** 245-54.

Olsson, M., and Lindahl, T. (1980). Repair of alkylated DNA in Escherichia coli. Methyl group transfer from O6-methylguanine to a protein cysteine residue. *J Biol Chem* **255**(22)**,** 10569-71.

Onorato, L., Stirmer, B., and Showe, M. K. (1978). Isolation and characterization of bacteriophage T4 mutant preheads. *J Virol* **27**(2)**,** 409-26.

Ovenden, J. R., and Mahon, R. J. (1984). Venereal transmission of Sindbis virus between individuals of Aedes australis (Diptera: Culicidae). *J Med Entomol* **21**(3)**,** 292-5.

Paessler, S., Fayzulin, R. Z., Anishchenko, M., Greene, I. P., Weaver, S. C., and Frolov, I. (2003). Recombinant sindbis/Venezuelan equine encephalitis virus is highly attenuated and immunogenic. *J Virol* **77**(17)**,** 9278-86.

Parat, M. O. (2009). The biology of caveolae: achievements and perspectives. *Int Rev Cell Mol Biol* **273,** 117-62.

Paredes, A. M., Brown, D. T., Rothnagel, R., Chiu, W., Schoepp, R. J., Johnston, R. E., and Prasad, B. V. (1993). Three-dimensional structure of a membrane-containing virus. *Proc Natl Acad Sci U S A* **90**(19)**,** 9095-9.

Paredes, A. M., Ferreira, D., Horton, M., Saad, A., Tsuruta, H., Johnston, R., Klimstra, W., Ryman, K., Hernandez, R., Chiu, W., and Brown, D. T. (2004). Conformational changes in Sindbis virions resulting from exposure to low pH and interactions with cells suggest that cell penetration may occur at the cell surface in the absence of membrane fusion. *Virology* **324**(2)**,** 373-86.

Pelkmans, L., and Helenius, A. (2003). Insider information: what viruses tell us about endocytosis. *Curr Opin Cell Biol* **15**(4)**,** 414-22.

Pelz, E. G., and Freier, J. E. (1990). Vertical transmission of St. Louis encephalitis virus to autogenously developed eggs of Aedes atropalpus mosquitoes. *J Am Mosq Control Assoc* **6**(4)**,** 658-61.

Peranen, J. (1991). Localization and phosphorylation of Semliki Forest virus non-structural protein nsP3 expressed in COS cells from a cloned cDNA. *J Gen Virol* **72 (Pt 1),** 195-9.

Peranen, J., Takkinen, K., Kalkkinen, N., and Kaariainen, L. (1988). Semliki Forest virus-specific non-structural protein nsP3 is a phosphoprotein. *J Gen Virol* **69 (Pt 9),** 2165-78.

Perez, L., and Carrasco, L. (1994). Involvement of the vacuolar H(+)-ATPase in animal virus entry. *J Gen Virol* **75 (Pt 10),** 2595-606.

Presely, J. F., and Brown, D. T. (1989). The proteolytic cleavage of PE2 to envelope glycoprotein E2 is not strictly required for the maturation of Sindbis virus. *J Virol* **63**(5)**,** 1975-80.

Prevention, C. F. D. C. a. (2010). CDC - Chikungunya, Vol. 2010, pp. CDC Chikungunya data. cdc.gov.

Ratajczak, R. (2000). Structure, function and regulation of the plant vacuolar H(+)-translocating ATPase. *Biochim Biophys Acta* **1465**(1-2)**,** 17-36.

Ren, J., Ding, T., Zhang, W., Song, J., and Ma, W. (2007). Does Japanese encephalitis virus share the same cellular receptor with other mosquito-borne flaviviruses on the C6/36 mosquito cells? *Virol J* **4,** 83.

Renz, D., and Brown, D. T. (1976). Characteristics of Sindbis virus temperature-sensitive mutants in cultured BHK-21 and Aedes albopictus (Mosquito) cells. *J Virol* **19**(3)**,** 775-81.

Rice, C. M., Levis, R., Strauss, J. H., and Huang, H. V. (1987). Production of infectious RNA transcripts from Sindbis virus cDNA clones: mapping of lethal mutations, rescue of a temperature-sensitive marker, and in vitro mutagenesis to generate defined mutants. *J Virol* **61**(12)**,** 3809-19.

Russo, A. T., White, M. A., and Watowich, S. J. (2006). The crystal structure of the Venezuelan equine encephalitis alphavirus nsP2 protease. *Structure* **14**(9)**,** 1449-58.

Ryan, C., Stevens, T. H., and Schlesinger, M. J. (1992). Inhibitory effects of HSP70 chaperones on nascent polypeptides. *Protein Sci* **1**(8)**,** 980-5.

Samson, L., and Cairns, J. (1977). A new pathway for DNA repair in Escherichia coli. *Nature* **267**(5608)**,** 281-3.

Sawicki, D., Barkhimer, D. B., Sawicki, S. G., Rice, C. M., and Schlesinger, S. (1990). Temperature sensitive shut-off of alphavirus minus strand RNA synthesis maps to a nonstructural protein, nsP4. *Virology* **174**(1)**,** 43-52.

Sawicki, D. L., and Sawicki, S. G. (1985). Functional analysis of the A complementation group mutants of Sindbis HR virus. *Virology* **144**(1)**,** 20-34.

Sawicki, D. L., and Sawicki, S. G. (1993). A second nonstructural protein functions in the regulation of alphavirus negative-strand RNA synthesis. *J Virol* **67**(6)**,** 3605-10.

Sawicki, D. L., Sawicki, S. G., Keranen, S., and Kaariainen, L. (1981). Specific Sindbis virus-coded function for minus-strand RNA synthesis. *J Virol* **39**(2)**,** 348-58.

Scheidel, L. M., Durbin, R. K., and Stollar, V. (1987). Sindbis virus mutants resistant to mycophenolic acid and ribavirin. *Virology* **158**(1)**,** 1-7.

Schendel, P. F., and Robins, P. E. (1978). Repair of O6-methylguanine in adapted Escherichia coli. *Proc Natl Acad Sci U S A* **75**(12)**,** 6017-20.

Scheuermann, R., Tam, S., Burgers, P. M., Lu, C., and Echols, H. (1983). Identification of the epsilon-subunit of Escherichia coli DNA polymerase III holoenzyme as the dnaQ gene product: a fidelity subunit for DNA replication. *Proc Natl Acad Sci U S A* **80**(23)**,** 7085-9.

Schlesinger, M. J., London, S. D., and Ryan, C. (1993). An in-frame insertion into the Sindbis virus 6K gene leads to defective proteolytic processing of the virus glycoproteins, a trans-dominant negative inhibition of normal virus formation, and interference in virus shut off of host-cell protein synthesis. *Virology* **193**(1)**,** 424-32.

Severs, N. J., and Robenek, H. (2008). Freeze-fracture cytochemistry in cell biology. *Methods Cell Biol* **88,** 181-204.

Shabman, R. S., Morrison, T. E., Moore, C., White, L., Suthar, M. S., Hueston, L., Rulli, N., Lidbury, B., Ting, J. P., Mahalingam, S., and Heise, M. T. (2007). Differential induction of type I interferon responses in myeloid dendritic cells by mosquito and mammalian-cell-derived alphaviruses. *J Virol* **81**(1)**,** 237-47.

Sharma, A., Yu, C., and Bernatchez, P. N. (2010). New insights into caveolae, caveolins and endothelial function. *Can J Cardiol* **26 Suppl A,** 5A-8A.

Shirako, Y., and Strauss, J. H. (1994). Regulation of Sindbis virus RNA replication: uncleaved P123 and nsP4 function in minus-strand RNA synthesis, whereas cleaved products from P123 are required for efficient plus-strand RNA synthesis. *J Virol* **68**(3)**,** 1874-85.

Showe, M. K., and Onorato, L. (1978). Kinetic factors and form determination of the head of bacteriophage T4. *Proc Natl Acad Sci U S A* **75**(9)**,** 4165-9.

Shroyer, D. A. (1990). Venereal transmission of St. Louis encephalitis virus by Culex quinquefasciatus males (Diptera: Culicidae). *J Med Entomol* **27**(3)**,** 334-7.

Sieczkarski, S. B., and Whittaker, G. R. (2002). Dissecting virus entry via endocytosis. *J Gen Virol* **83**(Pt 7)**,** 1535-45.

Sjoberg, M., and Garoff, H. (2003). Interactions between the transmembrane segments of the alphavirus E1 and E2 proteins play a role in virus budding and fusion. *J Virol* **77**(6)**,** 3441-50.

Smit, J. M., Li, G., Schoen, P., Corver, J., Bittman, R., Lin, K. C., and Wilschut, J. (2002a). Fusion of alphaviruses with liposomes is a non-leaky process. *FEBS Lett* **521**(1-3)**,** 62-6.

Smit, J. M., Waarts, B. L., Kimata, K., Klimstra, W. B., Bittman, R., and Wilschut, J. (2002b). Adaptation of alphaviruses to heparan sulfate: interaction of Sindbis and Semliki forest viruses with liposomes containing lipid-conjugated heparin. *J Virol* **76**(20)**,** 10128-37.

Smith, A. L., and Tignor, G. H. (1980). Host cell receptors for two strains of Sindbis virus. *Arch Virol* **66**(1)**,** 11-26.

Spotts, D. R., Reich, R. M., Kalkhan, M. A., Kinney, R. M., and Roehrig, J. T. (1998). Resistance to alpha/beta interferons correlates with the epizootic and virulence potential of Venezuelan equine encephalitis viruses and is determined by the 5' noncoding region and glycoproteins. *J Virol* **72**(12)**,** 10286-91.

Steere, R. L. (1957). Electron microscopy of structural detail in frozen biological specimens. *J Biophys Biochem Cytol* **3**(1)**,** 45-60.

Steere, R. L. (1989). Freeze-fracture: a personal history. *J Electron Microsc Tech* **13**(3)**,** 159-64.

Strauss, E. G., Levinson, R., Rice, C. M., Dalrymple, J., and Strauss, J. H. (1988). Nonstructural proteins nsP3 and nsP4 of Ross River and O'Nyong-nyong viruses: sequence and comparison with those of other alphaviruses. *Virology* **164**(1)**,** 265-74.

Strauss, E. G., Rice, C. M., and Strauss, J. H. (1984). Complete nucleotide sequence of the genomic RNA of Sindbis virus. *Virology* **133**(1)**,** 92-110.

Strauss, E. G., and Strauss, J. H. (1986). Structure and replication of the alphavirus genome. *The Togaviridae and Flaviviridae***,** 35-90.

Strauss, J. H., and Strauss, E. G. (1994). The Alphaviruses: Gene Expression, Replication, and Evolution. Micro. Rev. 58:491-562. *Micro. Rev* **58,** 491-562.

Suzuki, H., Nishikawa, K., Hiroaki, Y., and Fujiyoshi, Y. (2008). Formation of aquaporin-4 arrays is inhibited by palmitoylation of N-terminal cysteine residues. *Biochim Biophys Acta* **1778**(4)**,** 1181-9.

Talbot, P. J., and Vance, D. E. (1980). Evidence that Sindbis virus infects BHK-21 cells via a lysosomal route. *Can J Biochem* **58**(10)**,** 1131-7.

Talbot, P. J., and Vance, D. E. (1982). Biochemical studies on the entry of sindbis virus into BHK-21 cells and the effect of NH4Cl. *Virology* **118**(2)**,** 451-5.

Tomar, S., Hardy, R. W., Smith, J. L., and Kuhn, R. J. (2006). Catalytic core of alphavirus nonstructural protein nsP4 possesses terminal adenylyltransferase activity. *J Virol* **80**(20)**,** 9962-9.

Torrisi, M. R., and Bonatti, S. (1985). Immunocytochemical study of the partition and distribution of Sindbis virus glycoproteins in freeze-fractured membranes of infected baby hamster kidney cells. *J Cell Biol* **101**(4)**,** 1300-6.

Torrisi, M. R., Di Lazzaro, C., Pavan, A., Pereira, L., and Campadelli-Fiume, G. (1992). Herpes simplex virus envelopment and maturation studied by fracture label. *J Virol* **66**(1)**,** 554-61.

Ubol, S., and Griffin, D. E. (1991). Identification of a putative alphavirus receptor on mouse neural cells. *J Virol* **65**(12)**,** 6913-21.

VonBonsdorff, C. H., and Harrison, S. C. (1978). Sindbis virus glycoproteins form a regular icosahedral surface lattice. *J. Virol.* **28,** 578.

Waite, M. R., Brown, D. T., and Pfefferkorn, E. R. (1972). Inhibition of Sindbis virus release by media of low ionic strength: an electron microscope study. *J Virol* **10**(3)**,** 537-44.

Wang, G., Hernandez, R., Weninger, K., and Brown, D. T. (2007). Infection of cells by Sindbis virus at low temperature. *Virology* **362**(2)**,** 461-7.

Wang, K. S., Kuhn, R. J., Strauss, E. G., Ou, S., and Strauss, J. H. (1992). High-affinity laminin receptor is a receptor for Sindbis virus in mammalian cells. *J Virol* **66**(8)**,** 4992-5001.

Wang, K. S., Schmaljohn, A. L., Kuhn, R. J., and Strauss, J. H. (1991). Antiidiotypic antibodies as probes for the Sindbis virus receptor. *Virology* **181**(2)**,** 694-702.

Wang, Y., Inoue, T., and Forgac, M. (2005). Subunit a of the yeast V-ATPase participates in binding of bafilomycin. *J Biol Chem* **280**(49)**,** 40481-8.

Wang, Y. F., Sawicki, S. G., and Sawicki, D. L. (1991). Sindbis virus nsP1 functions in negative-strand RNA synthesis. *J Virol* **65**(2)**,** 985-8.

Wengler, G., Koschinski, A., and Dreyer, F. (2003). Entry of alphaviruses at the plasma membrane converts the viral surface proteins into an ion-permeable pore that can be detected by electrophysiological analyses of whole-cell membrane currents. *J Gen Virol* **84**(Pt 1)**,** 173-81.

Wengler, G., Koschinski, A., and Repp, H. (2004). During entry of alphaviruses, the E1 glycoprotein molecules probably form two separate populations that generate either a fusion pore or ion-permeable pores. *J Gen Virol* **85**(Pt 6)**,** 1695-701.

Wessels, L., Elting, M. W., Scimeca, D., and Weninger, K. (2007). Rapid membrane fusion of individual virus particles with supported lipid bilayers. *Biophys J* **93**(2)**,** 526-38.

West, J., Hernandez, R., Ferreira, D., and Brown, D. T. (2006). Mutations in the endodomain of sindbis virus glycoprotein e2 define sequences critical for virus assembly. *J Virol* **80**(9)**,** 4458-68.

White, J., and Helenius, A. (1980). pH-dependent fusion between the Semliki Forest virus membrane and lipsoomes. *Proceedings of the National Academy of Science* **77**(6)**,** 3273-3277.

White, J., Kartenbeck, J., and Helenius, A. (1980). Fusion of Semliki Forest Virus with the plasma membrane can be induced by low pH. *Journal of Cell Biology* **87,** 264-272.

Whitehurst, C. B., Soderblom, E. J., West, M. L., Hernandez, R., Goshe, M. B., and Brown, D. T. (2007). Location and role of free cysteinyl residues in the sindbis virus e1 and e2 glycoproteins. *J Virol* **81**(12)**,** 6231-40.

Whitehurst, C. B., Willis, J. H., Sinodis, C. N., Hernandez, R., and Brown, D. T. (2006). Single and multiple deletions in the transmembrane domain of the Sindbis virus E2 glycoprotein identify a region critical for normal virus growth. *Virology* **347**(1)**,** 199-207.

Wieczorek, H., Putzenlechner, M., Zeiske, W., and Klein, U. (1991). A vacuolar-type proton pump energizes K+/H+ antiport in an animal plasma membrane. *J Biol Chem* **266**(23)**,** 15340-7.

Wild, P., Senn, C., Manera, C. L., Sutter, E., Schraner, E. M., Tobler, K., Ackermann, M., Ziegler, U., Lucas, M. S., and Kaech, A. (2009). Exploring the nuclear envelope of herpes simplex virus 1-infected cells by high-resolution microscopy. *J Virol* **83**(1)**,** 408-19.

Zhang, W., Heil, M., Kuhn, R. J., and Baker, T. S. (2005). Heparin binding sites on Ross River virus revealed by electron cryo-microscopy. *Virology* **332**(2)**,** 511-8.

Zhang, W., Mukhopadhyay, S., Pletnev, S. V., Baker, T. S., Kuhn, R. J., and Rossmann, M. G. (2002). Placement of the structural proteins in sindbis virus. *J Virol* **76**(22)**,** 11645-58.